Multidecadal trends in CO_2 evasion and aquatic metabolism in a large temperate river

An Truong Nguyen[1*], Gwenaël Abril[2,3], Jacob S. Diamond[1,4], Raphaël Lamouroux[5], Cécile Martinet[6], Florentina Moatar[1]

[1] INRAE, UR RiverLy, 5 Rue de la Doua, 69100 Villeurbanne, France

[2] Laboratoire de Biologie des Organismes et Ecosystèmes Aquatiques (BOREA), UMR 8067, Muséum National d'Histoire Naturelle, CNRS, IRD, SU, UCN, UA, Paris, France.

[3] Programa de Geoquímica, Universidade Federal Fluminense, Niterói, Rio de Janeiro, Brazil

[4] Dipartimento di Scienze Ambientali, Informatica e Statistica, University of Venice Ca' Foscari, Via Torino 155, 30172 Venezia Mestre, Italy

[5] EDF – Recherche et Développement, Laboratoire National d'Hydraulique et Environnement, Chatou, France

[6] EDF – Division Technique Générale, Electricité de France, Grenoble, France

[*] Corresponding author: truongan9393@yahoo.com, truong-an.nguyen@inrae.fr

Abstract. Rivers play a critical role in the global carbon cycle. However, the environmental and hydro-climatic factors that control the sign and magnitude of river CO_2 fluxes across seasons and multi-decadal periods are less constrained. The origin of excess river CO_2—delivered by soils, wetlands and groundwater or produced by aquatic respiration of organic matter—remains an important unknown in linking terrestrial and aquatic carbon budgets. To address these knowledge gaps, we report on a 32-year high-frequency dataset (1990–2021) from the Loire River, a large, temperate river that underwent a shift from a ~~eutrophic,~~ phytoplankton-dominated ~~regime~~ regime to a~~n oligotrophic,~~ macrophyte-dominated ~~regime~~ regime in ca. 2005. We estimated daily river-atmosphere CO_2 flux (FCO_2) and river net ecosystem productivity (NEP) from hourly pH, alkalinity, dissolved oxygen, water temperature and solar radiation. We demonstrate that: i) annual FCO_2 varied an order of magnitude among years (range = 200–2600 g C m^2 yr^{-1}) with a long-term decrease trend, mainly linked to decreased groundwater contribution; ii) the mean annual contribution of aquatic metabolism to total FCO_2 was 40%, ~~but this also varied according to year and trophic regime, ranging from negative to 100% contribution~~increasing from 37 ± 27% in phytoplankton-dominated regime to 57 ± 10% in macrophyte-dominated regime; iii) while the river predominantly acted as a CO_2 source, it occasionally functioned as a CO_2 sink ($FCO_2 <$ 0) during summer, though this sink behavior constituted a minor component (-0.6%) of the FCO_2

31 budgetthe river occasionally acted as a CO₂ sink (FCO₂ < 0) during summer, especially during the
32 eutrophic period of 1990-2000, but this flux was negligible (-0.6% of the FCO₂ budget); and iv) FCO_2
33 exhibited strong seasonality linked to discharge, exhibiting hysteresis where FCO_2 levels at equivalent
34 discharge were 1.5 to 2 times higher during the rising limb (autumn) compared to the falling limb
35 (spring). The magnitude of this hysteresis diminished in the later macrophyte-dominated regime,
36 indicating a changing seasonal discharge controlhysteresis with discharge, with FCO₂ levels ranging
37 from 1.5 to 2 times higher in autumn compared to spring at equivalent discharge rates, and the degree
38 of which was depended on trophic regime. This study makes clear that river FCO_2—and its sourcethe
39 source of this CO₂—is dynamic within and across years, driven by hydro-climatic variations and
40 biological activity. and thatCatchment-scale hydrogeological changes can be a more dominant driver
41 of long-term riverine CO_2 evasion than in-stream ecological regime shifts, controlling the balance
42 between internal and external CO_2 productionglobal changes affecting the river trophic regime control
43 the balance between internal and external CO₂ production.

Keywords: internal contribution, autotrophic, heterotrophic, long-term trend, metabolic shift, Loire River

1. Introduction

Streams and rivers are a major component of inland water CO_2 evasion, with the most recent estimates for this flux at 2.0 ± 0.2 Pg C yr^{-1} (Liu et al., 2022). Earlier foundational work suggested this riverine flux accounted for approximately contribute 60% (1.8 Pg C yr⁻¹) of CO₂ evasion from all inland waters (Raymond et al., 2013). Most CO_2 flux (FCO_2) is often assumed to come emitted comes from "external" sources, delivered to streams via groundwater inputs and via temporary hydrologic connectivity with riparian wetlands (Abril & Borges, 2019; Hotchkiss et al., 2015). Additional, geochemical weathering and photochemical processes are also considered external sources to river FCO_2 (Hotchkiss et al., 2015). While geochemical weathering primarily affects river alkalinity and indirectly influences CO_2 dynamics through changes in water chemistry (J. B. Jones et al., 2003), photochemical processes make a relatively minor contribution to CO_2 production when compared to biological processes (Amaral et al., 2013; Koehler et al., 2014). The remainder of FCO_2 from rivers originates from in-stream respiration of organic matter (Cole et al., 2001), termed the "internal" source of CO_2. While the balance between internal versus external CO_2 sources is spatially predictable (Hotchkiss et al., 2015), its temporal variation is less clear. Most analyses on the origin of stream FCO_2 occur over one season (e.g., Bernal

61 et al., 2022; Rocher-Ros et al., 2020) or rely on discrete samplings (e.g., Hotchkiss et al., 2015).

62 Consequently, while progress has been made, a comprehensive understanding of the full spectrum of

63 temporal variability (seasonal to multidecadal) in FCO2 and its sources remains limited, particularly for

64 large river systems. Recent work by Young et al. (2025) highlighted this complexity by documenting

65 strong seasonal variability driven by hydrological events, temperature fluctuations, and biological

66 productivity in a temperate river. Their four-year study emphasized the need for longer-term datasets to

67 capture interannual variability, particularly in the context of ongoing climate and ecological changes.

68 The seasonal hydrology plays an important role in determining the magnitude and timing of CO_2

69 emissions from rivers, as changes in flow rates affect the transport of nutrient, organic carbon from

70 surrounding land as input for stream metabolism and the exchange of CO_2 between the river and the

71 atmosphere (Cole et al., 2007; Hotchkiss et al., 2015). There is thus a lack of understanding of the

72 temporal variability of FCO_2 and its sources, which are increasingly crucial under a changing climate

73 that increases water temperature and modifies river flow (Floury et al., 2012; Van Vliet et al., 2013).

74 This knowledge gap is most prominent in large rivers, leading to significant uncertainty in global FCO_2

75 assessment from inland waters (Battin et al., 2023; Hotchkiss et al., 2015).

76 The relative contribution of internal CO_2 sources can be quantified as the ratio between net ecosystem

77 productivity (NEP) and FCO_2. NEP is the balance between gross primary production (GPP) and

78 ecosystem respiration (ER) (NEP = GPP – ER). When NEP is negative (GPP < ER), the river is in a

79 "heterotrophic" state, and CO_2 is added to the water column by net organic matter respiration.

80 Assuming the river is a CO_2 source (FCO_2 > 0) and in a heterotrophic state, the –NEP/FCO$_2$ ratio yields

81 the ratio of internal source contribution to total emissions, and by difference, the ratio of external CO_2

82 source contribution (=1+ NEP/FCO$_2$). This ratio can be evaluated in response to environmental drivers

83 such as hydrology (Hotchkiss et al., 2015), light (Rocher-Ros et al., 2021), water temperature (Lynch et

84 al., 2010; Wallin et al., 2020), and organic matter source (Bernal et al., 2022; Reed et al., 2021).

85 However, rivers are not always CO_2 sources and can seasonally function as CO_2 sinks when high rates

86 of GPP deplete CO_2, leading to CO_2 undersaturation (Aho et al., 2021; Zhang et al., 2017). In this

87 "autotrophic" state (GPP > ER), positive NEP means a net production of organic matter within the

reach, leading to increases in biomass (e.g., algal, macrophyte) and potentially contributing to particulate and dissolved organic matter pools. Such autotrophic state, sometimes leading to CO_2 undersaturation, can be more prevalent or sustained in larger rivers due to factors like greater water residence times, increased light availability across wider channels, and potentially a greater buffering capacity against rapid changes in external CO_2 inputs compared to smaller streams (Hotchkiss et al., 2015)~~positive NEP yields local organic matter increases~~. However, these periods, especially if transient or occurring outside of typical low-flow summer conditions, ~~This period is most common in larger rivers but is typically missed by~~ can be missed FCO$_2$ sampling campaigns~~, furthering the need for high-frequency, long-term studies of coupled stream metabolism and CO$_2$ measurements~~ that are often infrequent or biased towards specific seasons, thus underestimating their occurrence and impact.

The eutrophic ~~Autotrophic periods~~ state ~~were~~ was common in large rivers throughout the 1980s and 1990s, characterized by high nutrient concentrations and high chlorophyll-*a*~~,~~, leading to a net autotrophic state ~~(i.e., an eutrophic regime)~~ (Dodds & Smith, 2016). The Loire River (France) ~~was classified as the most~~was one of the most eutrophic rivers in Europe at that time with total phosphorus (TP) concentrations frequently exceeding 0.2 mg P L^{-1} and chlorophyll-a concentrations often surpassing 100 μg L^{-1}, with summer peaks reaching over 200 μg L^{-1} (Minaudo et al., 2015; Moatar & Meybeck, 2005). Despite potential autotrophic activity, the CO_2 dynamics during these periods remains poorly documented due to the lack of comprehensive CO_2 data, leaving a gap in our understanding of whether the river predominantly acted as a CO_2 source or sink.

Following efforts to reduce nutrient inputs between the early 1990s and the mid-2000s, TP concentrations declined by approximately 50-70%, and mean summer chlorophyll-a concentrations decreased to <30 μg L^{-1} (Minaudo et al., 2015).~~From 1990 to 2005,~~ ~~t~~The Loire River underwent ecological shifts from planktonic autotrophic communities dominated by phytoplankton to benthic communities dominated by rooted macrophytes (Minaudo et al., 2015), which is termed ~~""~~re-oligotrophication~~"~~" (Ibáñez et al., 2022). The ecosystem transition was followed by a delayed shift in the river's metabolic regime around 2012–2014, with GPP declining and NEP decreasing by roughly 10% during the spring–summer growing season~~accompanied by a delayed shift in the river metabolic~~

115 ~~regime in 2012–2014, associated with reductions in GPP and NEP in the growing season (Diamond et~~

116 ~~al., 2022). As a result, approximately 10% of NEP was decreased~~ (Diamond et al., 2022)~~, which could~~

117 ~~potentially lead to an increase in FCO₂ due to decreased CO₂ consumption by stream metabolism~~. As

118 re-oligotrophication may become increasingly common in developed countries, its effects on FCO_2 and

119 CO_2 source variation remain unknown.

120 In this study, we used a 32-year daily dataset of coupled stream metabolism (NEP) and FCO_2 to assess

121 the temporal internal/external CO_2 source contributions in the Loire River. We hypothesized that the

122 FCO_2 and its internal source contribution would increase following the re-oligotrophication ecosystem

123 shift. Specifically, we predicted that these increases would manifest coincidentally with the shifts in

124 phytoplankton to macrophyte-dominated regime in 2005 and stream metabolism regime in 2012.

125 Finally, discharge influences FCO_2 through multiple mechanisms, including gas transfer velocity,

126 delivery of external CO_2, and inhibition of in-stream primary production. Phytoplankton GPP can be

127 sensitive to discharge (e.g., washout, turbidity), while macrophyte GPP may be less directly flow-

128 dependent~~because GPP under macrophytes is less flow-dependent than under phytoplankton~~ (Diamond

129 et al., 2022)~~,~~. We therefore predicted that the overall control of discharge (Q) on FCO2 would change

130 with the shift to macrophyte dominance. Specifically, we anticipated that the seasonal hysteresis patterns

131 observed in the FCO_2-Q relationship (where FCO_2 differs between rising and falling limbs of the

132 hydrograph at similar Q) would be altered, potentially becoming less pronounced or showing a different

133 shape if macrophyte GPP imparts a more stable baseline of CO_2 uptake across varying flow conditions

134 compared to phytoplankton ~~we predicted that discharge would become a weaker control on FCO₂ in the~~

135 ~~macrophyte-dominated state, but this changing control would vary seasonally~~.

136 **2. Methods**

137 **2.1. Study site**

138 The study site (47.6°N, 2.6°E) is located in the middle Loire River, France, 564 km from the source,

139 with a mean discharge of 300 m^3 s^{-1} (Supplementary Figure S1). Its 36,000 km² catchment is home to

140 over two million residents. The land cover consists of forests (42%), pasture (35%), and agriculture

141 (21%) (Moatar & Meybeck, 2005). The Loire River and its tributaries, upstream Dampierre drains

volcanic, granitic area and sedimentary basins characterized by extensive limestone and marl formations (Figure S1). After the confluence with Allier River (100 km upstream of the study site), the carbonate-rich catchment and its interaction with the Loire River significantly contribute to river alkalinity primarily through the dissolution of carbonate minerals (Binet et al., 2022). Soil types within the Loire catchment are heterogeneous and their nature is closely linked to the underlying lithology. In addition, the catchment includes significant areas of alluvial deposits, which feature more fertile and productive soils for extensive agriculture in the region (Moatar et al., 2022; Moatar & Meybeck, 2005). This river is an 8th-order river with an anabranching fluvial pattern resulting from a gentle slope (0.4 m km^{-1}). During summer, low flows (<150 m^3 s^{-1}), the study site is typically shallow (around 1 m deep) and wide (330 m); during winter, with higher discharges (e.g., >500 m^3 s^{-1}), depths can increase significantly, typically ranging from 2 to 3 mthe study site is shallow (1 m) and wide (330 m). The anabranching fluvial pattern leads to a broad range of lateral hydrologic connectivity between the main channel and secondary channels colonized by semi-terrestrial vegetation (Janssen et al., 2023). These vegetated side channels may behave like floodplains by acting as seasonal sources of organic carbon (Abril & Borges, 2019).

2.2. Data acquisition and processing

Hourly data of pH, temperature, electrical conductivity (EC) at 25°C, and dissolved oxygen (DO) from 1990–2021 were extracted from the monitoring program conducted by Électricité de France (EDF) upstream and downstream of the nuclear power plant Dampierre (47.6°N, 2.6°E) (Figure S2). Total alkalinity (TA) wasin the upstream station obtained from grab samples collected by both EDF and the Loire-Brittany Water Agency (AELB), with measurement frequency ranging from daily to monthly. was measured at varying intervals, ranging from every three days to weekly, by EDF and Naiades (www.naiades.eaufrance.fr). We reconstructed a continuous daily TA time series from the relationship between EC and TA (Appendix A, Figure A2). We reconstructed the daily TA based on the linear relationship between EC and TA (Supplementary Figure S2). This study used the upstream data to calculate daily FCO$_2$ and NEP, while the downstream data was used to support the data cleaning

168 procedure ~~(Supplementary section S1).~~. A full description of the data acquisition, quality control

169 framework, and data processing is available in **Appendix A**.

170 We obtained daily global radiation data (W m^{-2}) from a nearby meteorological station

171 (donneespubliques.meteofrance.fr). Mean daily discharge (m^3 s^{-1}) ~~and river depth (m) were~~ was

172 obtained from www.hydro.eaufrance.fr. We then estimated average river depth (m) using a local rating

173 curve (Depth (m)=0.0716×√(Q (m^3 s^{-1}) + 0.6171), which was established based on the hydraulic model

174 for the Loire River (Camenen et al., 2016).

2.3. NEP and FCO$_2$ estimation

2.3.1. Metabolism estimation

177 We estimated daily GPP, ER (~~mmol~~ g ~~C~~ O$_2$ m^{-2} d^{-1}), and the gas exchange rate coefficient (K$_{600}$, d^{-1}) by

178 using the inverse modelling approach that yields the best fit between modeled and observed DO. To

179 avoid the unrealistic estimates, the K$_{600}$ is constrained by daily river discharge and river depth with the

180 formulations proposed by Raymond et al., 2012, while the hourly DO, solar radiation and daily water

181 temperature data are required to further reduce equifinality of GPP, ER and K$_{600}$. These estimates are

182 supported by the *streamMetabolizer*, a R package (Appling et al., 2018). The model setup for the Loire

183 River was described by Diamond et al. (2021) and Diamond et al. (2025). GPP and ER were then

184 converted to carbon units (g C m^{-2} d^{-1}) using a fixed molar O$_2$:C ratio of 1:1. This assumption is widely

185 used in river metabolism studies and reflects the stoichiometry of aerobic metabolism (Trentman et al.,

186 2023). Although photosynthetic and respiratory quotients (PQ and RQ) can vary with autotrophic

187 community composition, recent long-term analysis of the Loire River by Diamond et al. (2025) showed

188 that such variability does not lead to cumulative bias in net ecosystem production or CO$_2$ budgets when

189 integrated over decadal timescales. Therefore, we adopt this approach as a reasonable and conservative

190 approximation for estimating long-term carbon dynamics, while acknowledging it as a source of short-

191 term uncertainty.

192 About 12% of samples (n=1391) were discarded due to physically impossible results in metabolism

193 estimation (i.e., negative values). Missing mean daily GPP and ER were then replaced by their daily

194 75th estimated percentile values provided by *streamMetabolizer*, as detailed in **Appendix B, Section**

195 **B1** ~~Supplementary section S3~~. We imputed the remaining 1.7% of missing data using the rolling 7-day

196 average. The K$_{600}$ values derived from the model were validated against established empirical equations

197 and found to be of the same order of magnitude, as detailed in **Appendix B, Section B2**. The covariance

198 between estimated ER and K600 was low (R^2 = 0.09), demonstrating reduced influence of equifinality

199 problem (Appling et al., 2018).

2.3.2. pCO₂~~CO₂~~ and FCO₂~~CO₂~~ estimation

201 Daily concentrations of partial pressure of CO_2 (pCO₂, µatm) were estimated by pyCO2SYS, a Python

202 package for the CO2SYS model (Humphreys et al., 2022), using mean daily pH, water temperature, and

203 TA. Carbonate dissociation constants K_1 and K_2 were chosen based on freshwater estimates (Millero,

204 1979). CO2SYS freshwater pCO₂ estimates are valid for water with TA > 1000 µmol L^{-1}, and results

205 have been previously validated for the Loire River (2–9% bias) (Abril et al., 2015). The daily TA data

206 in this study were estimated from daily EC with an average error of 190 µmol L^{-1}, leading to an

207 uncertainty in pCO2 estimation. PyCO2SYS can estimate pCO2 uncertainty by propagating the TA

208 uncertainty (Humphreys et al., 2022) ~~(Humphreys et al., 2022)~~. ~~Uncertainty~~The uncertainty of estimated

209 TA leads to ±11% uncertainty in pCO2 estimation, however there ~~is~~ was no significant difference in the

210 river's CO₂ state ~~compared~~ over 32 years, as detailed in the uncertainty analysis in **Appendix B, Section**

211 **B3** ~~(Supplementary section S4)~~.

212 ~~The~~ FCO₂ (mmol C m^{-2} d^{-1}) between the water and the atmosphere was calculated using ~~Fick's~~ Fick's

213 law, using the CO_2 transfer velocity (kCO₂, m d^{-1}) and the air-water CO_2 gradient (mmol m^{-3}) (Eq. 1).

214 We obtained kCO₂ (Eq. 2) using Schmidt number (Sc) at given water temperature (Eq. 3) scaling from

215 the gas transfer velocity k_{600} (m d^{-1}) (Raymond et al., 2012a). The k_{600} was calculated by multiplying

216 ~~with~~ river depth with K_{600}, an output of *streamMetabolizer*. ~~We compared k_{600} with seven fitted~~

217 ~~equations proposed by Raymond et al., (2012a) for streams and small rivers and found that they are~~

218 ~~within the same order of magnitude (Supplementary Figure S5).~~ The k600 estimates from the

219 StreamMetabolizer model were selected for FCO₂ calculations to ensure consistency with the NEP

220 calculations.

$$FCO_2 = k_{CO_2} \times (CO_{2\ water} - CO_{2\ air}) \qquad \text{Eq. 1}$$

$$k_{CO_2} = depth \times K_{600} / \left(600/Sc_{CO_2}\right)^{-0.5} \qquad \text{Eq. 2}$$

$$Sc_{CO_2} = 1911.1 - (118.1 \times T) + (3.45 \times T^2) - (0.0413 \times T^3) \qquad \text{Eq. 3}$$

221 CO₂,water is aqueous CO_2 (mmol m^{-3}) estimated by pyCO2SYS, and CO₂,air is CO_2 in equilibrium with

222 the atmosphere using global monthly atmospheric CO_2 from 1990–2021 from National Oceanic and

223 Atmospheric Administration Global Monitoring Laboratory (https://gml.noaa.gov/ccgg). K_{600} is the gas

224 exchange rate coefficient normalized to a Schmidt number of 600 (d^{-1}) from streamMetabolizer, Sc_{CO_2}

225 is the Schmidt number for CO_2 (unitless), T is the water temperature in degrees Celsius (°C). We used

226 ~~Henry's~~ Henry's law to convert pCO_2 in μatm into CO_2 in mmol m^{-3} using temperature-dependent

227 solubility constants.

2.3.3. Categorizing NEP-FCO₂ states by autotrophic/heterotrophic and source/sink states

229 We categorized the river into four trophic-flux states (or ~~"~~"trophlux~~"~~" states) based on daily NEP and

230 FCO_2. Following Odum (1956), ~~I~~if NEP is positive (GPP > ER), the river is autotrophic, while if NEP

231 is negative (GPP < ER), the river is heterotrophic. Likewise, if FCO_2 is positive, the river is a CO_2

232 source, while if FCO_2 is negative, the river is a CO_2 sink, relative to the atmosphere. The river could

233 thus be in four possible trophlux states: 1) autotrophic-sink, 2) autotrophic-source, 3) heterotrophic-sink,

234 and 4) heterotrophic-source. The autotrophic-sink and heterotrophic-source states imply that NEP and

235 FCO_2 vectors are moving CO_2 in the same direction, into water column biomass or out of the water

236 column, respectively (Bogard & Del Giorgio, 2016). The remaining two states imply opposite directions

237 between NEP and FCO_2. The autotrophic-source state implies that although there is a net conversion of

238 CO_2 into biomass, there is a surplus of water column CO_2 relative to autotrophic needs, leading to

239 continued positive FCO_2. The heterotrophic-sink state implies that despite the net conversion of biomass

240 into water column CO_2, there is still a CO_2 undersaturation relative to the atmosphere, likely due to prior

241 autotrophic uptake. We expect the heterotrophic-sink state to be a temporary occurrence, reflecting

242 temporal lags within the carbonate system buffering capacity during the short transition between

243 autotrophic and heterotrophic states. Recent work using this dataset has provided strong evidence for

244 this mechanism, showing that these events are temporary and typically follow periods of intense

245 autotrophic activity (Diamond et al., 2025). A more detailed discussion of methodological

246 considerations for this state is provided in **Appendix B, Section B4**.

247 Conventionally, the aquatic metabolism contribution to river CO_2 emissions (i.e., the internal CO_2

248 source) is calculated as –NEP/FCO_2 in the heterotrophic-source state (Bernal et al., 2022; Hotchkiss et

249 al., 2015; Kirk & Cohen, 2023).

2.4. Change points and long-term trend analysis

To test our hypothesis that FCO_2 would vary as a function of ecosystem state and metabolism shifts in the Loire River, we compared change points in FCO_2 with previously estimated change points in ecosystem regimestate (ca. 2005) and metabolic regime (ca. 2012) (Diamond et al., 2022; Minaudo et al., 2015). We used the *ruptures* Python package (Truong et al., 2020) with a five-year window interval to ensure that identified changes were sustained beyond year-to-year variation. The change point detection was also applied to the daily NEP and related variables (pH, alkalinity, pCO_2, k600, GPP, and ER). We also conducted change point detection on the seasonal decomposed time series of daily FCO_2 and NEP. This decomposition, performed using the *statsmodels* Python package (Seabold & Perktold, 2010), separates a time series into trend, seasonal, and residual components, allowing us to specifically identify change points in the characteristics of the seasonal cycle (e.g., amplitude changes) independently of the long-term trendto better identify changes in seasonal as opposed to long-term variations **(Appendix C, Section C1)**. To quantitatively assess differences between change point periods, we performed non-parametric Kruskal-Wallis tests followed by post-hoc Mann-Whitney U tests **(Appendix C, Section C2)**.

We further estimated long-term trends of FCO_2 and NEP as functions of hydroclimatic conditions (discharge, water temperature) in each trophlux state by using the Mann-Kendall test (*pyMannKendall* Python package) (Hussain & Mahmud, 2019).

2.5. Seasonal hysteresis of NEP and FCO_2 in response to discharge changes

To test the influence of discharge on CO_2 emissions, we evaluated the hysteresis of mean daily FCO_2 and NEP against mean daily discharge across the periods delineated by the change point analysis. We predicted that for the same discharge, FCO_2 would exhibit a range of magnitudes depending on the season but that this range would decrease systematically as a function of decreasing phytoplankton coverage in the Loire River. We evaluated the hysteresis loops by the direction of hysteresis (clockwise or counterclockwise) and the magnitude (i.e., difference of FCO_2 at the same discharge but in the rising and falling flow stage). We anticipated that the shift to a macrophyte-dominated regime, with potentially more stable GPP across flow conditions, might lead to a reduction in the magnitude (i.e., a "flattening")

277 of these hysteresis loops for FCO2 and NEP. We additionally calculated hysteresis magnitude for –NEP,

278 external source contribution (FCO_2 + NEP), and –NEP/FCO_2 at the mean discharge (300 m^3 s^{-1}, Table

279 2) during the rising (autumn) and falling stage (spring).

3. Results

3.1. Daily, seasonal, inter-annual FCO_2 emissions and NEP contribution for 32 years

282 FCO_2 and NEP exhibited strong daily, seasonal, and inter-annual variations (Figure 1). The pronounced

283 seasonal variability drove successive transitions among different trophlux states. Typically, the river

284 would shift from being heterotrophic and a CO_2 source in winter, towards becoming more autotrophic

285 in spring and potentially a CO_2 sink in summer during low flows, before returning to heterotrophic

286 source conditions in autumn with rising flows. This general seasonal pattern, involving changes in both

287 NEP (autotrophic/heterotrophic) and FCO_2 (sink/source), recurred each year, though its specific timing

288 and intensity varied resulted in the successive transition of different states of FCO_2 and NEP

289 (autotrophic/heterotrophic of NEP, sink/source of FCO_2) but with a recurring seasonal pattern each year

290 (Figure 1c). The corresponding hydro-climatic context, including mean annual discharge for each year,

291 is provided in the Supplementary Information (Figure S3) for a detailed comparison.

292
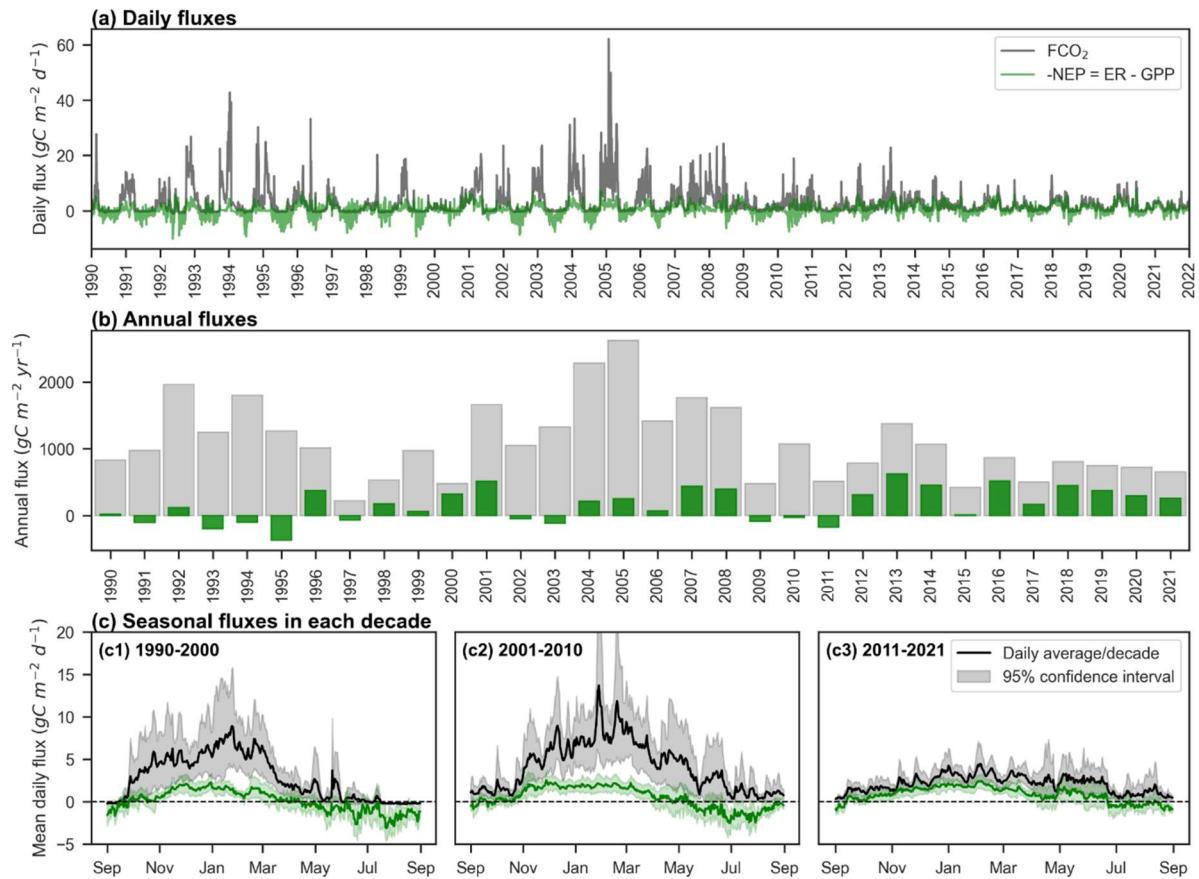
Figure 1. Evolution of FCO_2 and –NEP during 1990-2021. (a) Daily values (g C m^{-2} d^{-1}), (b) Cumulative annual fluxes (calendar year, g C m^{-2} y^{-1}), (c) Seasonal fluxes during hydrological year in each decade 1990-2000, 2001-2010, 2011-2021. In Figure 1c, the solid line and shaded area are the average and the 95% confidence interval of the daily fluxes each decade, calculated by 10 daily fluxes in the same day-year.

The daily average FCO_2 was 3 g C m^{-2} d^{-1}, with high peaks reaching 20 - 60 gC m^{-2} d^{-1} during high flow in winter (1000–2000 m^3 s^{-1}) and low peaks with negative FCO_2 of -0.8 gC m^{-2} d^{-1} during the low flow in summer (<150 m^3 s^{-1}) (Figure 1). The daily NEP was -0.45 gC m^{-2} d^{-1}, with average peaks from -4.0 gC m^{-2} d^{-1} in winter to 3.6 gC m^{-2} d^{-1} in summer (Figure 1a).

Cumulative annual FCO_2 ranged from 221 to 2633 g C m^{-2} y^{-1} and NEP from -383 to –584 g C m^{-2} yr^{-1}. Notably, there were 10 years from 1990–2011 when the Loire River was net autotrophic (Figure 1b, green bars), mainly in 1990-2000. Even during these years, the Loire River was a net source of CO_2 to the atmosphere (Figure 1b, grey bars). The contribution of external CO_2 sources (FCO_2 + NEP) ranged from 800–2400 g C m^{-2} y^{-1} in 1990–2010. However, the contribution of external CO_2 sources has significantly decreased to ca. 400 g C m^{-2} y^{-1} since 2011 (Figure 1b).

308
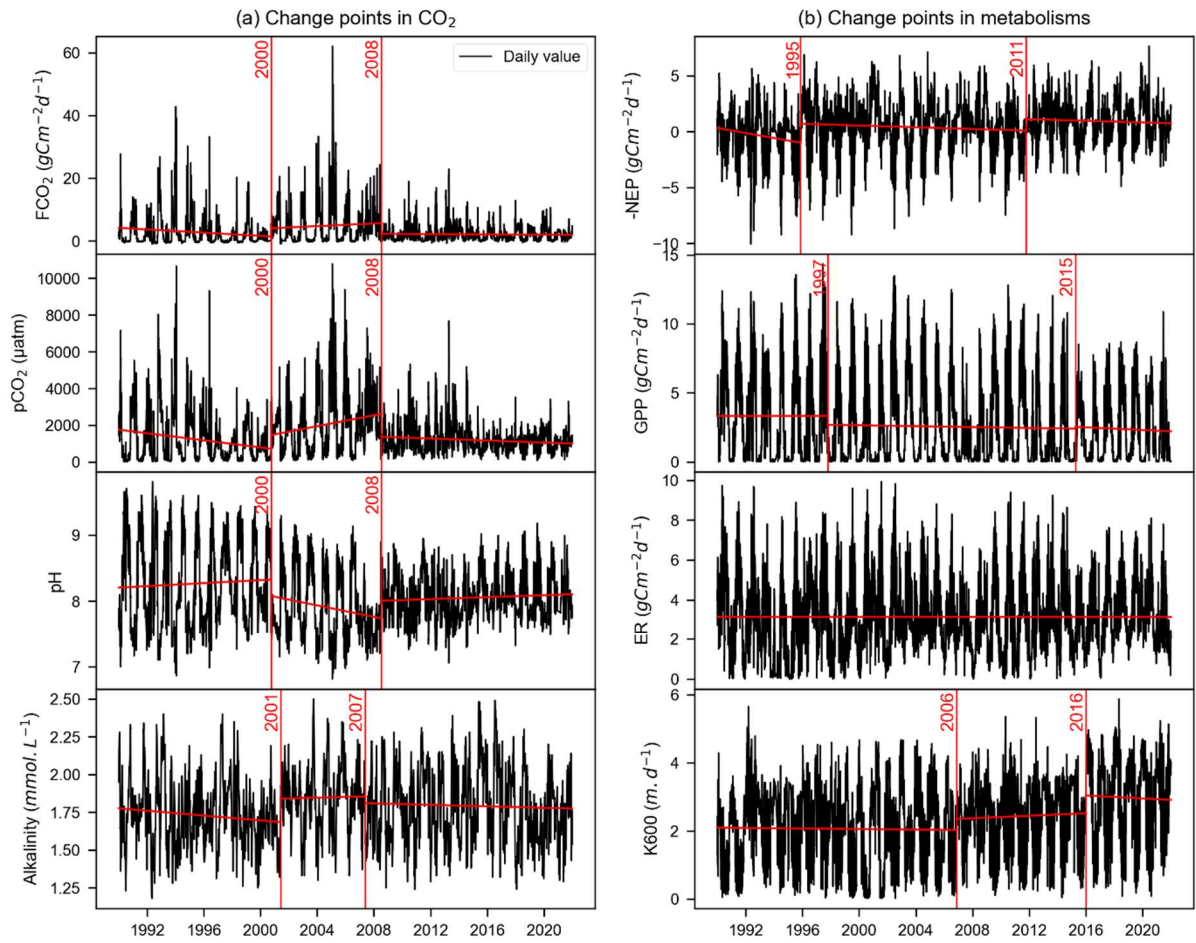
Figure 22. Change point detection in the daily time series of (a) FCO$_2$, pCO$_2$, pH, alkalinity and (b) – NEP, K600, GPP, ER during 1990-2021. The vertical red lines indicate the year of the change point.

The change point analysis on daily time series detected that the FCO$_2$ experienced two change points in 2000 and 2008 (Figure 2a), while the change points of –NEP were detected in 1995 and 2011 (Figure 2b). While change points in –NEP described a gradual increase, change points in FCO$_2$ indicated more abrupt fluctuations, with abnormal decreases in 2000 and 2008. The daily time series of pCO$_2$, pH, and alkalinity had similar change points to FCO$_2$. The change points of –NEP were mainly dependent on GPP, while there was no significant change in the ER time series (Figure 2b). In addition, the seasonal decomposition analysis detected the same change point in 2008 for the seasonal amplitude in both FCO$_2$ and NEP, indicating a significant decrease in the seasonal variations (Supplementary Figure S6C1).

The periods of change in both FCO$_2$ and NEP spanned roughly three decades: (i) 1990–2000, (ii) 2001–2010, and (iii) 2011–2021. These time frames were selected based on changepoint analysis, which identified shifts in FCO$_2$ around 2000 and 2008, in NEP around 1995 and 2011, and GPP around 1997

322 and 2015 (Figure 2). Despite some discrepancies in the exact timing of these changepoints between

323 FCO_2 and NEP, grouping the data by decades allowed for a coherent comparison of long-term trends in

324 ecosystem behavior. These periods corresponded to distinct phases in river metabolism and CO_2

325 emissions: (i) high primary productivity (cumulative annual GPP= 1113 ± 225 g C m^{-2} y^{-1}, ER= $1136 \pm$

326 241 g C m^{-2} y^{-1}) and low CO_2 emission ($FCO_2 = 1031 \pm 531$ g C m^{-2} y^{-1}) ; (ii) reduced primary

327 productivity (GPP= 973 ± 292 g C m^{-2} y^{-1}, ER= 1136 ± 128 g C m^{-2} y^{-1}) and high CO_2 emission (FCO_2

328 $= 1534 \pm 620$ g C m^{-2} y^{-1}), and (iii) low primary productivity (GPP= 867 ± 212 gC m^{-2} y^{-1}, ER= $1167 \pm$

329 163 g C m^{-2} y^{-1}) and low CO_2 emission ($FCO_2 = 773 \pm 272$ g C m^{-2} y^{-1}).

330 **3.2. Occurrence and contribution of trophlux states to CO_2 emissions**

331 At the seasonal time scale, the Loire River varied among trophlux states, with the heterotrophic-source

332 state predominating. The source state occurred the least (64% of time) in the first decade delineated by

333 change points (1990–2000) and occurred the most (92% of time) in the most recent decade (2011–2021).

334 Likewise, the heterotrophic state occurred at a minimum of 54% and a maximum of 67% of time during

335 those decades, respectively. The joint occurrence of the heterotrophic-source state thus ranged from 47.3

336 $\pm$ 9.4% in 1990-2000 to 66.8 $\pm$ 11.3% in 2011-2021 of time (Table 1), coinciding with low water

337 temperature and high discharge (Figure C2). This state contributed more than 90% of the total annual

338 CO_2 emissions. Within this heterotrophic-source state, the contribution of internal sources ($-NEP/FCO_2$)

339 to total CO_2 emissions varied across the decades: it was 37 ± 27% in 1990-2000, 28 ± 9% in 2001-2010,

340 and increased to 57 ± 10% in 2011-2021 (Table 1). This implies that external CO_2 sources accounted

341 for the remaining proportion in each periodstate, internal sources contributed an average of 28-57% of

342 total annual CO_2 emissions, implying external CO_2 source contributions of 72-43% in the Loire River.

343 The remaining three trophlux states (autotrophic-source, autotrophic-sink, and heterotrophic-sink) had

344 a combined net impact of contributed less than 10% to on total FCO_2 despite their regular occurrence

345 (e.g., up to 50% of time) during the 1990-2000 decade. ThThe autotrophic-sink state, driven by high

346 GPP, typically occurred for ere were often 1–3 months of CO$_2$ sink state due to high GPP in during the

347 summer growing season, coinciding with the highest water temperatures and the lowest discharge (Table

348 1). The autotrophic-sink reduced annual FCO_2 by -3.0 ± 4.2% 3% during 1990–2000 and by -0.4 ± 0.3%

349 0.3% in 2011–2021. In spring and autumn, the Loire River was regularly in an autotrophic state (17%

350 to 28% of time) but remained a CO_2 source, presumably attributed to external CO_2 sources. This

351 autotrophic-/source state contributed 8.2–9.2% to annual FCO_2 across years. The heterotrophic-sink

352 state occurred rarely (1–7% of time) and had a small influence on the annual FCO_2 budget (reducing it

353 by 0.1% to 0.8% across the decades0.1–0.8%). This state typically occurred as relatively short events of

354 1–14 days from June to August during the transition from autotrophic-sink state or heterotrophic-source

355 state.

356 **Table 1.** Summary of the occurrence, fluxes, and related hydroclimatic conditions of each trophlux

357 state in three decades, 1990-2021. The values within the table are depicted as the mean annual value ±

358 standard deviation, calculated for each decade (N=10 or 11).

359

Variable	Period	CO₂ source		CO₂ sink		All states
		Heterotrophic	Autotrophic	Heterotrophic	Autotrophic	
Occurrence (% of days)	1990-2000	47.3 ± 9.4	16.7 ± 9.2	7.3 ± 5.4	28.7 ± 7.0	100
	2001-2010	61.2 ± 12.7	25.3 ± 11.2	1.7 ± 1.1	15.5 ± 9.0	100
	2011-2021	65.8 ± 11.3	26.2 ± 8.6	1.1 ± 1.5	7.3 ± 5.7	100
FCO₂ budget (% of annual flux by each state)	1990-2000	94.6 ± 13.8	9.2 ± 11.4	-0.8 ± 1.4	-3.0 ± 4.2	100
	2001-2010	92.4 ± 11.3	8.2 ± 11.2	-0.1 ± 0.0	-0.6 ± 0.5	100
	2011-2021	91.8 ± 5.6	8.7 ± 5.8	-0.1 ± 0.2	-0.4 ± 0.3	100
–NEP ($gC\ m^{-2}\ y^{-1}$)	1990-2000	277 ± 158	-54 ± 46	25.5 ± 28.0	-225 ± 97	23 ± 222
	2001-2010	376 ± 127	-111 ± 83	3.8 ± 3.0	-131 ± 100	162 ± 234
	2011-2021	417 ± 173	-82 ± 48	2.0 ± 2.4	-36 ± 35	300 ± 232
FCO₂ ($gC\ m^{-2}\ y^{-1}$)	1990-2000	954 ± 514	102 ± 148	-4.4 ± 4.5	-21 ± 12	1031 ± 531
	2001-2010	1453 ± 666	88 ± 104	-0.6 ± 0.8	-7.8 ± 5.4	1534 ± 620
	2011-2021	717 ± 274	59 ± 28	-0.9 ± 1.8	-2.6 ± 2.1	773 ± 272
External CO₂ ($gC\ m^{-2}\ y^{-1}$)	1990-2000	677 ± 477	157 ± 92	-29 ± 32	204 ± 93	1008 ± 551
	2001-2010	1077 ± 595	199 ± 172	-4 ± 1	123 ± 95	1372 ± 528
	2011-2021	299 ± 140	140 ± 55	-2 ± 3	34 ± 31	472 ± 129
–NEP/FCO₂ (%)	1990-2000	37 ± 27	-123 ± 122*	*-697 ± 546	1535 ± 1413**	5 ± 29
	2001-2010	28 ± 9	-195 ± 137*	*-925 ± 786[NS]	1983 ± 828**	7 ± 15
	2011-2021	57 ± 10	-150 ± 59*	*-9204 [NS]	1480 ± 740**	34 ± 27
Temperature (°C)	1990-2000	8 ± 4	12 ± 4	18 ± 3	20 ± 3	13 ± 6
	2001-2010	10 ± 5	18 ± 5	18 ± 7	21 ± 3	13 ± 7
	2011-2021	11 ± 5	18 ± 5	10 ± 9	21 ± 3	14 ± 6
Discharge ($m^3\ s^{-1}$)	1990-2000	454 ± 326	276 ± 225	115 ± 60	111 ± 56	301 ± 290
	2001-2010	436 ± 323	160 ± 110	137 ± 69	115 ± 59	323 ± 296
	2011-2021	362 ± 278	120 ± 87	205 ± 136	80 ± 63	277 ± 259

* During the autotrophic/source state, the positive NEP reduces the outgassing of external CO₂, leading to a negative percentage ratio.Not applicable. In these cases, the –NEP/FCO₂ ratio does not represent a

360

3.3. The inter-annual trend of FCO$_2$ depending on trophlux states

The occurrence of heterotrophic-source and autotrophic-sink and their contribution to FCO$_2$ gradually changed from 1990~~–~~ to 2021 (Figure 3). The occurrence of the heterotrophic-source state increased from 140 days in 1990 to 250 days in 2021 (Figure 3a). However, the annual flux of –NEP within this state remained relatively stable (Figure 3b), while FCO$_2$ decreased with an average rate of 0.16 g C m^2 d^{-1} per year, resulting in a 62% reduction of FCO$_2$ in the heterotrophic-source state over the 32 years (Figure 3d). The annual decline in FCO$_2$ was uncorrelated ($R^2 = 0.09$) with the increase in annual water temperature (+5.7 °C/32 years), but it was positively correlated ($R^2 = 0.36$) with the decrease in annual discharge (-13%/32 years) (Table ~~S2~~D1). Since the annual –NEP remained stable and FCO$_2$ decreased, the ratio of –NEP/FCO$_2$ thus increased from 20–40% in the 1990s to 60-75% in recent years, +1.25% per year (Figure 3f). There were some abnormal increases of –NEP/FCO$_2$ observed in 1995–2000, with the ratio reaching 100% in 1997 and 90% in 1996~~,~~ and 2000. These peaks were associated with a significant drop in FCO$_2$ (Figure 3d) and, thus, in external CO_2 sources (Figure 3b).

The autotrophic-sink state occurrence decreased from 140 days in 1990–2000 to 30 days in recent years (Figure 3a), following a reduction in +NEP from about 2 to 1.5 gC m^{-2} d^{-1} (-25%/32 years), corresponding to -0.015 g C m^2 d^{-1} per year (Figure 3b). In this state, annual discharge and temperature did not show significant changes (p > 0.05) (Figure 3c, e). The decrease in +NEP was not significantly correlated with either annual discharge ($R^2 = 0.03$) ~~and~~ or annual temperature ($R^2 = 0.00$) (Table ~~S2~~D2).

Regarding the other two trophlux states, the autotrophic-source state showed a significant increasing trend in occurrence, similar to the heterotrophic-source state (Figure 3a). This state was also associated with increasing annual temperatures and decreasing annual discharge over time (Figure 3c,e). However, unlike the heterotrophic-source state, there was no significant long-term trend in FCO$_2$. In contrast, the

385
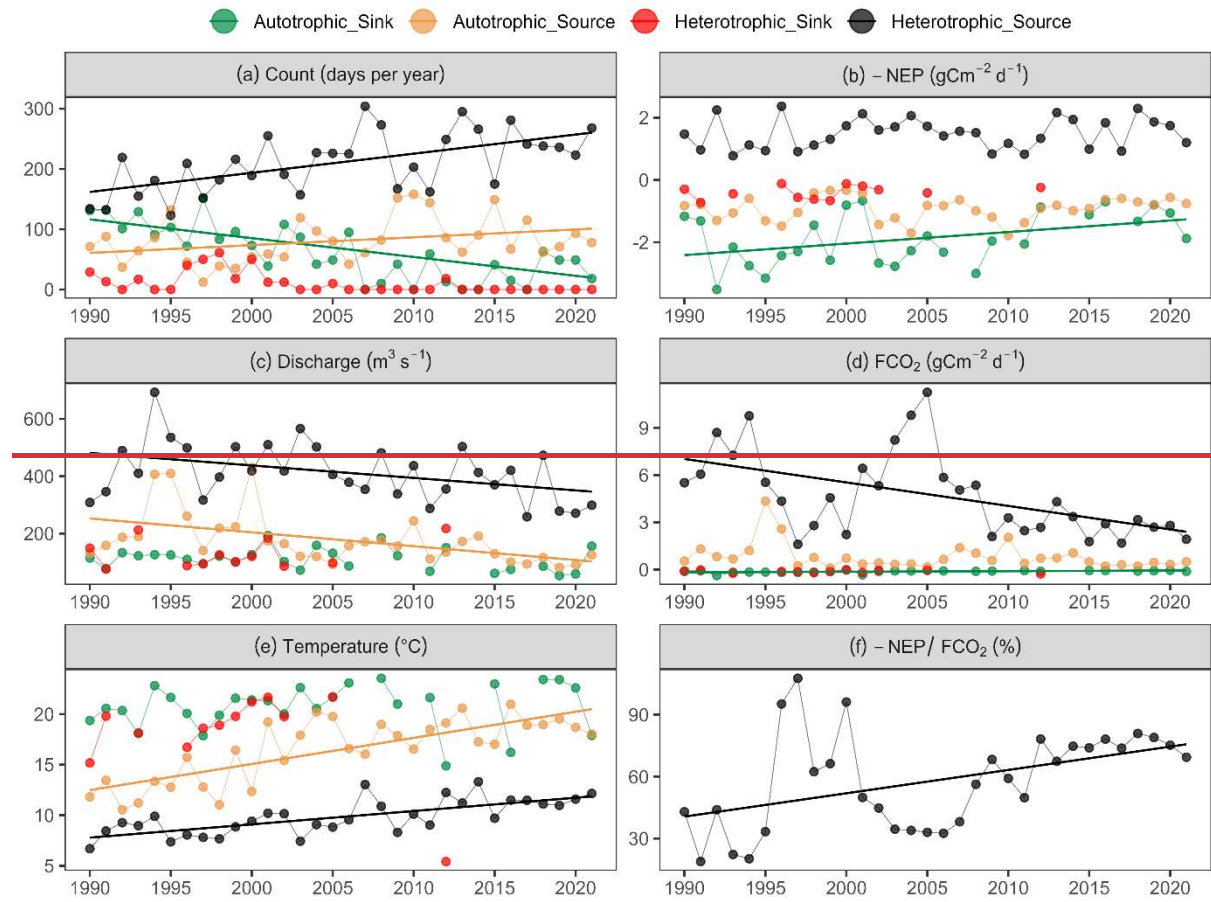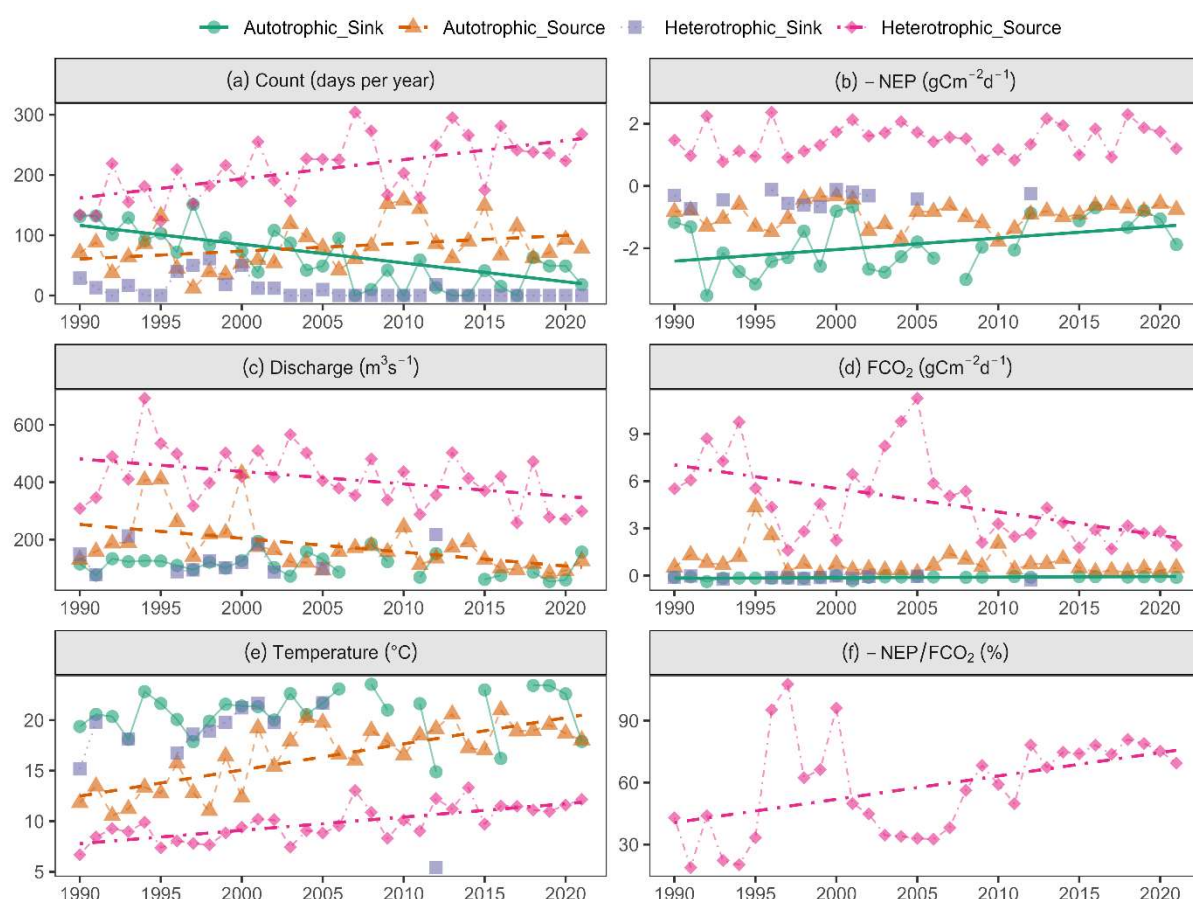
Figure 33. Long-term trends over 32 years of CO_2 fluxes, aquatic metabolism contribution, and hydroclimatic conditions on each trophlux state: a) occurrence per year, b) annual aquatic metabolism flux (–NEP), c) annual discharge, d) annual FCO_2, e) annual water temperature, f) –NEP/FCO_2. The points depicted on the graph were the annual averages. The regression lines were the Theil-Sen slopes with significant trends (p-value < 0.05).

3.4. Seasonal hysteresis of NEP and FCO_2 in relation to discharge

FCO_2 and NEP exhibited a similar clockwise hysteresis pattern in response to seasonal variations of discharge, i.e., higher fluxes in the rising discharge stage compared to the falling stage (Figure 4). Typically, hysteresis cycles started with FCO_2 minima and NEP maxima in July and August (mean discharge <150 m^3 s^{-1}, mean temperature 23 °C), with opposite peaks in January and February (mean discharge >500 m^3 s^{-1}, mean temperature 5 °C) (Figure 4a). As river discharge gradually increased from summer to winter, the river transitioned from an autotrophic to a heterotrophic state and from CO_2 sink to source. Subsequently, but along a different trajectory, the river shifted back to an autotrophic state during the spring-summer falling discharge stage (150–300 m^3 s^{-1}). During this time, however, the river continued to act as a CO_2 source, lasting two to three months (April–June) before returning to the FCO_2

402 minimum again in summer. The contribution of external CO$_2$ sources (FCO$_2$ + NEP) also exhibited a

403 clockwise hysteresis loop with discharge, with higher external contributions during the rising limb

404 (autumn/winter) and lower contributions during the falling limb (spring) at equivalent discharge rates,

405 generally mirroring the patterns observed for FCO$_2$ and –NEP ~~sources largely mirrored these patterns~~

406 (Figure 4, bottom row~~.~~).
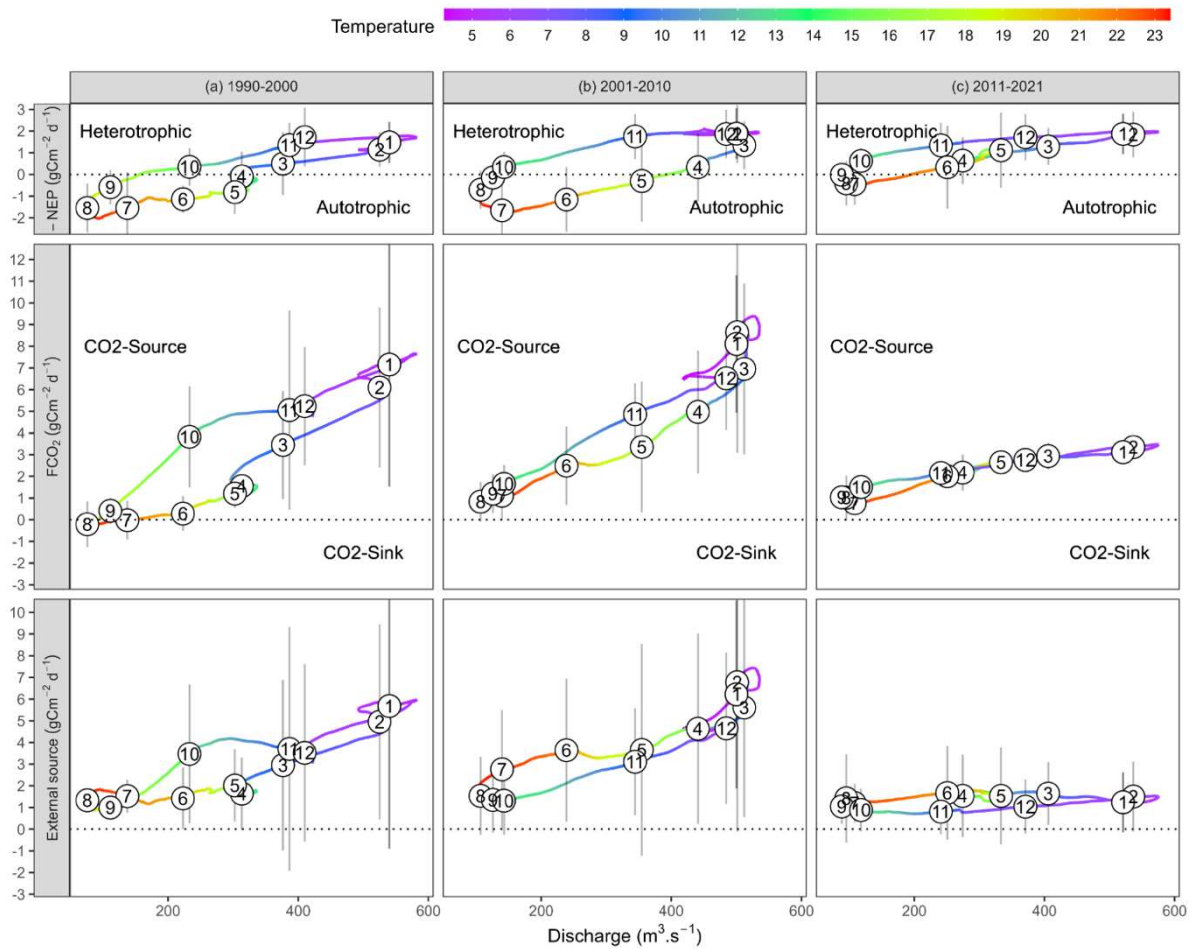
408 Figure 44. Hysteresis loops of –NEP, FCO$_2$, and external sources (FCO$_2$ + NEP) during the hydrological
409 cycle in each decade 1990-2000, 2001-2010, and 2011-2021. The color lines are the daily average fluxes
410 in each decade. The circle shape with numbers is the monthly average and standard deviation fluxes in
411 each decade.

412 The discharge trajectories of –NEP, FCO$_2$, and external sources varied across the three decades

413 delineated by the change point analysis. In three decades, all hysteresis loops exhibited positive

414 relationships with discharge, except the external CO$_2$ sources in 2011–2021. FCO$_2$ hysteresis magnitude

415 at 300 m^3 s^{-1} (autumn–spring) decreased from 3.2 g C m^{-2} d^{-1} in 1990–2000 to -0.09 g C m^{-2} d^{-1} in 2011–

416 2021. The near-zero FCO$_2$ hysteresis magnitude at 300 m^3 s^{-1} in 2011–2021 (Table 2) indicates that

FCO$_2$ values at this discharge were very similar during both the rising (autumn) and falling (spring) limbs of the hydrograph. This reduction in the hysteresis loop area suggests that the relationship between FCO$_2$ and discharge became less dependent on the seasonal progression of the hydrograph in recent years, making FCO$_2$ at a given moderate discharge more predictable regardless of season. ~~The lack of FCO$_2$-discharge hysteresis 2011–2021 indicates a more predictable and linear relationship in recent years.~~ Likewise, the magnitude of –NEP hysteresis at 300 m^3 s^{-1} was weakest in recent years (0.68 g C m^{-2} d^{-1}), but unlike FCO$_2$, it exhibited a peak (2.12 g C m^{-2} d^{-1}) in 2001–2010 (Table 2).

The internal source contribution of FCO$_2$ (–NEP/FCO$_2$) at 300 m^{3}s^{-1} between spring and autumn had contrasting ratios, with a positive CO$_2$ contribution in autumn (14 – 34%) but a negative contribution in spring (-26%, i.e., CO$_2$ consumption) in 1990-2000 and 2001-2010 (Table 2). In 2011-2021, internal source contributions of FCO$_2$ in autumn and spring were both positive, 64% and 34%, respectively.

Table 2. The mean ± standard deviation fluxes of daily –NEP, FCO$_2$, external CO$_2$, and –NEP/FCO$_2$ in spring and autumn at the mean river discharge of 300 ± 30 (m^3 s^{-1}).

	Flux*	1990–2000	2001–2010	2011–2021
River metabolism (g C m^{-2} d^{-1})	–NEP$_{300}$ spring	-0.28 ± 0.41	-0.69 ± 0.11	0.83 ± 0.18
	–NEP$_{300}$ autumn	0.66 ± 0.15	1.43 ± 0.13	1.5 ± 0.06
	–NEP$_{300}$ hysteresis	0.94 ± 0.43	2.12 ± 0.17	0.68 ± 0.18
Total CO$_2$ fluxes (g C m^{-2} d^{-1})	FCO$_{2\ 300}$ spring	1.55 ± 0.44	2.65 ± 0.15	2.42 ± 0.12
	FCO$_{2\ 300}$ autumn	4.77 ± 0.14	4.15 ± 0.25	2.34 ± 0.08
	FCO$_{2\ 300}$ hysteresis	3.22 ± 0.47	1.5 ± 0.29	-0.09 ± 0.14
External CO$_2$ flux (g C m^{-2} d^{-1})	(FCO$_{2\ 300}$+ NEP$_{300}$) spring	1.83 ± 0.2	3.34 ± 0.05	1.59 ± 0.14
	(FCO$_{2\ 300}$+NEP$_{300}$) autumn	4.12 ± 0.05	2.72 ± 0.12	0.83 ± 0.05
	(FCO$_{2\ 300}$+NEP$_{300}$) hysteresis	2.29 ± 0.2*	-0.62 ± 0.13**	-0.76 ± 0.15
–NEP/FCO$_2$ (%)	–NEP/FCO$_{2\ 300}$ spring	-26 ± 33%	-26 ± 5%	34 ± 6%
	–NEP/FCO$_{2\ 300}$ autumn	14 ± 3%	34 ± 1%	64 ± 1%
	–NEP/FCO$_{2\ 300}$ hysteresis	40 ± 34%	61 ± 5%	30 ± 6%

* The hysteresis flux is equal to the difference of flux in autumn and spring, i.e., 2.29 = 4.12–1.83, where the 300 subscript refers to the fact that these measurements are averages from mean discharge at 300 m^3 s^{-1}.
** Negative hysteresis flux indicates lower flux in autumn (rising waters stage), i.e., -0.62 = 2.72–3.34

4. Discussion

Our data analysis reveals important long-term changes in carbon fluxes of the Loire River. Re-oligotrophication led to an increase in the contribution of internal source ~~contribution~~ of FCO$_2$,

supporting our hypothesis but for reasons that ran counter to our predictions. Indeed, under oligotrophic conditions and macrophyte dominance, $-NEP/FCO_2$ increased by fourfold overall under the heterotrophic-source state, with $-NEP$ contributing up to 75% of FCO_2 at the monitoring station during the last decade (Figure 3). However, this change was largely due to decreases in total FCO_2 rather than an increase in the magnitude of $-NEP$. Instead, decreases in FCO_2 appeared to be due to an approximate halving of external CO_2 sources (Figure 5). Still, the timing of FCO_2 shifts, as detected by our change point analysis (ca. 2000 and 2010), broadly corresponded to our predictions based on previous studies (i.e., 2005 for trophic state change and 2012 for metabolism change), suggesting similar drivers of external and internal CO_2. Finally, we observed clear support for our prediction of weaker discharge controls on FCO_2 and $-NEP/FCO_2$ based on hysteresis analysis. However, this appeared to be most strongly due to a weakened discharge-external CO_2 source link rather than a weakened discharge-internal CO_2 source link.

4.1. Trophlux states and their contribution to CO_2 emissions

Large river systems function predominately as a source of CO_2 to the atmosphere (Battin et al., 2023; Butman & Raymond, 2011; Cole et al., 2007; Raymond et al., 2013; Abril and Borges 2019), and CO_2 sink states are rarely observed, even in large eutrophic rivers (Raymond et al., 1997). However, our unique dataset revealed the commonality of CO_2 sink behavior in the Loire River and further highlighted the seasonal transitions among all four possible trophlux states and how these transitions varied annually and across decades (Figure 1, Figure 4). This finding challenges the conventional understanding of large rivers as persistent CO_2 sources and demonstrates how ecosystem metabolism can fundamentally alter carbon cycling patterns. The frequency of CO_2 sink conditions in the Loire River reveals an important but often overlooked aspect of river carbon budgets that may be significant for other large temperate systems undergoing similar environmental changes. The transitions among these trophlux states are influenced by seasonal climatic drivers (temperature, solar radiation, discharge patterns, which themselves are subject to long-term climate change) and broader environmental changes like nutrient loading (e.g., re-oligotrophication) or external factors such as groundwater, making such long-term analyses critical for systems undergoing similar pressures.

We found that, regardless of the long-term trophic ~~or metabolic~~ regime, the heterotrophic/source state was the most prevalent (47–66% of time), while the autotrophic-source state occurred for approximately a quarter of the year (17–26% of time) (Figure 5). By contrast, the mean annual occurrence of the autotrophic-sink state depended strongly on the trophic ~~and metabolic regime~~conditions of the river, decreasing from $28.7 \pm 7.0\%$ of days in the eutrophic 1990-2000 period to $7.3 \pm 5.7\%$ in the oligotrophic 2011-2021 period ~~(7–29% of the time), with its decreasing decadal occurrence mirrored by the increasing decadal occurrence of the heterotrophic-source state~~ (~~Figure 5~~Table 1). This shift in trophlux state dominance reflects the ecosystem's response to re-oligotrophication ~~, where reduced nutrient availability has altered the balance between autotrophy and heterotrophy~~ (Diamond et al., 2022). Reduced nutrient availability, particularly phosphorus, directly restrained GPP more substantially than ER because ER is supported by both autochthonous organic matter (linked to GPP) and allochthonous inputs from the catchment. The declining prevalence of autotrophic-sink conditions indicates that the river's capacity to sequester atmospheric CO_2 has diminished with the transition from phytoplankton to macrophyte dominance. This demonstrates how long-term changes in trophic status can fundamentally alter carbon dynamics beyond simple changes in productivity rates.
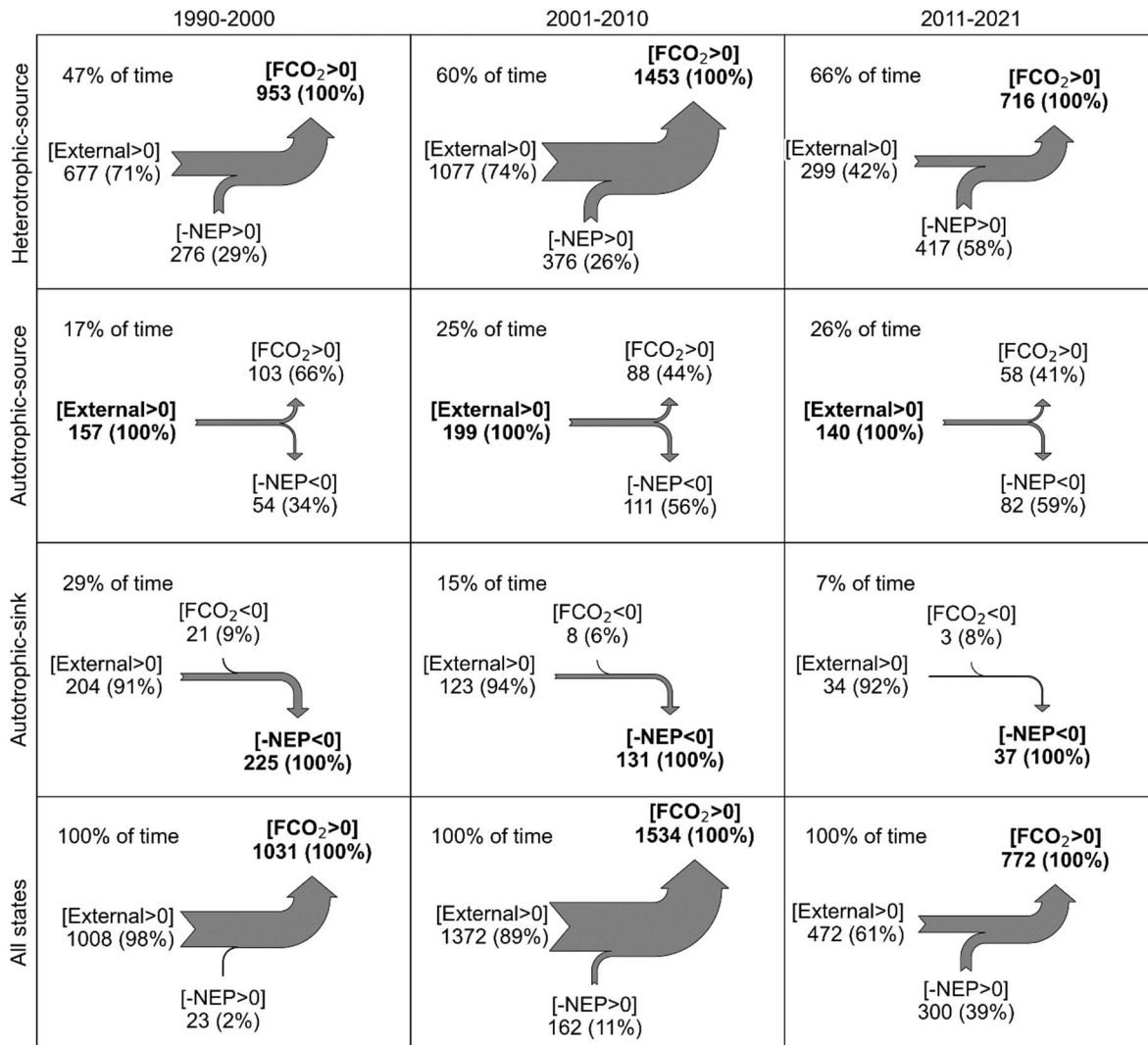
Figure 55. Annual CO₂ budget in three main trophlux states in 1990–2000, 2001–2010, and 2011–2021. All flux values are expressed in units of gC m^{-2} y^{-1}. The notation [FCO₂ > 0] denotes CO₂ emissions from rivers to the atmosphere, whereas [FCO₂ < 0] signifies CO₂ ingassing. The percentages in parentheses represent the proportion of each flux component, with the percentage calculated relative to the maximum flux component (shown in black bold).

4.2. Changes in CO₂ sources in relation to hydrology and re-oligotrophication

This work ~~adds an important data point~~ provides a significant long-term perspective to our understanding

of the contribution of internal and external sources to FCO₂ in large rivers. Despite this decades-old

research question (Cole et al., 2001), the capacity to ~~rigorously~~ quantify the relative strength of these

two fluxes is relatively recent (Bernal et al., 2022; Hotchkiss et al., 2015; Kirk & Cohen, 2023), and

data in mid-sized and large rivers are still limited. Utilizing a dataset comprising ~~5~~ five rivers with mean

discharge >100 m^3 s^{-1}, Hotchkiss et al. (2015) estimated an NEP of -0.51 to -1.01 g C m^{-2} d^{-1} and –

NEP/FCO₂ of 25% to 54%. More recently, Solano et al. (2023) highlighted the vast range of this

contribution, with values spanning from less than 10% to over 100%. Our results in the Loire River, which show strong seasonal variability in this metric, align with this broader context. This reinforces that within a single large river system, the contribution of internal metabolism to FCO_2 can be highly dynamic, covering much of the spectrum reported across diverse global systems. generally align with this range but further reveal that within a single river during a specific season (such as autumn or winter), the entire spectrum of these values can be observed.

While the magnitude of discharge is a known control discharge is known to exert an influence on CO_2 dynamics, our results highlight that the seasonal timing and the rising or falling limb of the hydrograph are equally crucial for determining CO_2 fluxes and sources, due to hysteresis effects we showed that the temporal evolution of discharge is equally important to its magnitude. Depending on the season, our results caution that measurements at the same discharge may yield contrasting estimates of the internal source contribution (Table 2, Figure 4). This difference was mainly explained by the difference in NEP magnitude and not by differences in FCO_2. For example, at the same mean discharge, NEP in autumn during the rising stage was more negative, and the river was more heterotrophic than in spring during the falling stage. This difference was only partly explained by differences in daily temperature between the two seasons (R^2=0.29, Supplementary Figure S7D1). First autumn floods are known to mobilize labile organic matter in temperate rivers, whose drying river beds in summer accumulate plant litter from riparian vegetation (Coynel et al., 2005; Etcheber et al., 2007). In the Middle Loire, the emergence of large, fertile riverbanks during the summer dry season may lead to organic matter deposition that is easily remobilized in autumn. Indeed, Minaudo et al. (2015) observed that the heterotrophy in the Middle Loire in autumn was strongly stimulated by a larger availability of biodegradable organic matter compared to spring. Such a seasonal hydrology-driven variability in river heterotrophy and associated CO_2 dynamics was also recently observed by Young et al. ((2025)) in the Upper Clark Fork River, USA. They reported pronounced seasonal variation in FCO_2 primarily linked to snowmelt-driven hydrological events mobilizing terrestrial carbon sources, reinforcing our observations that river CO_2 dynamics are strongly shaped by seasonal hydrological connectivity and terrestrial organic matter inputs.

515 Notably, Figure 4 reveals decadal changes in the magnitude of these hysteresis patterns. The FCO2

516 hysteresis magnitude at 300 m^3 s^{-1} decreased dramatically from 3.2 g C m^{-2} d^{-1} in 1990–2000 to -0.09

517 gC m^{-2} d^{-1} in 2011–2021, indicating a weakening discharge-FCO_2 relationship in recent years. Similarly,

518 external source hysteresis (bottom row, Figure 4) has flattened considerably in 2011-2021, suggesting

519 diminished influence of terrestrial carbon inputs on seasonal CO_2 dynamics. As these insights would

520 have been invisible without a high-frequency long-term dataset (Figure 1), we, therefore, encourage

521 future efforts to capture seasonality and varying discharges in the measurement campaigns.

522 During the 1990–2000 decade, the Loire River acted as a CO_2 sink had an annual CO_2 sink for almost

523 half the years due to high rates of GPP. The occurrence of this state has gradually declined over the three

524 decades (Table 1), highlighting an important environmental trade-off where improved water quality

525 from re-oligotrophication has diminished the river's capacity to act as a CO_2 sink. In 1990–2000, the

526 biogeochemical dynamics of the Loire River during the summer months coincided with long water

527 residence times, shallow waters, low discharge, high water temperature, and high eutrophication (>200

528 µg chlorophyll-a L^{-1}) (Moatar et al., 1999, 2001). These conditions were similar to eutrophic lakes,

529 which regularly act as CO_2 sinks (Bogard & Del Giorgio, 2016; He et al., 2022). In addition, autotrophy

530 can exert a stronger control on CO_2 dynamics in larger rivers compared to small streams. This is due to

531 factors such as increased light penetration across wider channels supporting higher areal GPP, and a

532 larger water volume where internal metabolic signals may be less rapidly overwhelmed by the

533 proportional influence of external CO_2 inputs from groundwater or riparian zones large river autotrophs

534 benefit from increased light penetration due to their greater width and from being less affected by

535 external CO_2 sources (Hotchkiss et al., 2015). Our data show that in the Loire, the long-term shift from

536 phytoplankton to macrophyte-dominance in 2005 has resulted in a decrease in NEP and greater

537 heterotrophy. Diamond et al. (2021) (2021) showed that the changes in stream metabolism in the Loire

538 River in 2010–2012 were related to the shift of other state variables in 2005 (turbidity, nutrient

539 concentrations, Corbicula fluminea densities, and chlorophyll-a), suggesting a decade lag for

540 metabolism shift. Moreover, while annual water temperature increased (+0.18°C per decade, +5.7°C

541 over 32 years) and annual river discharge decreased (-4% per decade, -13% over 32 years) (Figure 3,

542   Table D1), these hydroclimatic trends did not show a direct, strong correlation with the timing or

543   magnitude of these decadal metabolic shifts (Figure D2)~~the increase in annual water temperature and~~

544   ~~decrease in annual river discharge have no direct relationship with these metabolic shifts (Figure S8)~~,

545   suggesting that their manifestation on the magnitude of NEP is insignificant.

4.3. Long-term changes in the external CO$_2$ source

547   Contrary to our expectations, we observed a decreasing trend of FCO$_2$ attributable to an over 50%

548   reduction in external CO$_2$ sources in the Loire River. At first glance, this may appear to be due to overall

549   reductions in discharge and the magnitude of lateral CO$_2$ transport from groundwater and wetlands to

550   the river (Abril & Borges, 2019). While our data show a modest long-term decline in total river discharge

551   (~13% over 32 years), this alone is insufficient to explain the large reduction in external CO$_2$ inputs

552   (Figures D1 & D2). ~~However~~Besides, ~~this~~ the linkage between external CO$_2$ and river discharge is more

553   consistent with the seasonal variation (Figure 4, Figure ~~S7~~D1) rather than the inter-annual variation

554   (Figure ~~S8~~D2). In addition, while the discharge can explain ca. 37-48% of the decay in FCO$_2$ ~~(Figures~~

555   ~~S7 and S8)~~, it only explains ca. 19~~-2~~6% of the variation in external CO$_2$ source magnitude (Figures D1

556   and D2). Similarly, in a forested sandy watershed, Deirmendjian et al. (2018) reported that the export of

557   CO$_2$ flux from groundwater to the stream was independent of stream discharge and relatively constant

558   seasonally. This can be explained by the fact that higher discharge periods in these systems are

559   associated with low dissolved CO$_2$ groundwater concentrations and vice-versa. Still, to explain the >500

560   g C m^{-2} y^{-1} reduction in external CO$_2$ between 2001-2010 and 2011-2021, it seems clear that some

561   reduction in groundwater CO$_2$ is occurring. This decrease in external inputs must be driven by either a

562   decrease in the volume of contributing groundwater or a decrease in the CO$_2$ concentration of that

563   groundwater, or a combination of both.

564   In regions with carbonate bedrock, weathering of carbonate minerals can significantly contribute to the

565   CO$_2$ flux through the production of alkalinity (Vihermaa et al., 2014). Although this weathering reaction

566   does not directly release CO$_2$, it provides bicarbonate ions (HCO$_3^-$), which can equilibrate with CO$_2$ and

567   subsequently degas under certain conditions, influencing the CO$_2$ flux observed in groundwater and

568   rivers. Additionally, the transfer of CO$_2$ to groundwater depends on the spatiotemporal connections

between zones of maximal soil respiration and their intersection with the water table (Tsypin & Macpherson, 2012). If the water table remains disconnected from the topsoil where respiration is strongest, the transfer of soil CO_2 to groundwater becomes limited. Trend analysis of the groundwater table in France over the past 30 years shows low-frequency variations of multi-annual (~7 years) and decadal (~17 years) cycles in groundwater level (Baulon et al., 2022). Further evidence from a representative local borehole at Montifault (20 km from our site) shows a clearly decreasing trend in the piezometric level since 2003 (Appendix D, Figure D3). This regional decrease in groundwater levels supports a reduction in groundwater discharge to the river. ~~The groundwater table trend may explain the decay of annual external FCO_2 in the Loire River (Figure S9), although the spatiotemporal distribution of surface water and groundwater connections should be more deeply investigated to reach this conclusion.~~

To further explore the potential drivers behind the inferred long-term decrease in external CO_2 inputs, we analyzed available data of pH and TA during 1990-2021 from several groundwater monitoring stations situated in aquifers hydraulically connected to our study site. This analysis revealed a long-term increasing trend in groundwater pH, particularly after 2008, while groundwater TA remained relatively stable (Figure D4). At stable alkalinity, an increase in pH directly corresponds to a decrease in pCO_2. This inferred decline in groundwater pCO_2 provides a strong, complementary mechanism explaining the observed reduction in external CO_2 inputs to the river. Given the relative stability of in-river TA over the study period (Figure 2), it is likely that these shifts in the carbonate system are driven by changes in CO_2 supply rather than major changes in catchment-scale weathering rates. ~~Still, we can observe that peaks in groundwater level tend to lead to peaks in external CO_2 by approximately 3 years (Figure S9).~~ In addition, a study at a site located 20 km downstream from our study area in the Val ~~d'Orléans~~ d'Orléans fluviokarst aquifer reported that dissolved inorganic carbon flux from groundwater has decreased by about 20% along with the decrease of groundwater level between 2000 and 2020 (Binet et al., 2022). ~~In addition,~~ Binet et al.~~,~~ (2022) also assessed that there was no significant change in the carbonate weathering rate at this aquifer, which is similar to the relatively stable alkalinity at the Loire River (Figure 2). Together, the evidence for both reduced groundwater discharge and lower groundwater

pCO$_2$ provides a robust explanation for the observed multidecadal decline in external CO$_2$ sources to the Loire River ~~These observations suggest a need for future efforts to focus on surface water-groundwater connections as they relate to river hydrology and carbon supply~~.

~~5.~~

~~6.~~5.   Conclusions

In the middle Loire River, three main trophlux states alternately occur in the hydrological year cycle, predominated by the heterotrophic-source state. The heterotrophic-source state contributes more than 90% of annual CO$_2$ emissions, with an average of 40% from internal contribution (–NEP). Besides, in the 1990s, the autotrophic-sink state was still common; however, this state has gradually disappeared in recent years with the decline of phytoplankton, replaced by the dominance of macrophytes. Our analysis of seasonal hysteresis of NEP and CO$_2$ fluxes in relation to discharge indicates stronger heterotrophy in autumn during rising waters than in spring during the falling waters, and this is ~~a part~~partly explained by river temperature but more likely due to the remobilization of organic matter in floodplains and secondary channels during the first floods.

We report a strong long-term decrease in CO$_2$ fluxes (-62% over the 32 years) ~~but also~~and an increase in the contribution of heterotrophy (–NEP) to this CO$_2$ outgassing flux. While our study infers changes in external CO$_2$ sources, a full understanding of carbon transfer at the groundwater-river interface requires ~~Although we can call for~~ more DIC data from groundwaters and riparian zones~~acquisition in groundwaters, we must confess that the current dataset is far from sufficient to understand the transfer of carbon at the groundwater-river interface~~ (Deirmendjian & Abril, 2018; Duvert et al., 2018). Future work should focus on obtaining such data to quantify these fluxes better. ~~and therefore, future works are needed.~~ We also suggest that developing approaches to extrapolate findings from such detailed site studies across diverse river networks, integrating them with spatial hydrological and ecological data, will be key to better understanding and predicting how global changes will influence the balance between internal and external CO$_2$ production at broader scales, ultimately refining estimates of the role of rivers in the global carbon budget.~~We also suggest that new exploration of these types of datasets on large rivers and their extrapolation on river networks may help to understand better and predict the~~

623 ~~influence of global change on the balance between internal and external CO_2 production in the context~~

624 ~~of the global carbon budget.~~

Appendix A: Dataset integrity and validation

This appendix provides detailed information on the data acquisition, quality assurance/control (QA/QC) framework, and processing procedures used to generate the 32-year high-frequency dataset.

A1. Data acquisition and QA/QC framework

The dataset combines high-frequency continuous monitoring data from Électricité de France (EDF) with lower-frequency grab sample data from both EDF and the Loire-Brittany Water Agency (AELB).

The continuous measurement system of EDF is a floating platform with a temperature sensor and sensors for pH (range 0–14 pH unit), DO (range 0–20 mg L^{-1}), and conductivity (range 0–1000 μS cm^{-1}) (Campbell 1 ®). The surface water at 20 cm depth is pumped (ca. 0.5 L s^{-1}) through the system and measurements are recorded every 5 seconds, with average values saved every hour. It should be noted that data was collected both upstream and downstream of the nuclear power plant, with the upstream station located at the entrance of the dam and the downstream station located approximately 2-5km downstream of the dam. The data used for data analysis in this study was from the upstream station because of its data completeness. Grab sampling data was collected by EDF and Loire-Brittany Water Agency (AELB), including pH, conductivity, and TA in 1990-2021, with frequency ranging from daily to monthly. Grab sampling data exists only upstream of the nuclear power plant. While AELB provided data for the period of 1990 to 2003 for these parameters, EDF supplied data from 2007 to 2021.

EDF's environmental monitoring operates under mandatory oversight from ASN (Autorité de Sûreté Nucléaire), France's nuclear safety authority, with QA/QC protocols documented for two main periods. Prior to 2008, measurements were made with membrane sensors and validated using a multi-level quality control methodology that included routine calibrations and automated checks (Moatar et al., 2001), achieving an accuracy of approximately ±0.3 pH units and ±8% for DO. In 2008, the sensor technology was upgraded to optical sensors, and since 2009, all procedures have complied with ISO 17025:2005 standards, requiring documented calibration with certified reference standards and regular external audits.

We cross-validate the pH data from EDF with independent Water Agency grab samples (www.naiades.eaufrance.fr). The cross-validation confirms measurement continuity across the sensor transition, showing improved post-2008 agreement (pH residuals: -0.17±0.35 to -0.10±0.32 pH units) while preserving statistically significant long-term trends (**Figure A1**). Post-2008 optical sensors indicate fewer differences with the grab samples, but both continuous sensor data from EDF and grab sample data from the water agency are well consistent with the long-term trend. This demonstrates that

656 the sensor upgrade enhanced data quality rather than creating systematic artifacts, with the step change

657 in 2008 contributing to but not solely explaining the multidecadal trends.

658
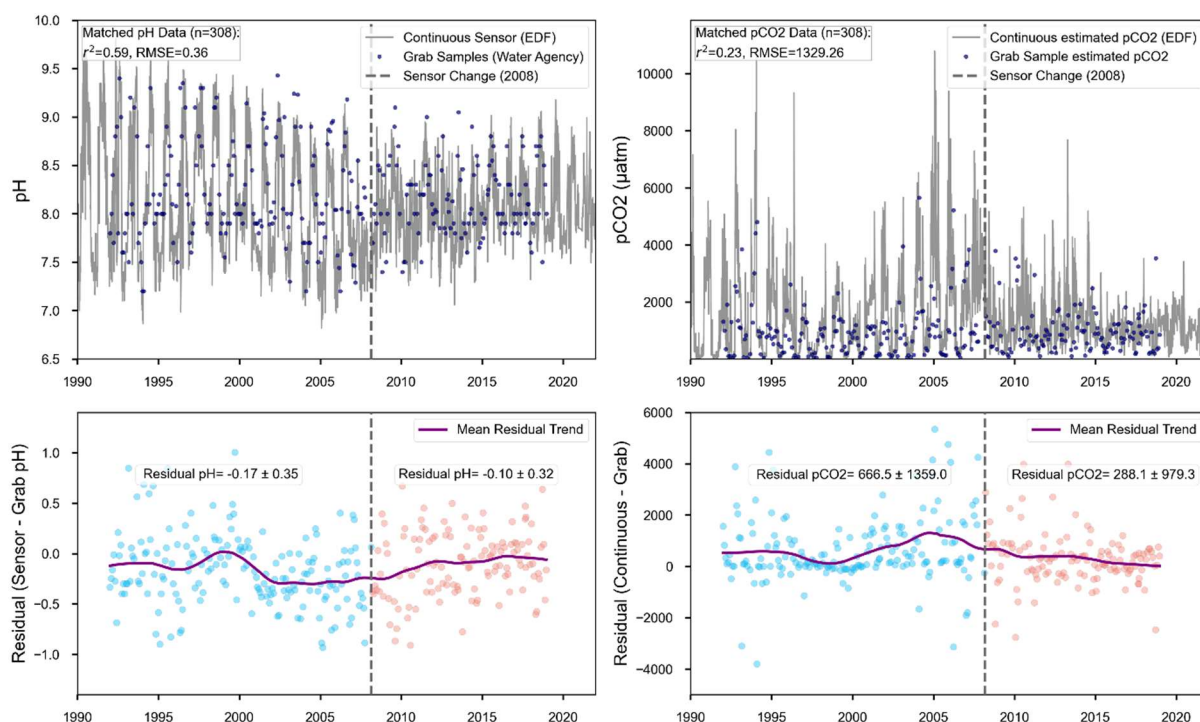
659 **Figure A1.** Comparison of continuous sensor (EDF) vs. independent grab samples from the water

660 agency for pH and estimated pCO_2 in 1990-2021. Bottom panels show residuals (Sensor - Grab) with

661 points colored pre/post sensor change in 2008, a LOWESS trend, and mean residual ± SD.

662 **A2. Data Processing and Reconstruction**

663 **Data Cleaning:** Although the sensors for pH and DO measurements were periodically calibrated by

664 EDF, the dataset still exhibited a notable number of anomalous values prior to 2008, which prompted

665 the implementation of comprehensive data control procedures. These procedures addressed sensor drift

666 and outlier removal, which were proposed by (Moatar et al., 2001). Data cleaning was conducted for the

667 hourly pH and dissolved oxygen data in this study, while the daily conductivity was carried out by EDF,

668 which was heavily based on visual inspection. Hourly temperature and alkalinity data from grab

669 sampling were only checked through a range check to eliminate unrealistic values, but there was minimal

670 significant removal of this data.

671 The following steps were carried out for the data cleaning and correction for hourly pH. Firstly,

672 performing the rules-based anomaly detection and correction as a first pass at quality control, including

673 range check (pH ranges from 6 to 10 in Loire River), data persistence check (pH relatively constant in

674 few days), significant change check (jump or drop within few hours), calibration and drift event

675 detection check. This step was performed automatically with the support of *pyhydroqc,* a Python

676 package for automating aquatic sensor data processing (A. S. Jones et al., 2022). Secondly, error

detection was manually inspected by comparing values between upstream and downstream, together with daily discharge. This step used the interactive plot with the support of *plotly* package to check the errors that were identified in previous steps. The use of daily discharge was to eliminate false detection of abnormal data, especially in the case of high discharge, where there are often sudden changes in pH and conductivity. There was 10.6% data (about 3 years of data) that was assessed as anomalous and was discarded. Finally, missing data will be completed based on several cases. Linear interpolation was applied for missing data within 6 hours (2.3% of data). Linear interpolation between upstream and downstream stations was applied for missing either upstream or downstream (7.5% of data). Linear interpolation between adjacent stations was applied when missing data in both upstream and downstream at the Dampierre station, but existed in adjacent stations (0.5% data). The remaining missing data was then filled based on the seasonal Kalman smoother, which estimates the missing values while considering the seasonal patterns and annual trend (*tsmoothie* package) (0.3% data).

The data cleaning procedure was similar for hourly DO. We first removed physically impossible values and then applied a low-pass filter to remove instrument noise in the DO signal. We then removed values that exceeded plausible hourly changes in DO (e.g., a leap from 10 to 15 mg L^{-1}) using 95% confidence intervals for hourly changes on a monthly basis as our cutoff. We finally used visual inspection to flag data of questionable validity and corrected for linear drift and anomalous drops or jumps in DO data. We then filled all remaining missing values with a seasonal Kalman filter (3% data). The data cleaning and correction for hourly DO were detailed by Diamond et al. (2025).

Alkalinity Reconstruction: As daily TA data were not available for the entire 32-year period, a continuous daily TA time series was reconstructed from the continuous daily conductivity data.

To reconstruct daily alkalinity from conductivity, we employed the *IterativeImputer* function with *BayesianRidge* estimator (i.e., regularized linear regression) by using *scikit-learn*, a Python package. The *BayesianRidge* estimator filled the missing daily alkalinity by iteratively modeling the linear relationship between daily conductivity and available alkalinity data, while regularization accounts for potential changes in their relationship over 32 years. This process begins by estimating data for the period with the fewest missing data, then continues iteratively until the imputed values converge, meaning subsequent iterations produce minimal changes in the estimates. This iterative process allows the imputer to adapt to underlying trends and shifts in the data. Besides, to verify the stability of the relationship between alkalinity and conductivity, we performed linear regressions on a 4-year period of 32 years dataset, which revealed quite similar slopes across all periods except 1990-1993 **(Figure A2)**.

$1990 - 1993, y = 121 + 5.82\,x, R^2 = 0.89, n = 32$
$1994 - 1997, y = -327 + 7.91\,x, R^2 = 0.80, n = 32$
$1998 - 2001, y = 61.7 + 6.58\,x, R^2 = 0.75, n = 32$
$2002 - 2005, y = -61.1 + 6.82\,x, R^2 = 0.80, n = 8$
$2006 - 2009, y = -114 + 6.99\,x, R^2 = 0.69, n = 439$
$2010 - 2013, y = -15 + 6.68\,x, R^2 = 0.60, n = 729$
$2014 - 2017, y = 55.5 + 6.75\,x, R^2 = 0.57, n = 858$
$2018 - 2021, y = -173 + 7.51\,x, R^2 = 0.46, n = 849$
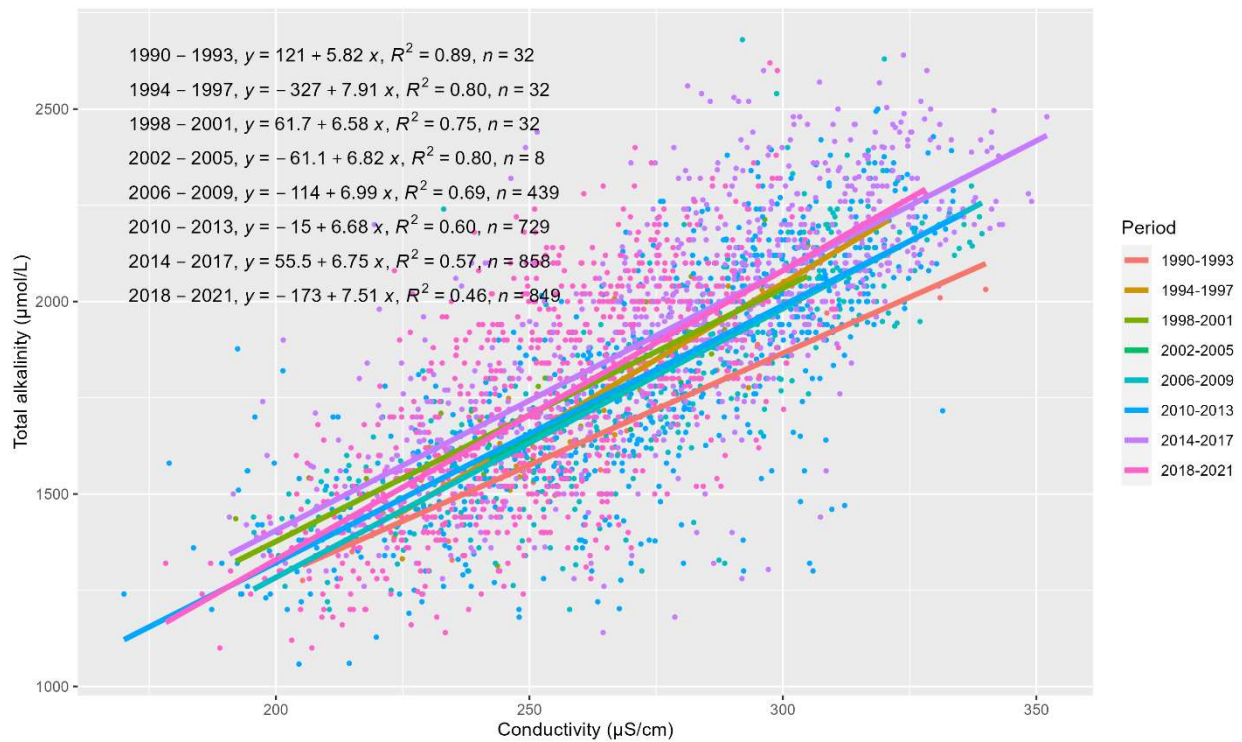
Figure A2. Relationship between measured total alkalinity and continuous measured conductivity in the Loire River.

Appendix B: Model Validation and Uncertainty

This appendix details the methods for handling model outputs, validates key model parameters, and assesses the impact of uncertainty on the final conclusions.

B1. Handling of Metabolism Model Outputs

The streamMetabolizer model can occasionally produce physically unrealistic values, such as negative GPP or positive ER. This issue typically arises when diel variations in dissolved oxygen (DO) are weak—meaning the DO levels are similar between day and night—making it difficult for the model to accurately separate the contributions of GPP and ER (Appling et al., 2018). When the diel DO signal is minimal, the GPP is likely close to zero, which can lead to the model estimating a negative median GPP value. Consequently, it is common practice to set these negative GPP estimates to zero (Blaszczak et al., 2019). In our study, rather than forcing these estimates to zero, we replaced unrealistic estimates with the 75th percentile of the modeled posterior distribution for that day. This approach avoids artificially setting values to zero while still acknowledging that the true value is likely small.

In general, this correction did not substantially alter the annual GPP or ER calculations. Replacing negative GPP with the 75th percentile increased annual GPP by an average of 1.3% (ranging from 0.1% to 5.3%), while setting negative GPP to zero resulted in a smaller increase, ranging from 0.04% to 3.4%

729 **(Figure B1).** Similarly, the annual ER calculations across different treatments for unrealistic ER values
730 show no significant differences, with an average flux variation of around 1%, except in 1995, where the
731 difference reaches 15% **(Figure B2).**

732
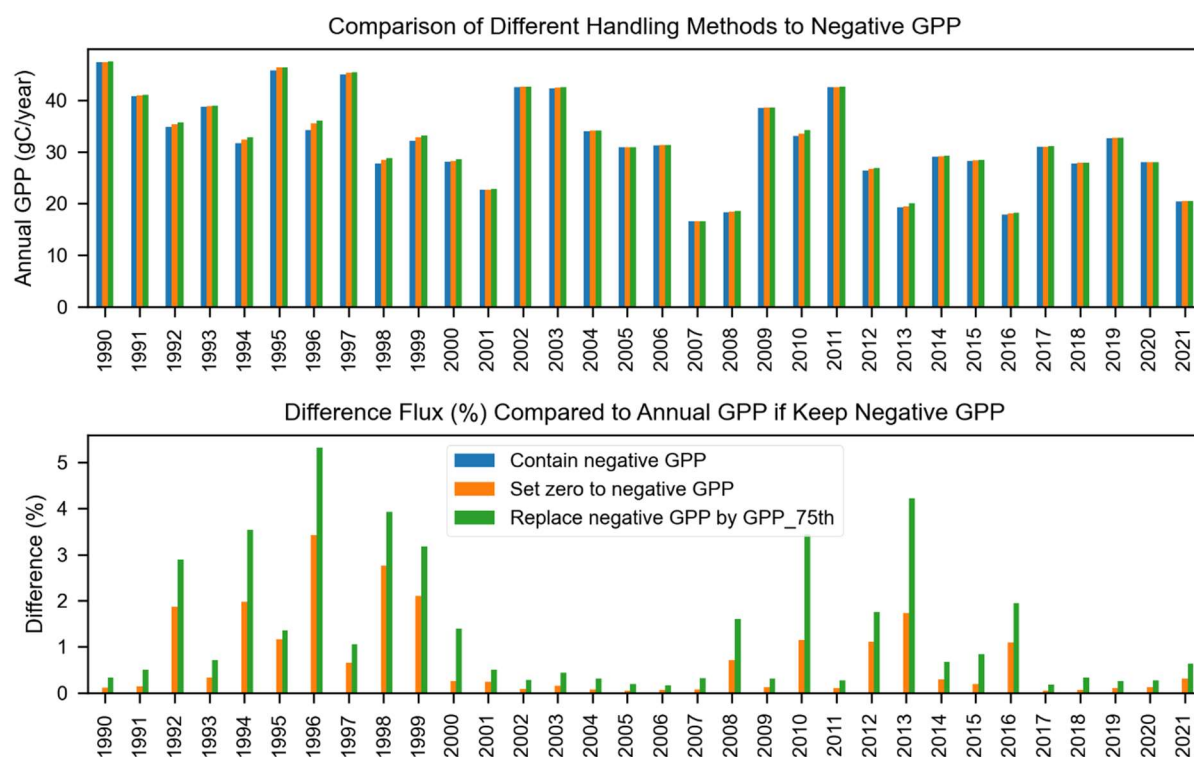
733 **Figure B1.** Comparison of annual GPP estimates based on different approaches for handling negative
734 GPP values: retaining negative GPP, setting negative GPP to zero, and replacing negative GPP with
735 the 75th percentile of estimated GPP from the *streamMetabolizer* model.
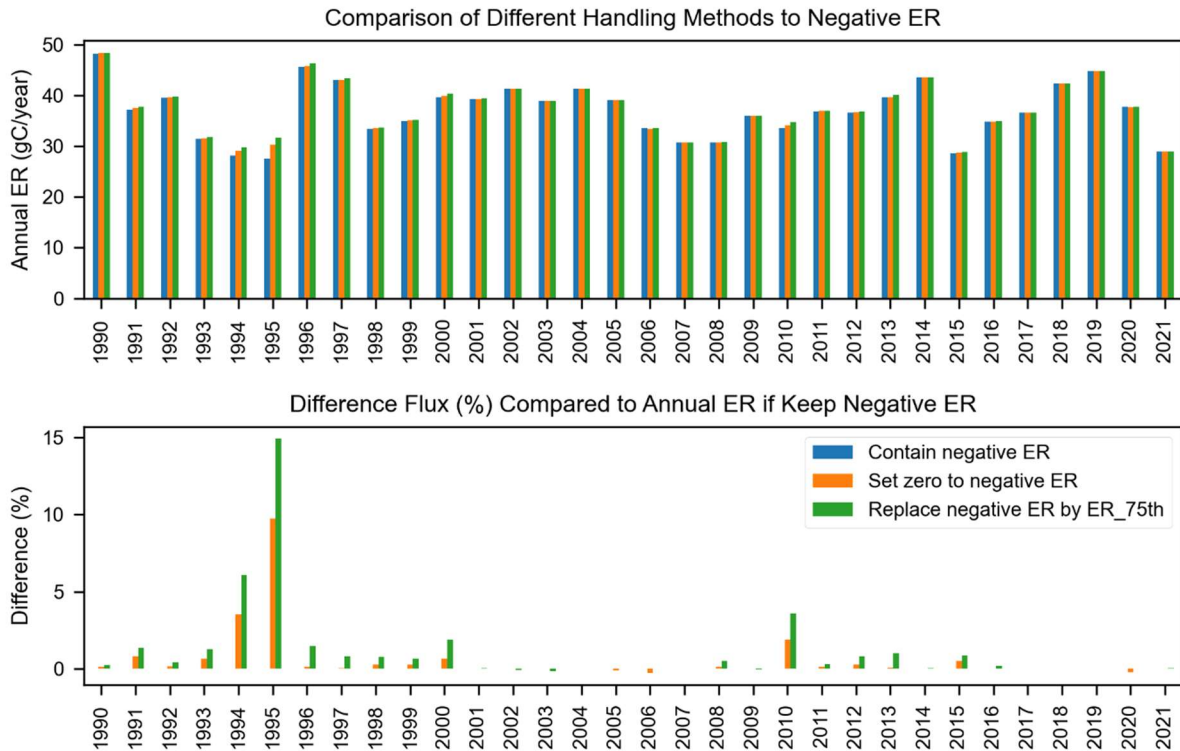
Figure B2. Comparison of annual ER estimates based on different approaches for handling negative ER values: retaining negative ER, setting negative ER to zero, and replacing negative ER with the 75th percentile of estimated ER from the *streamMetabolizer* model.

B2. Validation of the Gas exchange coefficient (k600)

The k600 values estimated by the StreamMetabolizer model were compared with the seven k600 values calculated from seven fitted equations proposed by Raymond et al. (2012b) for streams and small rivers. Both k600 estimates exhibited similar seasonal fluctuations, with the lowest values occurring in summer and the highest in winter (Figure **B3**). The comparison revealed that the mean absolute percentage error (MAPE) between the StreamMetabolizer estimates and the mean k600 from the seven fitted equations ranged from 36% to 62%. Specifically, the Raymond et al. (2012) k600 estimates tended to be higher in summer (low discharge) and lower in winter (high discharge) compared to those estimated by the StreamMetabolizer model (Figure **B4**). Such discrepancies can arise because streamMetabolizer co-estimates K600 with GPP and ER by fitting observed DO dynamics, making its estimate sensitive to the strength of the biological signal, whereas empirical equations rely solely on hydraulic proxies for turbulence. At high flow (winter), streamMetabolizer may underestimate k600 because the strong turbulence and deep water can weaken the biological signal (i.e., the daily change in dissolved oxygen), which the model relies on for its estimations. The Raymond et al. (2012) hydraulic equations, by contrast, are driven by high velocity and are less sensitive to this biological signal dampening. At low flow (summer), streamMetabolizer may estimate a higher k600 because the biological signal is very

strong and clear in the shallow, warm, and productive water. The model may attribute a larger portion of the observed oxygen change to gas exchange to best fit the data.

However, the k600 values derived from StreamMetabolizer fall within the same order of magnitude as those from the seven fitted equations (Figure **B3**). To maintain internal consistency between the metabolic and FCO_2 calculations, the k600 estimates from streamMetabolizer were used for all subsequent flux calculations.
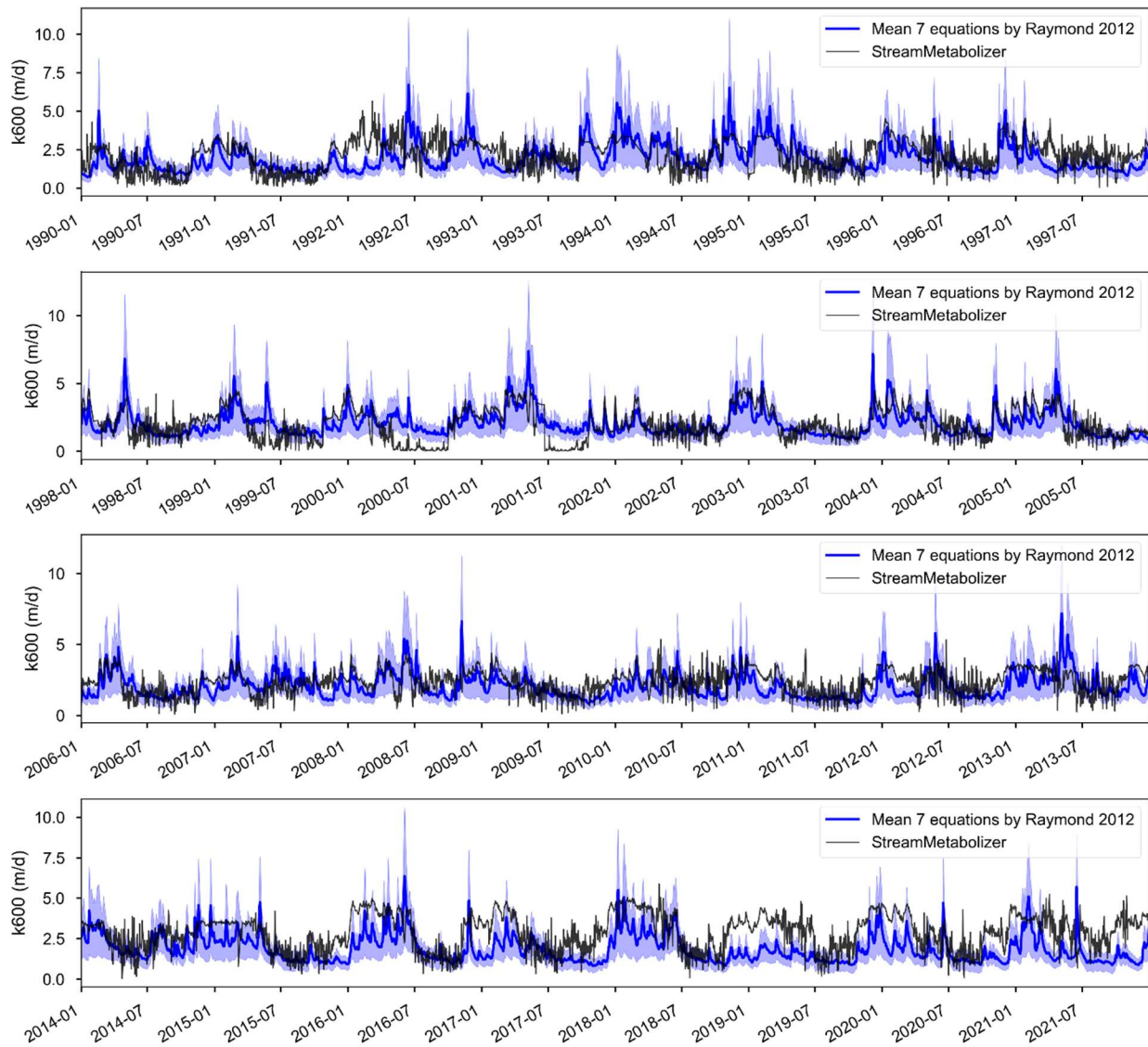
Figure B3. Comparison of the gas exchange coefficient (k600) estimated by streamMetabolizer (black line) with the mean and range (blue shaded area) of values derived from seven empirical equations from Raymond et al. (2012b).
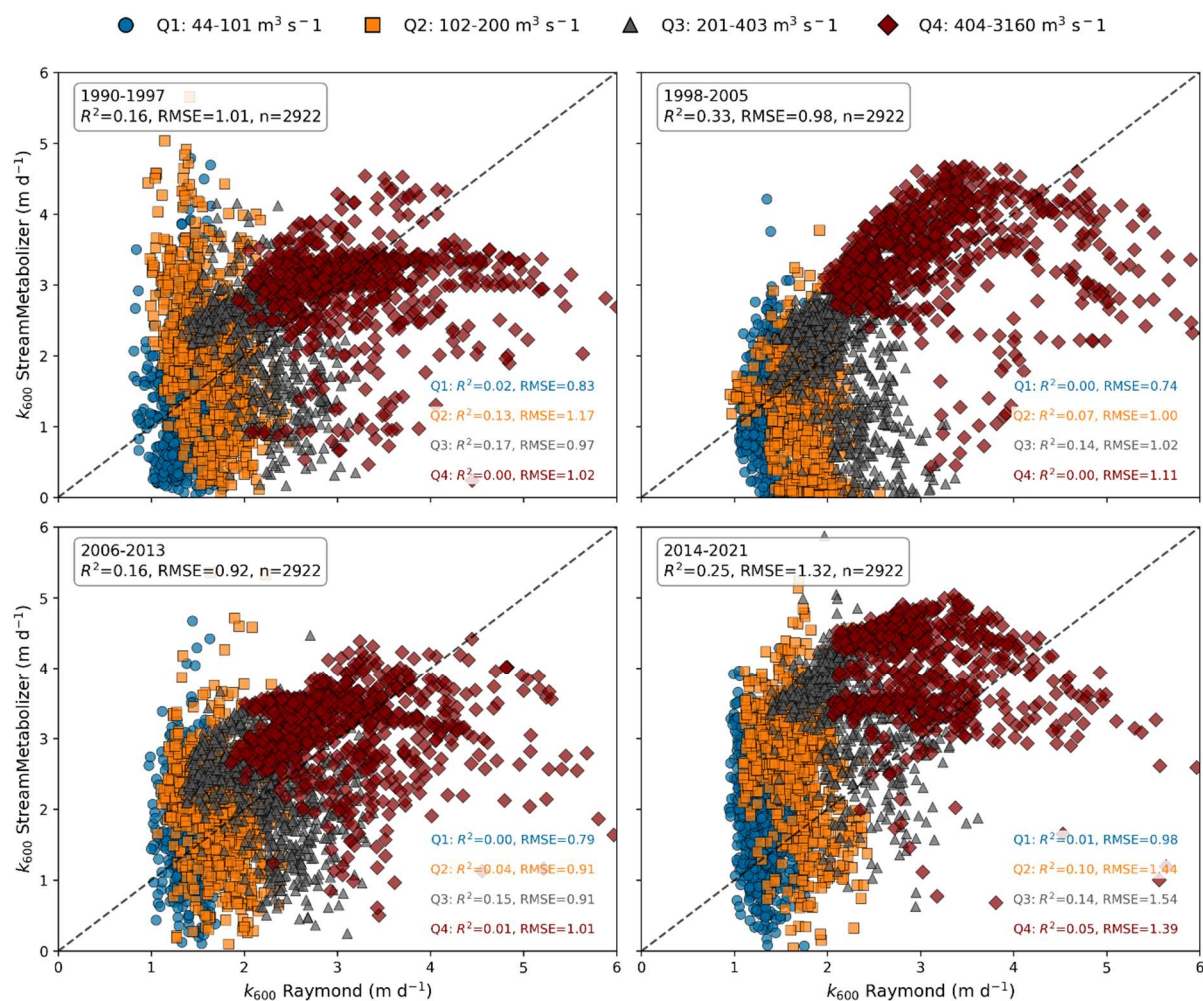
Figure B4. Compare the k600 between the mean of seven equations, Raymond et al. 2012, and StreamMetabolizer for 1990-2021. Colors indicate discharge quantiles (Q1-Q4, legend above). R^2 and RMSE are shown per discharge quantile range.

B3. Uncertainty Analysis

Estimating FCO_2 and NEP using models such as $PyCO_2SYS$ and streamMetabolizer often involves large uncertainties, particularly when considering the propagation of errors in all model input data and the summing/multiplying of these uncertainties in calculating fluxes (Battin et al., 2023; Kirk & Cohen, 2023). Estimating FCO_2 and NEP involves uncertainties from multiple sources. While a full error propagation was beyond the scope of this study, we assessed the impact of the largest source of input uncertainty: the reconstruction of daily TA, which was based on daily conductivity. The error in TA could potentially affect conclusions regarding the temporal distribution of CO_2 sink/source states throughout the year, as well as comparisons with NEP.

The average error in the reconstructed TA was ±190 µmol/L. Propagating this uncertainty through the $pyCO_2SYS$ model resulted in an uncertainty of ±11% in the final pCO_2 estimates. As shown in Table B1, this level of uncertainty did not alter the main conclusions of the study. The annual distribution of

785 trophic states remains consistent, with a maximum deviation of only 3% fluxes. Moreover, the
786 dominance of the CO_2 source–heterotrophic state throughout the year remains almost unchanged, with
787 less than a 1% difference under any range of TA uncertainty, though the magnitude of FCO_2 could vary
788 up to 602 to 841 gC m^{-2} y^{-1}.

789 **Table B1**. Impact of TA uncertainty on the occurrence and FCO_2 of each trophlux state.

| | | CO$_2$ source | | | | | | CO$_2$ sink | | | | | |
| | Period | Heterotrophic | | | Autotrophic | | | Heterotrophic | | | Autotrophic | | |
		Min	Mean	Max	Min	Mean	Max	Min	Mean	Max	Min	Mean	Max
% of days	1990-2000	47	47	48	16	17	18	8	7	7	30	29	28
	2001-2010	60	61	61	24	25	27	2	2	2	14	16	13
	2011-2021	65	66	66	25	26	28	1	1	1	9	7	6
FCO$_2$ (gC m^{-2} y^{-1}.)	1990-2000	831	954	1100	87	103	119	-5	-4	-4	-22	-21	-20
	2001-2010	1267	1454	1669	75	88	102	-1.3	-0.6	-1	-7.4	-7.8	-6.6
	2011-2021	602	717	841	49	59	71	-1.5	-0.9	-1.2	-3.4	-2.6	-2.1

790

791 **B4. Methodological considerations for the Heterotrophic-Sink State**

792 The Heterotrophic-Sink state (NEP < 0, FCO_2 < 0) represents a condition where the river is a net CO_2
793 sink from the atmosphere despite ongoing net ecosystem respiration. As discussed in the main text, we
794 primarily attribute this transient state to significant CO_2 undersaturation in the water column resulting
795 from intense prior autotrophic uptake. A recent analysis by Diamond et al. (2025) using this same dataset
796 provides strong evidence for this mechanism. They found that heterotrophic-sink events were
797 temporary, lasting an average of 4.7 ± 4.1 days, and that 76% of these events were immediately preceded
798 by an autotrophic-sink state. This confirms our interpretation that the heterotrophic-sink state is not a
799 stable condition but rather a short-lived transitionary phase as the river shifts from being an autotrophic-
800 sink to either an autotrophic-source or a heterotrophic-source state. An additional potential contributing
801 factor is the possible underestimation of GPP by the diel oxygen method. If oxygen produced within
802 dense benthic macrophyte beds does not fully mix into the water column on a diel timescale, the reach-
803 integrated GPP would be underestimated. This would result in a calculated NEP that is more negative
804 than the true value, which could contribute to the Heterotrophic-Sink state.

805 **Appendix C: Statistical Analyses of Long-Term Trends**

806 This appendix provides detailed results from the statistical analyses used to identify and quantify the
807 long-term changes discussed in the main text.

808 **C1. Change-Point Analysis**

809 We evaluated the long-term changes in FCO_2 and metabolism using a statistical change point analysis,
810 which identifies points in a time series where the statistical properties, such as the mean or variance,
811 undergo significant shifts. We first applied seasonal decomposition on daily time series to extract trend,
812 seasonal, and residual components using the *statsmodels* Python package (Seabold & Perktold, 2010).

813 The long-term trend component was analyzed using a piecewise linear regression method (model
814 ="linear" in *ruptures,* a Python package), while shift point detection by standard deviation (changes in
815 variance by model="normal" in *ruptures*) was employed for the seasonal components. This process was
816 also applied to related parameters, including daily discharge, temperature, GPP, and ER. The results of
817 this analysis (Figure C1) informed the division of the 32-year record into the three decadal periods used
818 for comparison throughout the manuscript.

819
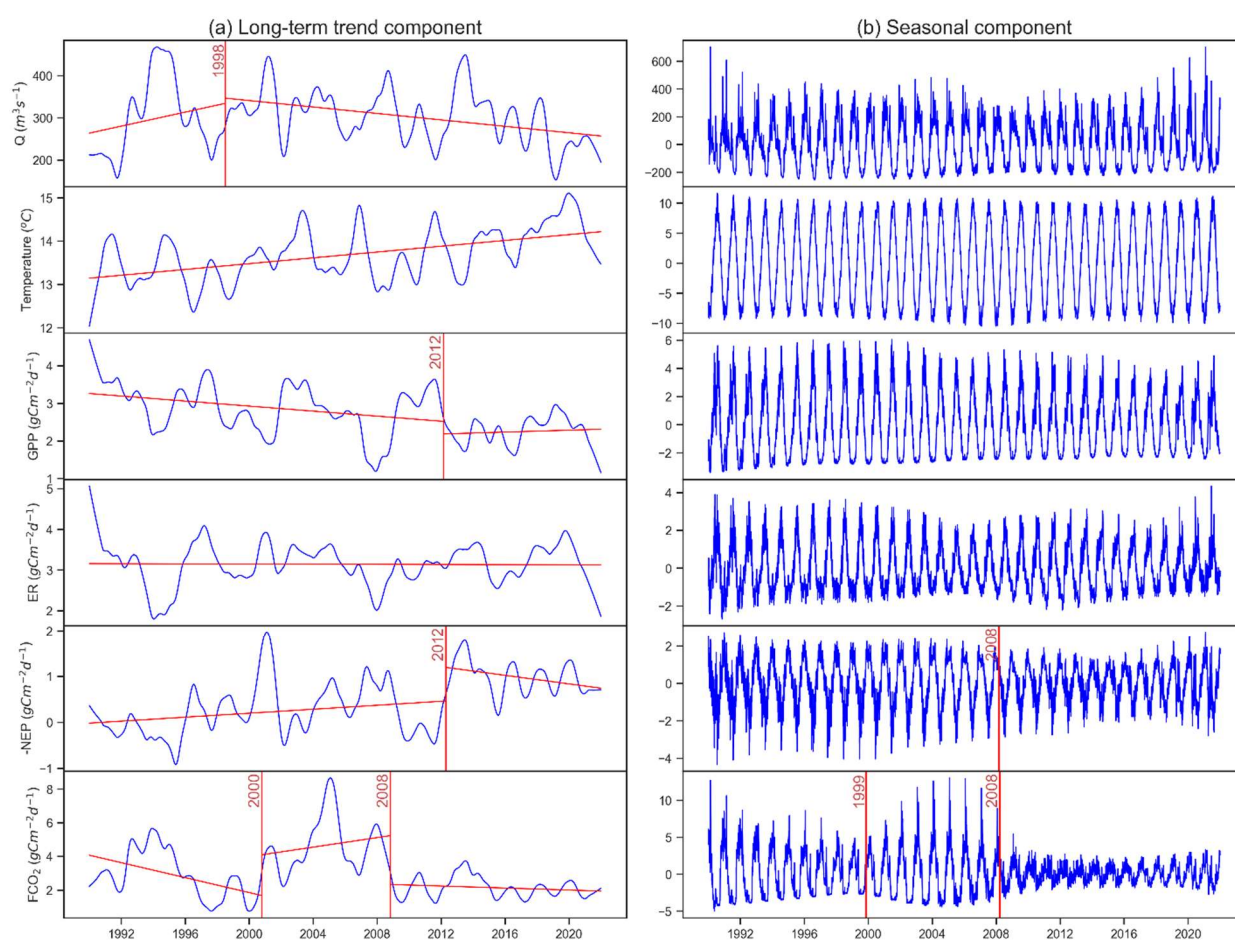
820 **Figure C1.** Change-point analysis on the decomposed time series: (a) long-term trend components and
821 (b) seasonal components of daily discharge, temperature, and fluxes of GPP, ER, -NEP, and FCO_2.
822   The red vertical lines indicate the change periods.

823 **C2. Inter-Decadal Statistical Comparisons**

824 To quantitatively assess differences between the three identified decades, we performed non-parametric
825 Kruskal-Wallis tests followed by post-hoc Mann-Whitney U tests. The results (Figure C2) provide
826 statistical validation for the observed shifts in key variables between the decadal periods.

827
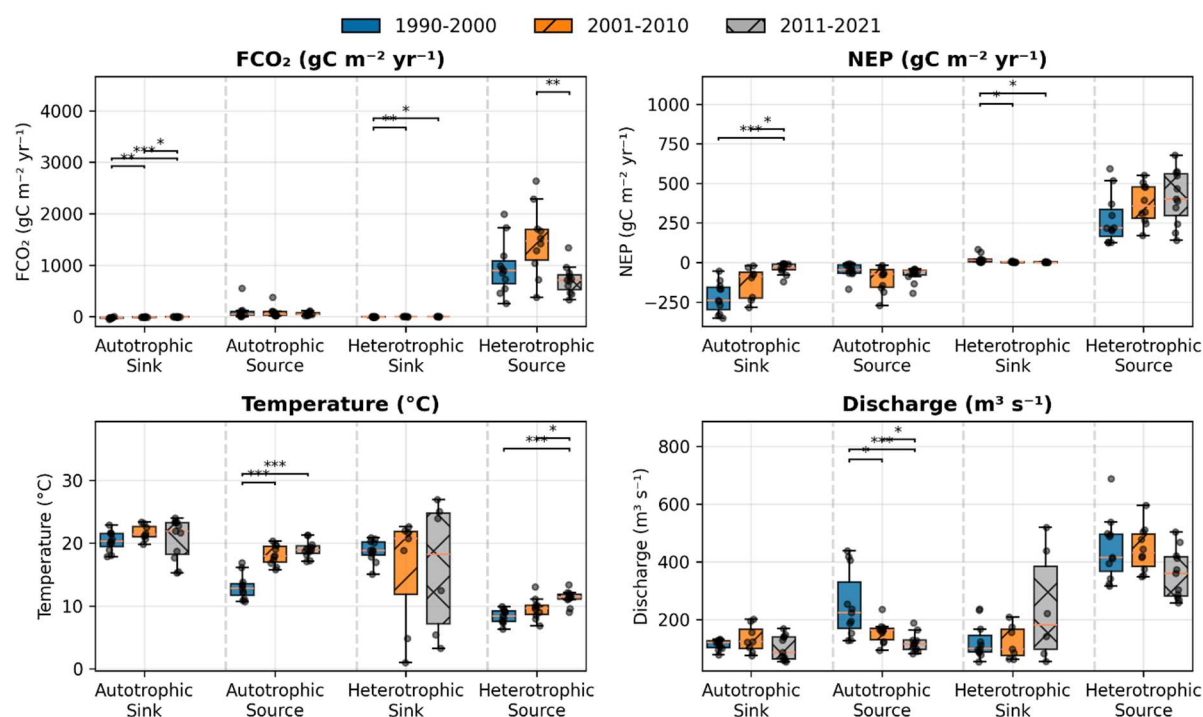
828 Figure C2. Statistical comparison of key variables across decades within each trophlux. Boxplots show
829 median (horizontal line), interquartile range (box), and distribution of annual values (black dots).
830 Colored boxes represent different decades: blue (1990-2000), purple (2001-2010), and orange (2011-
831 2021). Statistical significance of differences between decades was assessed using Kruskal-Wallis tests,
832 with significant pairwise differences (Mann-Whitney U test) indicated by horizontal bars with
833 asterisks (* $p<0.05$, ** $p<0.01$, *** $p<0.001$).

834 **Appendix D: Analysis of Hydroclimatic and External Drivers on FCO_2**

835 This appendix presents the analyses that explore the potential drivers behind the observed long-term
836 trends, particularly the decline in external CO_2 sources.

837 **Table D1.** The correlations (R^2) between annual FCO_2, -NEP, and hydroclimatic conditions
838 (discharge, temperature) in each trophlux state

Trophlux	Parameters	Days	Discharge	Temp	FCO_2	-NEP	-NEP/CO_2
Autotrophic Sink	**Days**	_	0.08	0.01	0.07	0.14	0.00
	Discharge	0.08	_	0.07	0.19	0.03	0.19
	Temp	0.01	0.07	_	0.04	0.00	0.00
	FCO_2	0.07	0.19	0.04	_	0.14	0.32
	-NEP	0.14	0.03	0.00	0.14	_	0.13
	-NEP/CO_2	0.00	0.19	0.00	0.32	0.13	_

		Days	Discharge	Temp	FCO_2	-NEP	-NEP/CO_2
Autotrophic Source	**Days**	_	0.00	0.06	0.06	0.16	0.00
	Discharge	0.00	_	0.34	0.41	0.00	0.36
	Temp	0.06	0.34	_	0.14	0.00	0.21
	FCO_2	0.06	0.41	0.14	_	0.13	0.32
	-NEP	0.16	0.00	0.00	0.13	_	0.01
	-NEP/CO_2	0.00	0.36	0.21	0.32	0.01	_
Heterotrophic Sink	**Days**	_	0.01	0.21	0.00	0.03	0.05
	Discharge	0.01	_	0.40	0.67	0.00	0.16
	Temp	0.21	0.40	_	0.40	0.10	0.90
	FCO_2	0.00	0.67	0.40	_	0.01	0.18
	-NEP	0.03	0.00	0.10	0.01	_	0.12
	-NEP/CO_2	0.05	0.16	0.90	0.18	0.12	_
Heterotrophic Source	**Days**	_	0.00	0.69	0.01	0.30	0.07
	Discharge	0.00	_	0.04	0.36	0.11	0.11
	Temp	0.69	0.04	_	0.09	0.07	0.06
	FCO_2	0.01	0.36	0.09	_	0.06	0.59
	-NEP	0.30	0.11	0.07	0.06	_	0.04
	-NEP/CO_2	0.07	0.11	0.06	0.59	0.04	_

839

840
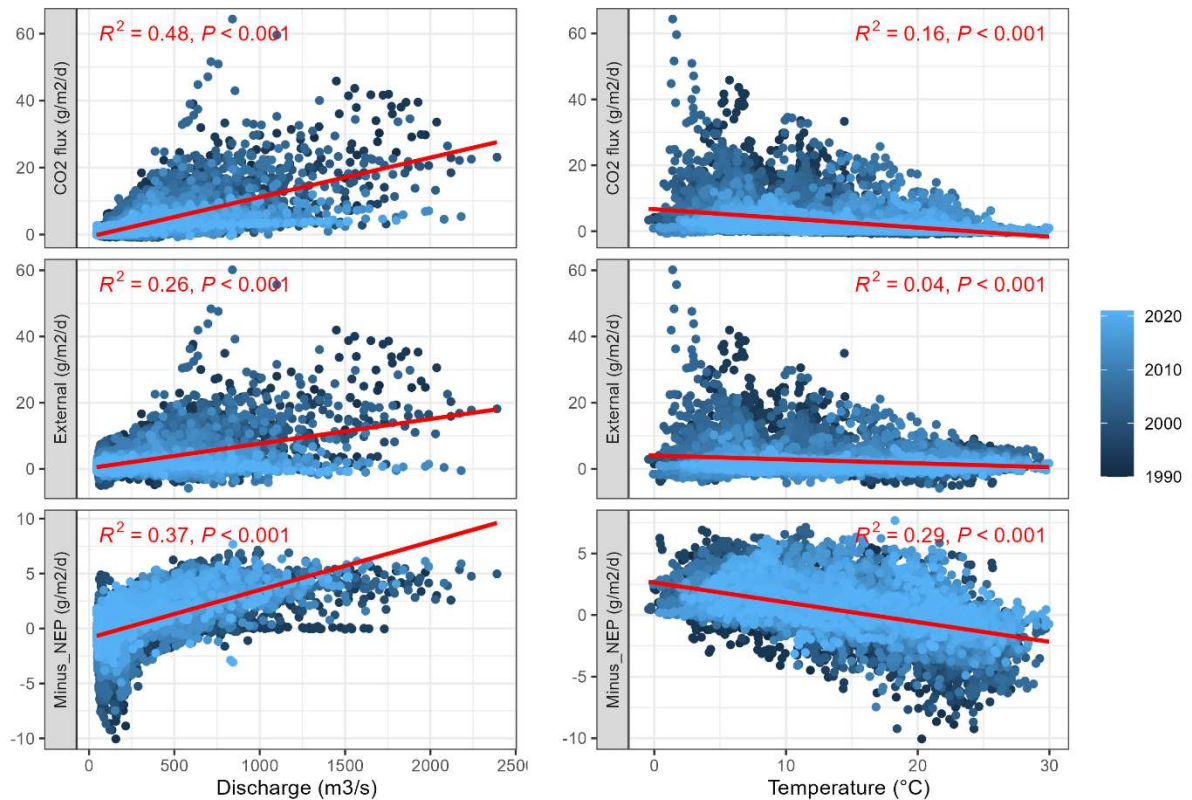
Figure D1. Relationship of daily fluxes and daily discharge or daily water temperature. Points are colored by year, as indicated by the color bar.

843

844
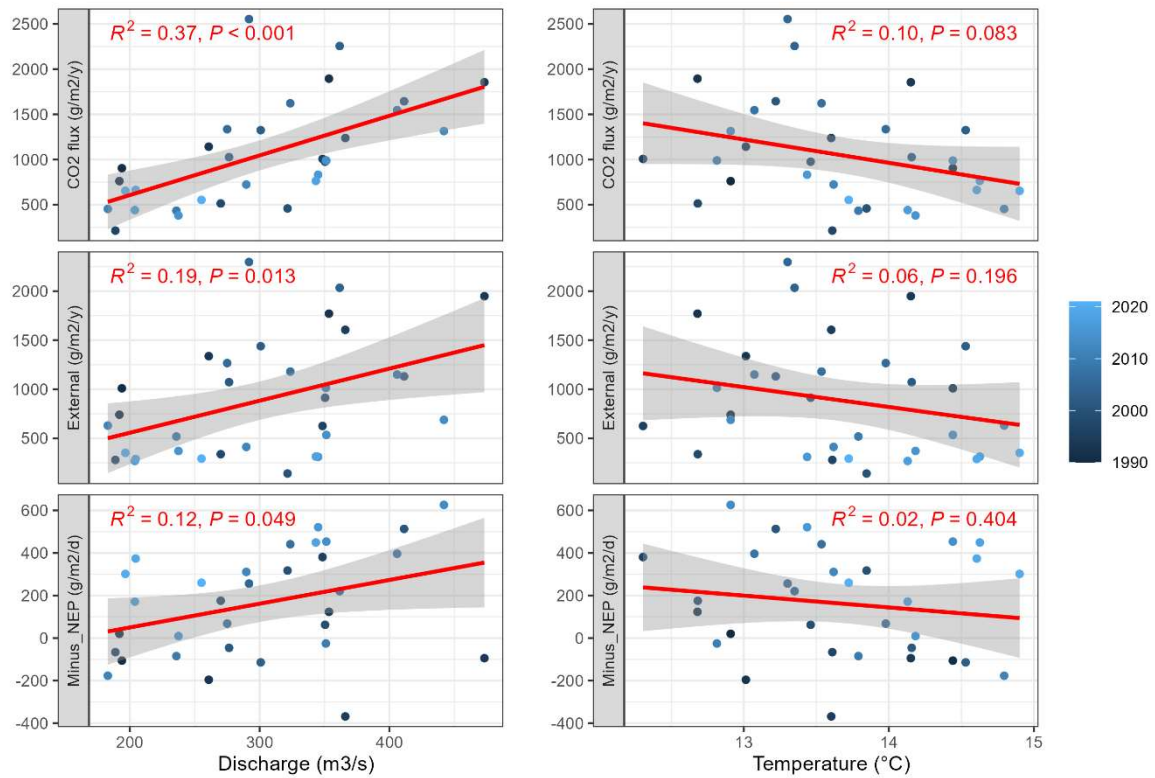
845 Figure D2. Relationship of annual fluxes and annual discharge or annual water temperature. Points are

846 colored by year, as indicated by the color bar.

847
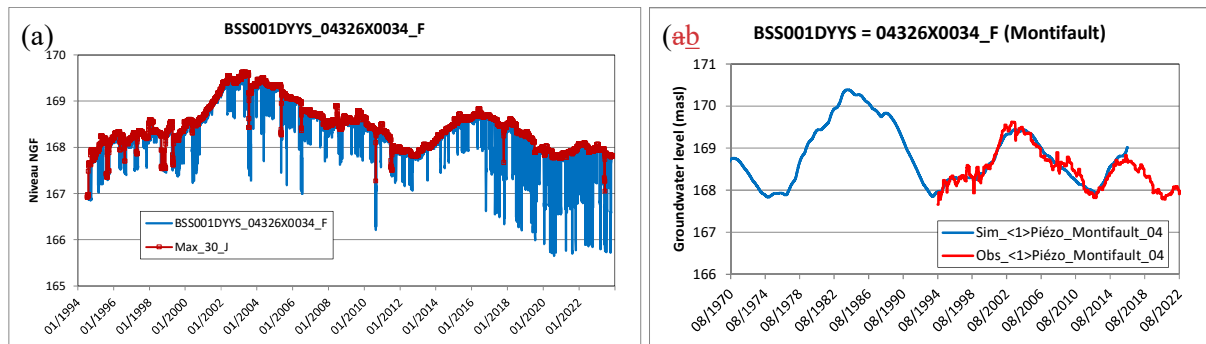
848 Figure D3. A decreasing trend in the groundwater level in Montifault (20 km from the study site). (a)

849 raw data, (b) after removing pumping effects with the EROS model (Data source: (Thiéry, 2018)).

850 NGF stands for "Nivellement Général de la France," which is the official vertical datum for France.
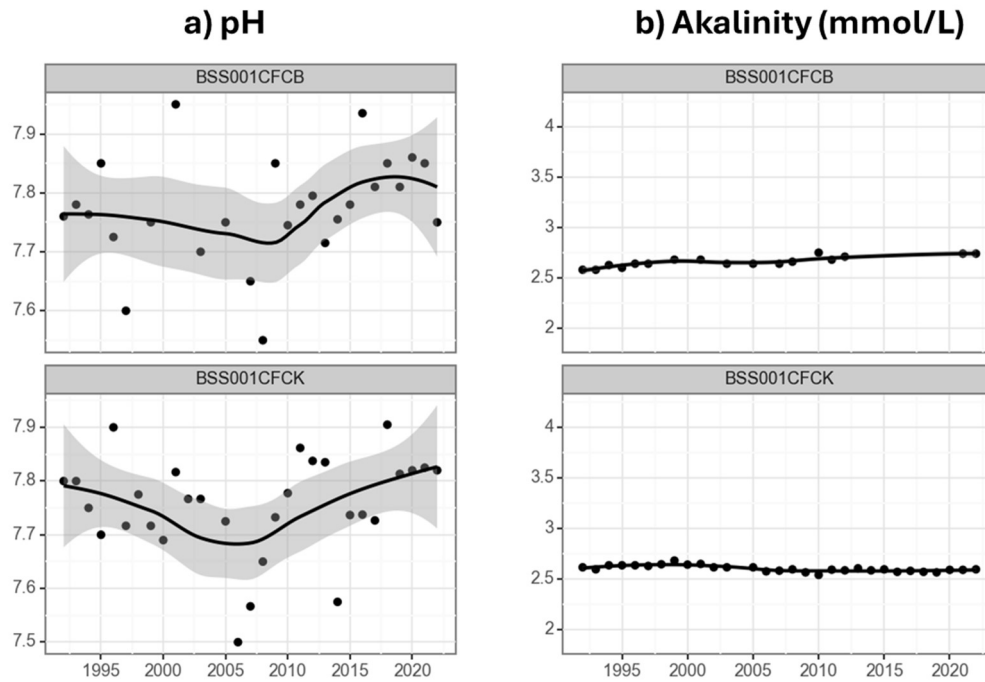
852 Figure D4. pH and alkalinity in groundwater monitoring stations in the vicinity (5 km radius) of the
853 Dampierre study site (1990-2021). Points represent individual measurements, and solid lines are
854 LOESS smoothers with 95% confidence intervals (shaded areas). Data source:
855 https://hubeau.eaufrance.fr/page/api-qualite-nappes

Data availability

The hourly temperature, conductivity, dissolved oxygen, and pH data used in this study are owned by Électricité de France (EDF). Due to ~~EDF's~~ EDF's data-sharing policy, these data are not publicly available but can be accessed upon reasonable request by contacting EDF directly. Other publicly available datasets used include discharge (https://www.hydro.eaufrance.fr), river water quality (www.naiades.eaufrance.fr).

Author Contribution

ANT led the manuscript effort. ANT, JSD, GA, and FM came up with the research question and designed the study approach. ANT and JSD conducted the data curation and preparation, and ANT conducted the statistical analyses. ANT wrote the paper with contributions from all authors.

Competing interests

The authors declare that they have no known competing financial interests or personal relationships that could have appeared to influence the work reported in this paper.

Acknowledgements

We express our gratitude to Electricité de France (EDF) for generously providing us with extensive long-term datasets in the Middle Loire River.

References

Abril, G., & Borges, A. V. (2019). Ideas and perspectives: Carbon leaks from flooded land: Do we need to replumb the inland water active pipe? Biogeosciences, 16(3), 769–784. https://doi.org/10.5194/bg-16-769-2019

Abril, G., Bouillon, S., Darchambeau, F., Teodoru, C. R., Marwick, T. R., Tamooh, F., Ochieng Omengo, F., Geeraert, N., Deirmendjian, L., Polsenaere, P., & Borges, A. V. (2015). Technical note: Large overestimation of pCO_2 calculated from pH and alkalinity in acidic, organic-rich freshwaters. Biogeosciences, 12(1), 67–78. https://doi.org/10.5194/bg-12-67-2015

Aho, K. S., Hosen, J. D., Logozzo, L. A., McGillis, W. R., & Raymond, P. A. (2021). Highest rates of gross primary productivity maintained despite CO_2 depletion in a temperate river network. Limnology and Oceanography Letters, 6(4), 200–206. https://doi.org/10.1002/lol2.10195

Amaral, J., Suhett, A., Melo, S., & Farjalla, V. (2013). Seasonal variation and interaction of photodegradation and microbial metabolism of DOC in black water Amazonian ecosystems. Aquatic Microbial Ecology, 70(2), 157–168. https://doi.org/10.3354/ame01651

Appling, A. P., Hall, R. O., Yackulic, C. B., & Arroita, M. (2018). Overcoming Equifinality: Leveraging Long Time Series for Stream Metabolism Estimation. Journal of Geophysical Research: Biogeosciences, 123(2), 624–645. https://doi.org/10.1002/2017JG004140

Battin, T. J., Lauerwald, R., Bernhardt, E. S., Bertuzzo, E., Gener, L. G., Hall, R. O., Hotchkiss, E. R., Maavara, T., Pavelsky, T. M., Ran, L., Raymond, P., Rosentreter, J. A., & Regnier, P. (2023). River ecosystem metabolism and carbon biogeochemistry in a changing world. Nature, 613(7944), 449–459. https://doi.org/10.1038/s41586-022-05500-8

Baulon, L., Allier, D., Massei, N., Bessiere, H., Fournier, M., & Bault, V. (2022). Influence of low-frequency variability on groundwater level trends. Journal of Hydrology, 606, 127436. https://doi.org/10.1016/j.jhydrol.2022.127436

Bernal, S., Cohen, M. J., Ledesma, J. L. J., Kirk, L., Martí, E., & Lupon, A. (2022). Stream metabolism sources a large fraction of carbon dioxide to the atmosphere in two hydrologically contrasting headwater streams. Limnology and Oceanography, 67(12), 2621–2634. https://doi.org/10.1002/lno.12226

Binet, S., Charlier, J.-B., Jozja, N., Défarge, C., & Moquet, J.-S. (2022). Evidence of long term biogeochemical interactions in carbonate weathering: The role of planktonic microorganisms and riverine bivalves in a large fluviokarst system. Science of the Total Environment, 842, 156823. https://doi.org/10.1016/j.scitotenv.2022.156823

Blaszczak, J. R., Delesantro, J. M., Urban, D. L., Doyle, M. W., & Bernhardt, E. S. (2019). Scoured or suffocated: Urban stream ecosystems oscillate between hydrologic and dissolved oxygen extremes. Limnology and Oceanography, 64(3), 877–894.

Bogard, M. J., & Del Giorgio, P. A. (2016). The role of metabolism in modulating CO_2 fluxes in boreal lakes. Global Biogeochemical Cycles, 30(10), 1509–1525. https://doi.org/10.1002/2016GB005463

Butman, D., & Raymond, P. A. (2011). Significant efflux of carbon dioxide from streams and rivers in the united states. Nature Geoscience, 4(12), Article 12. https://doi.org/10.1038/ngeo1294

Camenen, B., Grabowski, R. C., Latapie, A., Paquier, A., Solari, L., & Rodrigues, S. (2016). On the estimation of the bed-material transport and budget along a river segment: Application to the Middle Loire River, France. Aquatic Sciences, 78(1), 71–81. https://doi.org/10.1007/s00027-015-0442-3

Cole, J. J., Cole, J. J., Caraco, N. F., & Caraco, N. F. (2001). Carbon in catchments: Connecting terrestrial carbon losses with aquatic metabolism. Marine and Freshwater Research, 52(1), 101. https://doi.org/10.1071/MF00084

Cole, J. J., Prairie, Y. T., Caraco, N. F., McDowell, W. H., Tranvik, L. J., Striegl, R. G., Duarte, C. M., Kortelainen, P., Downing, J. A., Middelburg, J. J., & Melack, J. (2007). Plumbing the global carbon cycle: Integrating inland waters into the terrestrial carbon budget. Ecosystems, 10(1), 171–184. https://doi.org/10.1007/s10021-006-9013-8

Coynel, A., Etcheber, H., Abril, G., Maneux, E., Dumas, J., & Hurtrez, J.-E. (2005). Contribution of small mountainous rivers to particulate organic carbon input in the bay of biscay. Biogeochemistry, 74(2), 151–171.

Deirmendjian, L., & Abril, G. (2018). Carbon dioxide degassing at the groundwater-stream-atmosphere interface: Isotopic equilibration and hydrological mass balance in a sandy watershed. Journal of Hydrology, 558, 129–143. https://doi.org/10.1016/j.jhydrol.2018.01.003

Diamond, J. S., Bernal, S., Boukra, A., Cohen, M. J., Lewis, D., Masson, M., Moatar, F., & Pinay, G. (2021). Stream network variation in dissolved oxygen: Metabolism proxies and biogeochemical controls. Ecological Indicators, 131(September), 108233. https://doi.org/10.1016/j.ecolind.2021.108233

Diamond, J. S., Moatar, F., Cohen, M. J., Poirel, A., Martinet, C., Maire, A., & Pinay, G. (2022). Metabolic regime shifts and ecosystem state changes are decoupled in a large river. Limnology and Oceanography, 67(S1). https://doi.org/10.1002/lno.11789

Diamond, J. S., Truong, A. N., Abril, G., Bertuzzo, E., Chanudet, V., Lamouroux, R., & Moatar, F. (2025). Inorganic carbon dynamics and their relation to autotrophic community regime shift over three decades in a large, alkaline river. Limnology and Oceanography, n/a(n/a). https://doi.org/10.1002/lno.70016

Dodds, W. K., & Smith, V. H. (2016). Nitrogen, phosphorus, and eutrophication in streams. Inland Waters, 6(2), 155–164. https://doi.org/10.5268/IW-6.2.909

Duvert, C., Butman, D. E., Marx, A., Ribolzi, O., & Hutley, L. B. (2018). CO2 evasion along streams driven by groundwater inputs and geomorphic controls. Nature Geoscience, 11(11), Article 11. https://doi.org/10.1038/s41561-018-0245-y

Etcheber, H., Taillez, A., Abril, G., Garnier, J., Servais, P., Moatar, F., & Commarieu, M.-V. (2007). Particulate organic carbon in the estuarine turbidity maxima of the gironde, loire and seine estuaries: Origin and lability. Hydrobiologia, 588(1), 245–259. https://doi.org/10.1007/s10750-007-0667-9

Floury, M., Delattre, C., Ormerod, S. J., & Souchon, Y. (2012). Global versus local change effects on a large european river. Science of the Total Environment, 441, 220–229. https://doi.org/10.1016/j.scitotenv.2012.09.051

He, H., Wang, Y., Liu, Z., Bao, Q., Wei, Y., Chen, C., & Sun, H. (2022). Lake metabolic processes and their effects on the carbonate weathering CO2 sink: Insights from diel variations in the hydrochemistry of a typical karst lake in SW china. Water Research, 222, 118907. https://doi.org/10.1016/j.watres.2022.118907

Hotchkiss, E. R., Hall Jr, R. O., Sponseller, R. A., Butman, D., Klaminder, J., Laudon, H., Rosvall, M., & Karlsson, J. (2015). Sources of and processes controlling CO_2 emissions change with the size of streams and rivers. Nature Geoscience, 8(9), 696–699. https://doi.org/10.1038/ngeo2507

Humphreys, M. P., Lewis, E. R., Sharp, J. D., & Pierrot, D. (2022). PyCO2SYS v1.8: Marine carbonate system calculations in python. Geoscientific Model Development, 15(1), 15–43. https://doi.org/10.5194/gmd-15-15-2022

Hussain, Md., & Mahmud, I. (2019). pyMannKendall: A python package for non parametric mann kendall family of trend tests. Journal of Open Source Software, 4(39), 1556. https://doi.org/10.21105/joss.01556

Ibáñez, C., Caiola, N., Barquín, J., Belmar, O., Benito, X., Casals, F., Fennessy, S., Hughes, J., Palmer, M., Peñuelas, J., Romero, E., Sardans, J., & Williams, M. (2022). Ecosystem-level effects of re-oligotrophication and N:P imbalances in rivers and estuaries on a global scale. Global Change Biology, n/a(n/a). https://doi.org/10.1111/gcb.16520

Janssen, P., Chevalier, R., Chantereau, M., Dupré, R., Evette, A., Hémeray, D., Mårell, A., Martin, H., Rodrigues, S., Villar, M., & Greulich, S. (2023). Can vegetation clearing operations and reprofiling of bars be considered as an ecological restoration measure? Lessons from a 10-year vegetation monitoring program (loire river, france). Restoration Ecology, 31(3), e13704. https://doi.org/10.1111/rec.13704

Jones, A. S., Jones, T. L., & Horsburgh, J. S. (2022). Toward automating post processing of aquatic sensor data. Environmental Modelling and Software, 151, 105364. https://doi.org/10.1016/j.envsoft.2022.105364

Jones, J. B., Stanley, E. H., & Mulholland, P. J. (2003). Long-term decline in carbon dioxide supersaturation in rivers across the contiguous united states. Geophysical Research Letters, 30(10), 2003GL017056. https://doi.org/10.1029/2003GL017056

Kirk, L., & Cohen, M. J. (2023). River corridor sources dominate CO_2 emissions from a lowland river network. Journal of Geophysical Research: Biogeosciences, 128(1), e2022JG006954. https://doi.org/10.1029/2022JG006954

Koehler, B., Landelius, T., Weyhenmeyer, G. A., Machida, N., & Tranvik, L. J. (2014). Sunlight-induced carbon dioxide emissions from inland waters. Global Biogeochemical Cycles, 28(7), 696–711. https://doi.org/10.1002/2014GB004850

Liu, S., Kuhn, C., Amatulli, G., Aho, K., Butman, D. E., Allen, G. H., Lin, P., Pan, M., Yamazaki, D., Brinkerhoff, C., Gleason, C., Xia, X., & Raymond, P. A. (2022). The importance of hydrology in routing terrestrial carbon to the atmosphere via global streams and rivers. Proceedings of the National Academy of Sciences, 119(11), e2106322119. https://doi.org/10.1073/pnas.2106322119

Lynch, J. K., Beatty, C. M., Seidel, M. P., Jungst, L. J., & DeGrandpre, M. D. (2010). Controls of riverine CO_2 over an annual cycle determined using direct, high temporal resolution pCO_2 measurements. Journal of Geophysical Research: Biogeosciences, 115(G3), 2009JG001132. https://doi.org/10.1029/2009JG001132

Millero, F. J. (1979). The thermodynamics of the carbonate system in seawater. Geochimica et Cosmochimica Acta, 43(10), 1651–1661. https://doi.org/10.1016/0016-7037(79)90184-4

Minaudo, C., Meybeck, M., Moatar, F., Gassama, N., & Curie, F. (2015). Eutrophication mitigation in rivers: 30 years of trends in spatial and seasonal patterns of biogeochemistry of the loire river (1980–2012). Biogeosciences, 12(8), 2549–2563. https://doi.org/10.5194/bg-12-2549-2015

Moatar, F., Descy, J.-P., Rodrigues, S., Souchon, Y., Floury, M., Grosbois, C., Minaudo, C., Leitao, M., Wantzen, K. M., & Bertrand, F. (2022). Chapter 7—The loire river basin. In K. Tockner, C. Zarfl, & C. T. Robinson (Eds.), Rivers of Europe (Second Edition) (pp. 245–271). Elsevier. https://doi.org/10.1016/B978-0-08-102612-0.00007-9

Moatar, F., Fessant, F., & Poirel, A. (1999). pH modelling by neural networks. Application of control and validation data series in the middle loire river. Ecological Modelling, 120(2–3), 141–156. https://doi.org/10.1016/S0304-3800(99)00098-8

Moatar, F., & Meybeck, M. (2005). Compared performances of different algorithms for estimating annual nutrient loads discharged by the eutrophic River Loire. Hydrological Processes, 19(2), 429–444. https://doi.org/10.1002/hyp.5541

Moatar, F., Miquel, J., & Poirel, A. (2001). A quality-control method for physical and chemical monitoring data. Application to dissolved oxygen levels in the river loire (france). Journal of Hydrology, 252(1–4), 25–36. https://doi.org/10.1016/S0022-1694(01)00439-5

NOAA. (n.d.). Trends in atmospheric carbon dioxide. Global Monitoring Laboratory - Carbon Cycle Greenhouse Gases. https://gml.noaa.gov/ccgg/trends/data.html

Odum, H. T. (1956). Primary Production in Flowing Waters. Limnology and Oceanography, 1(2), 102–117. https://doi.org/10.4319/lo.1956.1.2.0102

Raymond, P. A., Caraco, N. F., & Cole, J. J. (1997). Carbon dioxide concentration and atmospheric flux in the hudson river. Estuaries, 20(2), 381. https://doi.org/10.2307/1352351

Raymond, P. A., Hartmann, J., Lauerwald, R., Sobek, S., McDonald, C., Hoover, M., Butman, D., Striegl, R., Mayorga, E., Humborg, C., Kortelainen, P., Dürr, H., Meybeck, M., Ciais, P., & Guth, P. (2013). Global carbon dioxide emissions from inland waters. Nature, 503(7476), 355–359. https://doi.org/10.1038/nature12760

Raymond, P. A., Zappa, C. J., Butman, D., Bott, T. L., Potter, J., Mulholland, P., Laursen, A. E., McDowell, W. H., & Newbold, D. (2012a). Scaling the gas transfer velocity and hydraulic geometry in streams and small rivers. Limnology and Oceanography: Fluids and Environments, 2(1), 41–53. https://doi.org/10.1215/21573689-1597669

Raymond, P. A., Zappa, C. J., Butman, D., Bott, T. L., Potter, J., Mulholland, P., Laursen, A. E., McDowell, W. H., & Newbold, D. (2012b). Scaling the gas transfer velocity and hydraulic geometry in streams and small rivers. Limnology and Oceanography: Fluids and Environments, 2(1), 41–53. https://doi.org/10.1215/21573689-1597669

Reed, A. P., Stets, E. G., Murphy, S. F., & Mullins, E. A. (2021). Aquatic-terrestrial linkages control metabolism and carbon dynamics in a mid-sized, urban stream influenced by snowmelt. Journal of Geophysical Research: Biogeosciences, 126(9), e2021JG006296. https://doi.org/10.1029/2021JG006296

Rocher-Ros, G., Harms, T. K., Sponseller, R. A., Väisänen, M., Mörth, C.-M., & Giesler, R. (2021). Metabolism overrides photo-oxidation in CO2 dynamics of Arctic permafrost streams. Limnology and Oceanography, 66(S1), S169–S181. https://doi.org/10.1002/lno.11564

Rocher-Ros, G., Sponseller, R. A., Bergström, A., Myrstener, M., & Giesler, R. (2020). Stream metabolism controls diel patterns and evasion of CO 2 in arctic streams. Global Change Biology, 26(3), 1400–1413. https://doi.org/10.1111/gcb.14895

Seabold, S., & Perktold, J. (2010). Statsmodels: Econometric and statistical modeling with python. 92–96. https://doi.org/10.25080/Majora-92bf1922-011

Solano, V., Duvert, C., Birkel, C., Maher, D. T., García, E. A., & Hutley, L. B. (2023). Stream respiration exceeds CO_2 evasion in a low-energy, oligotrophic tropical stream. Limnology and Oceanography, 68(5), 1132–1146. https://doi.org/10.1002/lno.12334

Thiéry, D. (2018). EROS: A semi-global hydrological modelling application for a catchment area divided into sub-basins | BRGM. https://www.brgm.fr/en/software/eros-semi-global-hydrological-modelling-application-catchment-area-divided-sub-basins

Trentman, M. T., Hall, R. O., & Valett, H. M. (2023). Exploring the mismatch between the theory and application of photosynthetic quotients in aquatic ecosystems. Limnology and Oceanography Letters. https://doi.org/10.1002/lol2.10326

Truong, C., Oudre, L., & Vayatis, N. (2020). Selective review of offline change point detection methods. Signal Processing, 167, 107299. https://doi.org/10.1016/j.sigpro.2019.107299

Tsypin, M., & Macpherson, G. L. (2012). The effect of precipitation events on inorganic carbon in soil and shallow groundwater, konza prairie LTER site, NE kansas, USA. Applied Geochemistry, 27(12), 2356–2369. https://doi.org/10.1016/j.apgeochem.2012.07.008

Van Vliet, M. T. H., Franssen, W. H. P., Yearsley, J. R., Ludwig, F., Haddeland, I., Lettenmaier, D. P., & Kabat, P. (2013). Global river discharge and water temperature under climate change. Global Environmental Change, 23(2), 450–464. https://doi.org/10.1016/j.gloenvcha.2012.11.002

Vihermaa, L. E., Waldron, S., Garnett, M. H., & Newton, J. (2014). Old carbon contributes to aquatic emissions of carbon dioxide in the Amazon. Biogeosciences, 11(13), 3635–3645. https://doi.org/10.5194/bg-11-3635-2014

Wallin, M. B., Audet, J., Peacock, M., Sahlée, E., & Winterdahl, M. (2020). Carbon dioxide dynamics in an agricultural headwater stream driven by hydrology and primary production. Biogeosciences, 17(9), 2487–2498. https://doi.org/10.5194/bg-17-2487-2020

Young, F. L., Colman, B. P., Carter, A. M., Fiejó De Lima, R., Shangguan, Q., Payn, R. A., & DeGrandpre, M. D. (2025). Variability and Controls of p CO_2 and Air-Water CO_2 Fluxes in a Temperate River. Journal of Geophysical Research: Biogeosciences, 130(2), e2024JG008434. https://doi.org/10.1029/2024JG008434

Zhang, T., Li, J., Pu, J., Martin, J. B., Khadka, M. B., Wu, F., Li, L., Jiang, F., Huang, S., & Yuan, D. (2017). River sequesters atmospheric carbon and limits the CO_2 degassing in karst area, southwest China. Science of the Total Environment, 609, 92–101. https://doi.org/10.1016/j.scitotenv.2017.07.143

Abril, G., & Borges, A. V. (2019). Ideas and perspectives: Carbon leaks from flooded land: Do we need to replumb the inland water active pipe? *Biogeosciences*, *16*(3), 769–784. https://doi.org/10.5194/bg-16-769-2019

Abril, G., Bouillon, S., Darchambeau, F., Teodoru, C. R., Marwick, T. R., Tamooh, F., Ochieng Omengo, F., Geeraert, N., Deirmendjian, L., Polsenaere, P., & Borges, A. V. (2015). Technical note: Large overestimation of pCO_2 calculated from pH and alkalinity in acidic, organic-rich freshwaters. *Biogeosciences*, *12*(1), 67–78. https://doi.org/10.5194/bg-12-67-2015

Aho, K. S., Hosen, J. D., Logozzo, L. A., McGillis, W. R., & Raymond, P. A. (2021). Highest rates of gross primary productivity maintained despite CO_2 depletion in a temperate river network. *Limnology and Oceanography Letters*, *6*(4), 200–206. https://doi.org/10.1002/lol2.10195

Amaral, J., Suhett, A., Melo, S., & Farjalla, V. (2013). Seasonal variation and interaction of photodegradation and microbial metabolism of DOC in black water Amazonian ecosystems. *Aquatic Microbial Ecology*, *70*(2), 157–168. https://doi.org/10.3354/ame01651

Appling, A. P., Hall, R. O., Yackulic, C. B., & Arroita, M. (2018). Overcoming Equifinality: Leveraging Long Time Series for Stream Metabolism Estimation. *Journal of Geophysical Research: Biogeosciences*, *123*(2), 624–645. https://doi.org/10.1002/2017JG004140

Battin, T. J., Lauerwald, R., Bernhardt, E. S., Bertuzzo, E., Gener, L. G., Hall, R. O., Hotchkiss, E. R., Maavara, T., Pavelsky, T. M., Ran, L., Raymond, P., Rosentreter, J. A., & Regnier, P. (2023). River ecosystem metabolism and carbon biogeochemistry in a changing world. *Nature*, *613*(7944), 449–459. https://doi.org/10.1038/s41586-022-05500-8

Baulon, L., Allier, D., Massei, N., Bessiere, H., Fournier, M., & Bault, V. (2022). Influence of low-frequency variability on groundwater level trends. *Journal of Hydrology*, *606*, 127436. https://doi.org/10.1016/j.jhydrol.2022.127436

Bernal, S., Cohen, M. J., Ledesma, J. L. J., Kirk, L., Martí, E., & Lupon, A. (2022). Stream metabolism sources a large fraction of carbon dioxide to the atmosphere in two hydrologically contrasting headwater streams. *Limnology and Oceanography*, *67*(12), 2621–2634. https://doi.org/10.1002/lno.12226

Binet, S., Charlier, J. B., Jozja, N., Défarge, C., & Moquet, J. S. (2022). Evidence of long term biogeochemical interactions in carbonate weathering: The role of planktonic microorganisms and riverine bivalves in a large fluviokarst system. *Science of the Total Environment*, *842*, 156823. https://doi.org/10.1016/j.scitotenv.2022.156823

Blaszczak, J. R., Delesantro, J. M., Urban, D. L., Doyle, M. W., & Bernhardt, E. S. (2019). Scoured or suffocated: Urban stream ecosystems oscillate between hydrologic and dissolved oxygen extremes. *Limnology and Oceanography*, *64*(3), 877–894.

1105   Bogard, M. J., & Del Giorgio, P. A. (2016). The role of metabolism in modulating CO_2 fluxes in boreal

1106   lakes.   *Global   Biogeochemical   Cycles*,   *30*(10),   1509–1525.

1107   https://doi.org/10.1002/2016GB005463

1108   Butman, D., & Raymond, P. A. (2011). Significant efflux of carbon dioxide from streams and rivers in

1109   the united states. *Nature Geoscience*, *4*(12), Article 12. https://doi.org/10.1038/ngeo1294

1110   Camenen, B., Grabowski, R. C., Latapie, A., Paquier, A., Solari, L., & Rodrigues, S. (2016). On the

1111   estimation of the bed material transport and budget along a river segment: Application to the

1112   Middle Loire River, France. *Aquatic Sciences*, *78*(1), 71–81. https://doi.org/10.1007/s00027-

1113   015-0442-3

1114   Cole, J. J., Cole, J. J., Caraco, N. F., & Caraco, N. F. (2001). Carbon in catchments: Connecting

1115   terrestrial carbon losses with aquatic metabolism. *Marine and Freshwater Research*, *52*(1), 101.

1116   https://doi.org/10.1071/MF00084

1117   Cole, J. J., Prairie, Y. T., Caraco, N. F., McDowell, W. H., Tranvik, L. J., Striegl, R. G., Duarte, C. M.,

1118   Kortelainen, P., Downing, J. A., Middelburg, J. J., & Melack, J. (2007). Plumbing the global

1119   carbon cycle: Integrating inland waters into the terrestrial carbon budget. *Ecosystems*, *10*(1),

1120   171–184. https://doi.org/10.1007/s10021-006-9013-8

1121   Coynel, A., Etcheber, H., Abril, G., Maneux, E., Dumas, J., & Hurtrez, J. E. (2005). Contribution of

1122   small mountainous rivers to particulate organic carbon input in the bay of biscay.

1123   *Biogeochemistry*, *74*(2), 151–171.

1124   Deirmendjian, L., & Abril, G. (2018). Carbon dioxide degassing at the groundwater-stream-atmosphere

1125   interface: Isotopic equilibration and hydrological mass balance in a sandy watershed. *Journal

1126   of Hydrology*, *558*, 129–143. https://doi.org/10.1016/j.jhydrol.2018.01.003

1127   Diamond, J. S., Bernal, S., Boukra, A., Cohen, M. J., Lewis, D., Masson, M., Moatar, F., & Pinay, G.

1128   (2021). Stream network variation in dissolved oxygen: Metabolism proxies and biogeochemical

1129   controls.   *Ecological   Indicators*,   *131*(September),   108233.

1130   https://doi.org/10.1016/j.ecolind.2021.108233

Diamond, J. S., Moatar, F., Cohen, M. J., Poirel, A., Martinet, C., Maire, A., & Pinay, G. (2022). Metabolic regime shifts and ecosystem state changes are decoupled in a large river. *Limnology and Oceanography*, *67*(S1). https://doi.org/10.1002/lno.11789

Diamond, J. S., Truong, A. N., Abril, G., Bertuzzo, E., Chanudet, V., Lamouroux, R., & Moatar, F. (2025). Inorganic carbon dynamics and their relation to autotrophic community regime shift over three decades in a large, alkaline river. *Limnology and Oceanography*, *n/a*(n/a). https://doi.org/10.1002/lno.70016

Dodds, W. K., & Smith, V. H. (2016). Nitrogen, phosphorus, and eutrophication in streams. *Inland Waters*, *6*(2), 155–164. https://doi.org/10.5268/IW-6.2.909

Duvert, C., Butman, D. E., Marx, A., Ribolzi, O., & Hutley, L. B. (2018). CO2 evasion along streams driven by groundwater inputs and geomorphic controls. *Nature Geoscience*, *11*(11), Article 11. https://doi.org/10.1038/s41561-018-0245-y

Etcheber, H., Taillez, A., Abril, G., Garnier, J., Servais, P., Moatar, F., & Commarieu, M. V. (2007). Particulate organic carbon in the estuarine turbidity maxima of the gironde, loire and seine estuaries: Origin and lability. *Hydrobiologia*, *588*(1), 245–259. https://doi.org/10.1007/s10750-007-0667-9

Floury, M., Delattre, C., Ormerod, S. J., & Souchon, Y. (2012). Global versus local change effects on a large european river. *Science of the Total Environment*, *441*, 220–229. https://doi.org/10.1016/j.scitotenv.2012.09.051

He, H., Wang, Y., Liu, Z., Bao, Q., Wei, Y., Chen, C., & Sun, H. (2022). Lake metabolic processes and their effects on the carbonate weathering CO2 sink: Insights from diel variations in the hydrochemistry of a typical karst lake in SW china. *Water Research*, *222*, 118907. https://doi.org/10.1016/j.watres.2022.118907

Hotchkiss, E. R., Hall Jr, R. O., Sponseller, R. A., Butman, D., Klaminder, J., Laudon, H., Rosvall, M., & Karlsson, J. (2015). Sources of and processes controlling CO2 emissions change with the size of streams and rivers. *Nature Geoscience*, *8*(9), 696–699. https://doi.org/10.1038/ngeo2507

1157 Humphreys, M. P., Lewis, E. R., Sharp, J. D., & Pierrot, D. (2022). PyCO2SYS v1.8: Marine carbonate

1158   system calculations in python. *Geoscientific Model Development*, *15*(1), 15–43.

1159   https://doi.org/10.5194/gmd-15-15-2022

1160 Hussain, Md., & Mahmud, I. (2019). pyMannKendall: A python package for non parametric mann

1161   kendall family of trend tests. *Journal of Open Source Software*, *4*(39), 1556.

1162   https://doi.org/10.21105/joss.01556

1163 Ibáñez, C., Caiola, N., Barquín, J., Belmar, O., Benito, X., Casals, F., Fennessy, S., Hughes, J., Palmer,

1164   M., Peñuelas, J., Romero, E., Sardans, J., & Williams, M. (2022). Ecosystem-level effects of re-

1165   oligotrophication and N:P imbalances in rivers and estuaries on a global scale. *Global Change*

1166   *Biology*, *n/a*(n/a). https://doi.org/10.1111/gcb.16520

1167 Janssen, P., Chevalier, R., Chantereau, M., Dupré, R., Evette, A., Hémeray, D., Mårell, A., Martin, H.,

1168   Rodrigues, S., Villar, M., & Greulich, S. (2023). Can vegetation clearing operations and

1169   reprofiling of bars be considered as an ecological restoration measure? Lessons from a 10-year

1170   vegetation monitoring program (loire river, france). *Restoration Ecology*, *31*(3), e13704.

1171   https://doi.org/10.1111/rec.13704

1172 Jones, A. S., Jones, T. L., & Horsburgh, J. S. (2022). Toward automating post processing of aquatic

1173   sensor data. *Environmental Modelling and Software*, *151*, 105364.

1174   https://doi.org/10.1016/j.envsoft.2022.105364

1175 Jones, J. B., Stanley, E. H., & Mulholland, P. J. (2003). Long-term decline in carbon dioxide

1176   supersaturation in rivers across the contiguous united states. *Geophysical Research Letters*,

1177   *30*(10), 2003GL017056. https://doi.org/10.1029/2003GL017056

1178 Kirk, L., & Cohen, M. J. (2023). River corridor sources dominate CO_2 emissions from a lowland river

1179   network. *Journal of Geophysical Research: Biogeosciences*, *128*(1), e2022JG006954.

1180   https://doi.org/10.1029/2022JG006954

1181 Koehler, B., Landelius, T., Weyhenmeyer, G. A., Machida, N., & Tranvik, L. J. (2014). Sunlight-

1182   induced carbon dioxide emissions from inland waters. *Global Biogeochemical Cycles*, *28*(7),

1183   696–711. https://doi.org/10.1002/2014GB004850

Liu, S., Kuhn, C., Amatulli, G., Aho, K., Butman, D. E., Allen, G. H., Lin, P., Pan, M., Yamazaki, D., Brinkerhoff, C., Gleason, C., Xia, X., & Raymond, P. A. (2022). The importance of hydrology in routing terrestrial carbon to the atmosphere via global streams and rivers. *Proceedings of the National Academy of Sciences, 119*(11), e2106322119. https://doi.org/10.1073/pnas.2106322119

Lynch, J. K., Beatty, C. M., Seidel, M. P., Jungst, L. J., & DeGrandpre, M. D. (2010). Controls of riverine CO_2 over an annual cycle determined using direct, high temporal resolution pCO_2 measurements. *Journal of Geophysical Research: Biogeosciences, 115*(G3), 2009JG001132. https://doi.org/10.1029/2009JG001132

Millero, F. J. (1979). The thermodynamics of the carbonate system in seawater. *Geochimica et Cosmochimica Acta, 43*(10), 1651–1661. https://doi.org/10.1016/0016-7037(79)90184-4

Minaudo, C., Meybeck, M., Moatar, F., Gassama, N., & Curie, F. (2015). Eutrophication mitigation in rivers: 30 years of trends in spatial and seasonal patterns of biogeochemistry of the loire river (1980–2012). *Biogeosciences, 12*(8), 2549–2563. https://doi.org/10.5194/bg-12-2549-2015

Moatar, F., Descy, J.-P., Rodrigues, S., Souchon, Y., Floury, M., Grosbois, C., Minaudo, C., Leitao, M., Wantzen, K. M., & Bertrand, F. (2022). Chapter 7 - The loire river basin. In K. Tockner, C. Zarfl, & C. T. Robinson (Eds.), *Rivers of Europe (Second Edition)* (pp. 245–271). Elsevier. https://doi.org/10.1016/B978-0-08-102612-0.00007-9

Moatar, F., Fessant, F., & Poirel, A. (1999). pH modelling by neural networks. Application of control and validation data series in the middle loire river. *Ecological Modelling, 120*(2-3), 141–156. https://doi.org/10.1016/S0304-3800(99)00098-8

Moatar, F., & Meybeck, M. (2005). Compared performances of different algorithms for estimating annual nutrient loads discharged by the eutrophic River Loire. *Hydrological Processes, 19*(2), 429–444. https://doi.org/10.1002/hyp.5541

Moatar, F., Miquel, J., & Poirel, A. (2001). A quality-control method for physical and chemical monitoring data. Application to dissolved oxygen levels in the river loire (france). *Journal of Hydrology, 252*(1-4), 25–36. https://doi.org/10.1016/S0022-1694(01)00439-5

NOAA. (n.d.). *Trends in atmospheric carbon dioxide*. Global Monitoring Laboratory - Carbon Cycle Greenhouse Gases. https://gml.noaa.gov/ccgg/trends/data.html

Odum, H. T. (1956). Primary Production in Flowing Waters. *Limnology and Oceanography*, *1*(2), 102–117. https://doi.org/10.4319/lo.1956.1.2.0102

Raymond, P. A., Caraco, N. F., & Cole, J. J. (1997). Carbon dioxide concentration and atmospheric flux in the hudson river. *Estuaries*, *20*(2), 381. https://doi.org/10.2307/1352351

Raymond, P. A., Hartmann, J., Lauerwald, R., Sobek, S., McDonald, C., Hoover, M., Butman, D., Striegl, R., Mayorga, E., Humborg, C., Kortelainen, P., Dürr, H., Meybeck, M., Ciais, P., & Guth, P. (2013). Global carbon dioxide emissions from inland waters. *Nature*, *503*(7476), 355–359. https://doi.org/10.1038/nature12760

Raymond, P. A., Zappa, C. J., Butman, D., Bott, T. L., Potter, J., Mulholland, P., Laursen, A. E., McDowell, W. H., & Newbold, D. (2012a). Scaling the gas transfer velocity and hydraulic geometry in streams and small rivers. *Limnology and Oceanography: Fluids and Environments*, *2*(1), 41–53. https://doi.org/10.1215/21573689-1597669

Raymond, P. A., Zappa, C. J., Butman, D., Bott, T. L., Potter, J., Mulholland, P., Laursen, A. E., McDowell, W. H., & Newbold, D. (2012b). Scaling the gas transfer velocity and hydraulic geometry in streams and small rivers. *Limnology and Oceanography: Fluids and Environments*, *2*(1), 41–53. https://doi.org/10.1215/21573689-1597669

Reed, A. P., Stets, E. G., Murphy, S. F., & Mullins, E. A. (2021). Aquatic-terrestrial linkages control metabolism and carbon dynamics in a mid-sized, urban stream influenced by snowmelt. *Journal of Geophysical Research: Biogeosciences*, *126*(9), e2021JG006296. https://doi.org/10.1029/2021JG006296

Rocher-Ros, G., Harms, T. K., Sponseller, R. A., Väisänen, M., Mörth, C. M., & Giesler, R. (2021). Metabolism overrides photo-oxidation in CO_2 dynamics of Arctic permafrost streams. *Limnology and Oceanography*, *66*(S1), S169–S181. https://doi.org/10.1002/lno.11564

Rocher-Ros, G., Sponseller, R. A., Bergström, A., Myrstener, M., & Giesler, R. (2020). Stream metabolism controls diel patterns and evasion of CO_2 in arctic streams. *Global Change Biology*, *26*(3), 1400–1413. https://doi.org/10.1111/gcb.14895

Seabold, S., & Perktold, J. (2010). *Statsmodels: Econometric and statistical modeling with python.* 92–96. https://doi.org/10.25080/Majora-92bf1922-011

Solano, V., Duvert, C., Birkel, C., Maher, D. T., García, E. A., & Hutley, L. B. (2023). Stream respiration exceeds CO_2 evasion in a low-energy, oligotrophic tropical stream. *Limnology and Oceanography*, *68*(5), 1132–1146. https://doi.org/10.1002/lno.12334

Thiéry, D. (2018). *ÉROS: A semi-global hydrological modelling application for a catchment area divided into sub-basins | BRGM.* https://www.brgm.fr/en/software/eros-semi-global-hydrological-modelling-application-catchment-area-divided-sub-basins

Trentman, M. T., Hall, R. O., & Valett, H. M. (2023). Exploring the mismatch between the theory and application of photosynthetic quotients in aquatic ecosystems. *Limnology and Oceanography Letters*. https://doi.org/10.1002/lol2.10326

Truong, C., Oudre, L., & Vayatis, N. (2020). Selective review of offline change point detection methods. *Signal Processing*, *167*, 107299. https://doi.org/10.1016/j.sigpro.2019.107299

Tsypin, M., & Macpherson, G. L. (2012). The effect of precipitation events on inorganic carbon in soil and shallow groundwater, konza prairie LTER site, NE kansas, USA. *Applied Geochemistry*, *27*(12), 2356–2369. https://doi.org/10.1016/j.apgeochem.2012.07.008

Van Vliet, M. T. H., Franssen, W. H. P., Yearsley, J. R., Ludwig, F., Haddeland, I., Lettenmaier, D. P., & Kabat, P. (2013). Global river discharge and water temperature under climate change. *Global Environmental Change*, *23*(2), 450–464. https://doi.org/10.1016/j.gloenvcha.2012.11.002

Vihermaa, L. E., Waldron, S., Garnett, M. H., & Newton, J. (2014). Old carbon contributes to aquatic emissions of carbon dioxide in the Amazon. *Biogeosciences*, *11*(13), 3635–3645. https://doi.org/10.5194/bg-11-3635-2014

Wallin, M. B., Audet, J., Peacock, M., Sahlée, E., & Winterdahl, M. (2020). Carbon dioxide dynamics in an agricultural headwater stream driven by hydrology and primary production. *Biogeosciences*, *17*(9), 2487–2498. https://doi.org/10.5194/bg-17-2487-2020

Young, F. L., Colman, B. P., Carter, A. M., Fiejó De Lima, R., Shangguan, Q., Payn, R. A., & DeGrandpre, M. D. (2025). Variability and Controls of p CO_2 and Air-Water CO_2 Fluxes in a

Temperate River. *Journal of Geophysical Research: Biogeosciences, 130*(2), e2024JG008434. https://doi.org/10.1029/2024JG008434

Zhang, T., Li, J., Pu, J., Martin, J. B., Khadka, M. B., Wu, F., Li, L., Jiang, F., Huang, S., & Yuan, D. (2017). River sequesters atmospheric carbon and limits the CO2 degassing in karst area, southwest China. *Science of the Total Environment, 609*, 92-101. https://doi.org/10.1016/j.scitotenv.2017.07.143

Abril, G., & Borges, A. V. (2019). Ideas and perspectives: Carbon leaks from flooded land: Do we need to replumb the inland water active pipe? *Biogeosciences, 16*(3), 769-784. https://doi.org/10.5194/bg-16-769-2019

Abril, G., Bouillon, S., Darchambeau, F., Teodoru, C. R., Marwick, T. R., Tamooh, F., Ochieng Omengo, F., Geeraert, N., Deirmendjian, L., Polsenaere, P., & Borges, A. V. (2015). Technical note: Large overestimation of pCO_2 calculated from pH and alkalinity in acidic, organic-rich freshwaters. *Biogeosciences, 12*(1), 67-78. https://doi.org/10.5194/bg-12-67-2015

Aho, K. S., Hosen, J. D., Logozzo, L. A., McGillis, W. R., & Raymond, P. A. (2021). Highest rates of gross primary productivity maintained despite CO_2 depletion in a temperate river network. *Limnology and Oceanography Letters, 6*(4), 200-206. https://doi.org/10.1002/lol2.10195

Amaral, J., Suhett, A., Melo, S., & Farjalla, V. (2013). Seasonal variation and interaction of photodegradation and microbial metabolism of DOC in black water Amazonian ecosystems. *Aquatic Microbial Ecology, 70*(2), 157-168. https://doi.org/10.3354/ame01651

Appling, A. P., Hall, R. O., Yackulic, C. B., & Arroita, M. (2018). Overcoming Equifinality: Leveraging Long Time Series for Stream Metabolism Estimation. *Journal of Geophysical Research: Biogeosciences, 123*(2), 624-645. https://doi.org/10.1002/2017JG004140

Battin, T. J., Lauerwald, R., Bernhardt, E. S., Bertuzzo, E., Gener, L. G., Hall, R. O., Hotchkiss, E. R., Maavara, T., Pavelsky, T. M., Ran, L., Raymond, P., Rosentreter, J. A., & Regnier, P. (2023). River ecosystem metabolism and carbon biogeochemistry in a changing world. *Nature, 613*(7944), 449-459. https://doi.org/10.1038/s41586-022-05500-8

Baulon, L., Allier, D., Massei, N., Bessiere, H., Fournier, M., & Bault, V. (2022). Influence of low-frequency variability on groundwater level trends. *Journal of Hydrology*, *606*, 127436. https://doi.org/10.1016/j.jhydrol.2022.127436

Bernal, S., Cohen, M. J., Ledesma, J. L. J., Kirk, L., Martí, E., & Lupon, A. (2022). Stream metabolism sources a large fraction of carbon dioxide to the atmosphere in two hydrologically contrasting headwater streams. *Limnology and Oceanography*, *67*(12), 2621–2634. https://doi.org/10.1002/lno.12226

Binet, S., Charlier, J. B., Jozja, N., Défarge, C., & Moquet, J. S. (2022). Evidence of long term biogeochemical interactions in carbonate weathering: The role of planktonic microorganisms and riverine bivalves in a large fluviokarst system. *Science of the Total Environment*, *842*, 156823. https://doi.org/10.1016/j.scitotenv.2022.156823

Blaszczak, J. R., Delesantro, J. M., Urban, D. L., Doyle, M. W., & Bernhardt, E. S. (2019). Scoured or suffocated: Urban stream ecosystems oscillate between hydrologic and dissolved oxygen extremes. *Limnology and Oceanography*, *64*(3), 877–894.

Bogard, M. J., & Del Giorgio, P. A. (2016). The role of metabolism in modulating CO_2 fluxes in boreal lakes. *Global Biogeochemical Cycles*, *30*(10), 1509–1525. https://doi.org/10.1002/2016GB005463

Butman, D., & Raymond, P. A. (2011). Significant efflux of carbon dioxide from streams and rivers in the united states. *Nature Geoscience*, *4*(12), Article 12. https://doi.org/10.1038/ngeo1294

Camenen, B., Grabowski, R. C., Latapie, A., Paquier, A., Solari, L., & Rodrigues, S. (2016). On the estimation of the bed material transport and budget along a river segment: Application to the Middle Loire River, France. *Aquatic Sciences*, *78*(1), 71–81. https://doi.org/10.1007/s00027-015-0442-3

Cole, J. J., Cole, J. J., Caraco, N. F., & Caraco, N. F. (2001). Carbon in catchments: Connecting terrestrial carbon losses with aquatic metabolism. *Marine and Freshwater Research*, *52*(1), 101. https://doi.org/10.1071/MF00084

Cole, J. J., Prairie, Y. T., Caraco, N. F., McDowell, W. H., Tranvik, L. J., Striegl, R. G., Duarte, C. M., Kortelainen, P., Downing, J. A., Middelburg, J. J., & Melack, J. (2007). Plumbing the global

carbon cycle: Integrating inland waters into the terrestrial carbon budget. *Ecosystems, 10*(1), 171–184. https://doi.org/10.1007/s10021-006-9013-8

Coynel, A., Etcheber, H., Abril, G., Maneux, E., Dumas, J., & Hurtrez, J.-E. (2005). Contribution of small mountainous rivers to particulate organic carbon input in the bay of biscay. *Biogeochemistry, 74*(2), 151–171.

Deirmendjian, L., & Abril, G. (2018). Carbon dioxide degassing at the groundwater-stream-atmosphere interface: Isotopic equilibration and hydrological mass balance in a sandy watershed. *Journal of Hydrology, 558*, 129–143. https://doi.org/10.1016/j.jhydrol.2018.01.003

Diamond, J. S., Bernal, S., Boukra, A., Cohen, M. J., Lewis, D., Masson, M., Moatar, F., & Pinay, G. (2021). Stream network variation in dissolved oxygen: Metabolism proxies and biogeochemical controls. *Ecological Indicators, 131*(September), 108233. https://doi.org/10.1016/j.ecolind.2021.108233

Diamond, J. S., Moatar, F., Cohen, M. J., Poirel, A., Martinet, C., Maire, A., & Pinay, G. (2022). Metabolic regime shifts and ecosystem state changes are decoupled in a large river. *Limnology and Oceanography, 67*(S1). https://doi.org/10.1002/lno.11789

Diamond, J. S., Truong, A. N., Abril, G., Bertuzzo, E., Chanudet, V., Lamouroux, R., & Moatar, F. (2025). Inorganic carbon dynamics and their relation to autotrophic community regime shift over three decades in a large, alkaline river. *Limnology and Oceanography, n/a*(n/a). https://doi.org/10.1002/lno.70016

Dodds, W. K., & Smith, V. H. (2016). Nitrogen, phosphorus, and eutrophication in streams. *Inland Waters, 6*(2), 155–164. https://doi.org/10.5268/IW-6.2.909

Duvert, C., Butman, D. E., Marx, A., Ribolzi, O., & Hutley, L. B. (2018). CO2 evasion along streams driven by groundwater inputs and geomorphic controls. *Nature Geoscience, 11*(11), Article 11. https://doi.org/10.1038/s41561-018-0245-y

Etcheber, H., Taillez, A., Abril, G., Garnier, J., Servais, P., Moatar, F., & Commarieu, M. V. (2007). Particulate organic carbon in the estuarine turbidity maxima of the gironde, loire and seine estuaries: Origin and lability. *Hydrobiologia, 588*(1), 245–259. https://doi.org/10.1007/s10750-007-0667-9

Floury, M., Delattre, C., Ormerod, S. J., & Souchon, Y. (2012). Global versus local change effects on a large european river. *Science of the Total Environment*, *441*, 220–229. https://doi.org/10.1016/j.scitotenv.2012.09.051

He, H., Wang, Y., Liu, Z., Bao, Q., Wei, Y., Chen, C., & Sun, H. (2022). Lake metabolic processes and their effects on the carbonate weathering CO_2 sink: Insights from diel variations in the hydrochemistry of a typical karst lake in SW china. *Water Research*, *222*, 118907. https://doi.org/10.1016/j.watres.2022.118907

Hotchkiss, E. R., Hall Jr, R. O., Sponseller, R. A., Butman, D., Klaminder, J., Laudon, H., Rosvall, M., & Karlsson, J. (2015). Sources of and processes controlling CO_2 emissions change with the size of streams and rivers. *Nature Geoscience*, *8*(9), 696–699. https://doi.org/10.1038/ngeo2507

Humphreys, M. P., Lewis, E. R., Sharp, J. D., & Pierrot, D. (2022). PyCO2SYS v1.8: Marine carbonate system calculations in python. *Geoscientific Model Development*, *15*(1), 15–43. https://doi.org/10.5194/gmd-15-15-2022

Hussain, Md., & Mahmud, I. (2019). pyMannKendall: A python package for non parametric mann kendall family of trend tests. *Journal of Open Source Software*, *4*(39), 1556. https://doi.org/10.21105/joss.01556

Ibáñez, C., Caiola, N., Barquín, J., Belmar, O., Benito, X., Casals, F., Fennessy, S., Hughes, J., Palmer, M., Peñuelas, J., Romero, E., Sardans, J., & Williams, M. (2022). Ecosystem-level effects of re-oligotrophication and N:P imbalances in rivers and estuaries on a global scale. *Global Change Biology*, *n/a*(n/a). https://doi.org/10.1111/gcb.16520

Janssen, P., Chevalier, R., Chantereau, M., Dupré, R., Evette, A., Hémeray, D., Mårell, A., Martin, H., Rodrigues, S., Villar, M., & Greulich, S. (2023). Can vegetation clearing operations and reprofiling of bars be considered as an ecological restoration measure? Lessons from a 10-year vegetation monitoring program (loire river, france). *Restoration Ecology*, *31*(3), e13704. https://doi.org/10.1111/rec.13704

Jones, A. S., Jones, T. L., & Horsburgh, J. S. (2022). Toward automating post processing of aquatic sensor data. *Environmental Modelling and Software*, *151*, 105364. https://doi.org/10.1016/j.envsoft.2022.105364

Jones, J. B., Stanley, E. H., & Mulholland, P. J. (2003). Long-term decline in carbon dioxide supersaturation in rivers across the contiguous united states. *Geophysical Research Letters*, *30*(10), 2003GL017056. https://doi.org/10.1029/2003GL017056

Kirk, L., & Cohen, M. J. (2023). River corridor sources dominate CO_2 emissions from a lowland river network. *Journal of Geophysical Research: Biogeosciences*, *128*(1), e2022JG006954. https://doi.org/10.1029/2022JG006954

Koehler, B., Landelius, T., Weyhenmeyer, G. A., Machida, N., & Tranvik, L. J. (2014). Sunlight-induced carbon dioxide emissions from inland waters. *Global Biogeochemical Cycles*, *28*(7), 696–711. https://doi.org/10.1002/2014GB004850

Liu, S., Kuhn, C., Amatulli, G., Aho, K., Butman, D. E., Allen, G. H., Lin, P., Pan, M., Yamazaki, D., Brinkerhoff, C., Gleason, C., Xia, X., & Raymond, P. A. (2022). The importance of hydrology in routing terrestrial carbon to the atmosphere via global streams and rivers. *Proceedings of the National Academy of Sciences*, *119*(11), e2106322119. https://doi.org/10.1073/pnas.2106322119

Lynch, J. K., Beatty, C. M., Seidel, M. P., Jungst, L. J., & DeGrandpre, M. D. (2010). Controls of riverine CO_2 over an annual cycle determined using direct, high temporal resolution pCO_2 measurements. *Journal of Geophysical Research: Biogeosciences*, *115*(G3), 2009JG001132. https://doi.org/10.1029/2009JG001132

Millero, F. J. (1979). The thermodynamics of the carbonate system in seawater. *Geochimica et Cosmochimica Acta*, *43*(10), 1651–1661. https://doi.org/10.1016/0016-7037(79)90184-4

Minaudo, C., Meybeck, M., Moatar, F., Gassama, N., & Curie, F. (2015). Eutrophication mitigation in rivers: 30 years of trends in spatial and seasonal patterns of biogeochemistry of the loire river (1980–2012). *Biogeosciences*, *12*(8), 2549–2563. https://doi.org/10.5194/bg-12-2549-2015

Moatar, F., Descy, J. P., Rodrigues, S., Souchon, Y., Floury, M., Grosbois, C., Minaudo, C., Leitao, M., Wantzen, K. M., & Bertrand, F. (2022). Chapter 7 – The loire river basin. In K. Tockner, C. Zarfl, & C. T. Robinson (Eds.), *Rivers of Europe (Second Edition)* (pp. 245–271). Elsevier. https://doi.org/10.1016/B978-0-08-102612-0.00007-9

Moatar, F., Fessant, F., & Poirel, A. (1999). pH modelling by neural networks. Application of control and validation data series in the middle loire river. *Ecological Modelling*, *120*(2–3), 141–156. https://doi.org/10.1016/S0304-3800(99)00098-8

Moatar, F., & Meybeck, M. (2005). Compared performances of different algorithms for estimating annual nutrient loads discharged by the eutrophic River Loire. *Hydrological Processes*, *19*(2), 429–444. https://doi.org/10.1002/hyp.5541

Moatar, F., Miquel, J., & Poirel, A. (2001). A quality control method for physical and chemical monitoring data. Application to dissolved oxygen levels in the river loire (france). *Journal of Hydrology*, *252*(1–4), 25–36. https://doi.org/10.1016/S0022-1694(01)00439-5

NOAA. (n.d.). *Trends in atmospheric carbon dioxide*. Global Monitoring Laboratory – Carbon Cycle Greenhouse Gases. https://gml.noaa.gov/ccgg/trends/data.html

Odum, H. T. (1956). Primary Production in Flowing Waters. *Limnology and Oceanography*, *1*(2), 102–117. https://doi.org/10.4319/lo.1956.1.2.0102

Raymond, P. A., Caraco, N. F., & Cole, J. J. (1997). Carbon dioxide concentration and atmospheric flux in the hudson river. *Estuaries*, *20*(2), 381. https://doi.org/10.2307/1352351

Raymond, P. A., Hartmann, J., Lauerwald, R., Sobek, S., McDonald, C., Hoover, M., Butman, D., Striegl, R., Mayorga, E., Humborg, C., Kortelainen, P., Dürr, H., Meybeck, M., Ciais, P., & Guth, P. (2013). Global carbon dioxide emissions from inland waters. *Nature*, *503*(7476), 355–359. https://doi.org/10.1038/nature12760

Raymond, P. A., Zappa, C. J., Butman, D., Bott, T. L., Potter, J., Mulholland, P., Laursen, A. E., McDowell, W. H., & Newbold, D. (2012a). Scaling the gas transfer velocity and hydraulic geometry in streams and small rivers. *Limnology and Oceanography: Fluids and Environments*, *2*(1), 41–53. https://doi.org/10.1215/21573689-1597669

Raymond, P. A., Zappa, C. J., Butman, D., Bott, T. L., Potter, J., Mulholland, P., Laursen, A. E., McDowell, W. H., & Newbold, D. (2012b). Scaling the gas transfer velocity and hydraulic geometry in streams and small rivers. *Limnology and Oceanography: Fluids and Environments*, *2*(1), 41–53. https://doi.org/10.1215/21573689-1597669

Reed, A. P., Stets, E. G., Murphy, S. F., & Mullins, E. A. (2021). Aquatic-terrestrial linkages control metabolism and carbon dynamics in a mid-sized, urban stream influenced by snowmelt. *Journal of Geophysical Research: Biogeosciences*, *126*(9), e2021JG006296. https://doi.org/10.1029/2021JG006296

Rocher-Ros, G., Harms, T. K., Sponseller, R. A., Väisänen, M., Mörth, C. M., & Giesler, R. (2021). Metabolism overrides photo-oxidation in CO2 dynamics of Arctic permafrost streams. *Limnology and Oceanography*, *66*(S1), S169–S181. https://doi.org/10.1002/lno.11564

Rocher-Ros, G., Sponseller, R. A., Bergström, A., Myrstener, M., & Giesler, R. (2020). Stream metabolism controls diel patterns and evasion of CO_2 in arctic streams. *Global Change Biology*, *26*(3), 1400–1413. https://doi.org/10.1111/gcb.14895

Seabold, S., & Perktold, J. (2010). *Statsmodels: Econometric and statistical modeling with python.* 92–96. https://doi.org/10.25080/Majora-92bf1922-011

Thiéry, D. (2018). *ÉROS: A semi-global hydrological modelling application for a catchment area divided into sub-basins | BRGM.* https://www.brgm.fr/en/software/eros-semi-global-hydrological-modelling-application-catchment-area-divided-sub-basins

Trentman, M. T., Hall, R. O., & Valett, H. M. (2023). Exploring the mismatch between the theory and application of photosynthetic quotients in aquatic ecosystems. *Limnology and Oceanography Letters*. https://doi.org/10.1002/lol2.10326

Truong, C., Oudre, L., & Vayatis, N. (2020). Selective review of offline change point detection methods. *Signal Processing*, *167*, 107299. https://doi.org/10.1016/j.sigpro.2019.107299

Tsypin, M., & Macpherson, G. L. (2012). The effect of precipitation events on inorganic carbon in soil and shallow groundwater, konza prairie LTER site, NE kansas, USA. *Applied Geochemistry*, *27*(12), 2356–2369. https://doi.org/10.1016/j.apgeochem.2012.07.008

Van Vliet, M. T. H., Franssen, W. H. P., Yearsley, J. R., Ludwig, F., Haddeland, I., Lettenmaier, D. P., & Kabat, P. (2013). Global river discharge and water temperature under climate change. *Global Environmental Change*, *23*(2), 450–464. https://doi.org/10.1016/j.gloenvcha.2012.11.002

Vihermaa, L. E., Waldron, S., Garnett, M. H., & Newton, J. (2014). Old carbon contributes to aquatic emissions of carbon dioxide in the Amazon. *Biogeosciences*, *11*(13), 3635–3645. https://doi.org/10.5194/bg-11-3635-2014

Wallin, M. B., Audet, J., Peacock, M., Sahlée, E., & Winterdahl, M. (2020). Carbon dioxide dynamics in an agricultural headwater stream driven by hydrology and primary production. *Biogeosciences*, *17*(9), 2487–2498. https://doi.org/10.5194/bg-17-2487-2020

Young, F. L., Colman, B. P., Carter, A. M., Fiejó De Lima, R., Shangguan, Q., Payn, R. A., & DeGrandpre, M. D. (2025). Variability and Controls of p CO_2 and Air-Water CO_2 Fluxes in a Temperate River. *Journal of Geophysical Research: Biogeosciences*, *130*(2), e2024JG008434. https://doi.org/10.1029/2024JG008434

Zhang, T., Li, J., Pu, J., Martin, J. B., Khadka, M. B., Wu, F., Li, L., Jiang, F., Huang, S., & Yuan, D. (2017). River sequesters atmospheric carbon and limits the CO2 degassing in karst area, southwest China. *Science of the Total Environment*, *609*, 92–101. https://doi.org/10.1016/j.scitotenv.2017.07.143

Abril, G., & Borges, A. V. (2019). Ideas and perspectives: Carbon leaks from flooded land: Do we need to replumb the inland water active pipe? *Biogeosciences*, *16*(3), 769–784. https://doi.org/10.5194/bg-16-769-2019

Abril, G., Bouillon, S., Darchambeau, F., Teodoru, C. R., Marwick, T. R., Tamooh, F., Ochieng Omengo, F., Geeraert, N., Deirmendjian, L., Polsenaere, P., & Borges, A. V. (2015). Technical note: Large overestimation of pCO2 calculated from pH and alkalinity in acidic, organic-rich freshwaters. *Biogeosciences*, *12*(1), 67–78. https://doi.org/10.5194/bg-12-67-2015

Aho, K. S., Hosen, J. D., Logozzo, L. A., McGillis, W. R., & Raymond, P. A. (2021). Highest rates of gross primary productivity maintained despite CO_2 depletion in a temperate river network. *Limnology and Oceanography Letters*, *6*(4), 200–206. https://doi.org/10.1002/lol2.10195

Amaral, J., Suhett, A., Melo, S., & Farjalla, V. (2013). Seasonal variation and interaction of photodegradation and microbial metabolism of DOC in black water Amazonian ecosystems. *Aquatic Microbial Ecology*, *70*(2), 157–168. https://doi.org/10.3354/ame01651

Appling, A. P., Hall, R. O., Yackulic, C. B., & Arroita, M. (2018). Overcoming Equifinality: Leveraging Long Time Series for Stream Metabolism Estimation. *Journal of Geophysical Research: Biogeosciences*, *123*(2), 624–645. https://doi.org/10.1002/2017JG004140

Battin, T. J., Lauerwald, R., Bernhardt, E. S., Bertuzzo, E., Gener, L. G., Hall, R. O., Hotchkiss, E. R., Maavara, T., Pavelsky, T. M., Ran, L., Raymond, P., Rosentreter, J. A., & Regnier, P. (2023). River ecosystem metabolism and carbon biogeochemistry in a changing world. *Nature*, *613*(7944), 449–459. https://doi.org/10.1038/s41586-022-05500-8

Baulon, L., Allier, D., Massei, N., Bessiere, H., Fournier, M., & Bault, V. (2022). Influence of low-frequency variability on groundwater level trends. *Journal of Hydrology*, *606*, 127436. https://doi.org/10.1016/j.jhydrol.2022.127436

Bernal, S., Cohen, M. J., Ledesma, J. L. J., Kirk, L., Martí, E., & Lupon, A. (2022). Stream metabolism sources a large fraction of carbon dioxide to the atmosphere in two hydrologically contrasting headwater streams. *Limnology and Oceanography*, *67*(12), 2621–2634. https://doi.org/10.1002/lno.12226

Binet, S., Charlier, J.-B., Jozja, N., Défarge, C., & Moquet, J.-S. (2022). Evidence of long term biogeochemical interactions in carbonate weathering: The role of planktonic microorganisms and riverine bivalves in a large fluviokarst system. *Science of the Total Environment*, *842*, 156823. https://doi.org/10.1016/j.scitotenv.2022.156823

Blaszczak, J. R., Delesantro, J. M., Urban, D. L., Doyle, M. W., & Bernhardt, E. S. (2019). Scoured or suffocated: Urban stream ecosystems oscillate between hydrologic and dissolved oxygen extremes. *Limnology and Oceanography*, *64*(3), 877–894.

Bogard, M. J., & Del Giorgio, P. A. (2016). The role of metabolism in modulating CO_2 fluxes in boreal lakes. *Global Biogeochemical Cycles*, *30*(10), 1509–1525. https://doi.org/10.1002/2016GB005463

Butman, D., & Raymond, P. A. (2011). Significant efflux of carbon dioxide from streams and rivers in the united states. *Nature Geoscience*, *4*(12), Article 12. https://doi.org/10.1038/ngeo1294

Camenen, B., Grabowski, R. C., Latapie, A., Paquier, A., Solari, L., & Rodrigues, S. (2016). On the estimation of the bed material transport and budget along a river segment: Application to the

Middle Loire River, France. *Aquatic Sciences*, *78*(1), 71–81. https://doi.org/10.1007/s00027-015-0442-3

Cole, J. J., Cole, J. J., Caraco, N. F., & Caraco, N. F. (2001). Carbon in catchments: Connecting terrestrial carbon losses with aquatic metabolism. *Marine and Freshwater Research*, *52*(1), 101. https://doi.org/10.1071/MF00084

Cole, J. J., Prairie, Y. T., Caraco, N. F., McDowell, W. H., Tranvik, L. J., Striegl, R. G., Duarte, C. M., Kortelainen, P., Downing, J. A., Middelburg, J. J., & Melack, J. (2007). Plumbing the global carbon cycle: Integrating inland waters into the terrestrial carbon budget. *Ecosystems*, *10*(1), 171–184. https://doi.org/10.1007/s10021-006-9013-8

Coynel, A., Etcheber, H., Abril, G., Maneux, E., Dumas, J., & Hurtrez, J. E. (2005). Contribution of small mountainous rivers to particulate organic carbon input in the bay of biscay. *Biogeochemistry*, *74*(2), 151–171.

Deirmendjian, L., & Abril, G. (2018). Carbon dioxide degassing at the groundwater-stream-atmosphere interface: Isotopic equilibration and hydrological mass balance in a sandy watershed. *Journal of Hydrology*, *558*, 129–143. https://doi.org/10.1016/j.jhydrol.2018.01.003

Diamond, J. S., Bernal, S., Boukra, A., Cohen, M. J., Lewis, D., Masson, M., Moatar, F., & Pinay, G. (2021). Stream network variation in dissolved oxygen: Metabolism proxies and biogeochemical controls. *Ecological Indicators*, *131*(September), 108233. https://doi.org/10.1016/j.ecolind.2021.108233

Diamond, J. S., Moatar, F., Cohen, M. J., Poirel, A., Martinet, C., Maire, A., & Pinay, G. (2022). Metabolic regime shifts and ecosystem state changes are decoupled in a large river. *Limnology and Oceanography*, *67*(S1). https://doi.org/10.1002/lno.11789

Diamond, J. S., Truong, A. N., Abril, G., Bertuzzo, E., Chanudet, V., Lamouroux, R., & Moatar, F. (2025). Inorganic carbon dynamics and their relation to autotrophic community regime shift over three decades in a large, alkaline river. *Limnology and Oceanography*, *n/a*(n/a). https://doi.org/10.1002/lno.70016

Dodds, W. K., & Smith, V. H. (2016). Nitrogen, phosphorus, and eutrophication in streams. *Inland Waters*, *6*(2), 155–164. https://doi.org/10.5268/IW-6.2.909

Duvert, C., Butman, D. E., Marx, A., Ribolzi, O., & Hutley, L. B. (2018). CO2 evasion along streams driven by groundwater inputs and geomorphic controls. *Nature Geoscience*, *11*(11), Article 11. https://doi.org/10.1038/s41561-018-0245-y

Etcheber, H., Taillez, A., Abril, G., Garnier, J., Servais, P., Moatar, F., & Commarieu, M. V. (2007). Particulate organic carbon in the estuarine turbidity maxima of the gironde, loire and seine estuaries: Origin and lability. *Hydrobiologia*, *588*(1), 245–259. https://doi.org/10.1007/s10750-007-0667-9

Floury, M., Delattre, C., Ormerod, S. J., & Souchon, Y. (2012). Global versus local change effects on a large european river. *Science of the Total Environment*, *441*, 220–229. https://doi.org/10.1016/j.scitotenv.2012.09.051

He, H., Wang, Y., Liu, Z., Bao, Q., Wei, Y., Chen, C., & Sun, H. (2022). Lake metabolic processes and their effects on the carbonate weathering CO2 sink: Insights from diel variations in the hydrochemistry of a typical karst lake in SW china. *Water Research*, *222*, 118907. https://doi.org/10.1016/j.watres.2022.118907

Hotchkiss, E. R., Hall Jr, R. O., Sponseller, R. A., Butman, D., Klaminder, J., Laudon, H., Rosvall, M., & Karlsson, J. (2015). Sources of and processes controlling CO2 emissions change with the size of streams and rivers. *Nature Geoscience*, *8*(9), 696–699. https://doi.org/10.1038/ngeo2507

Humphreys, M. P., Lewis, E. R., Sharp, J. D., & Pierrot, D. (2022). PyCO2SYS v1.8: Marine carbonate system calculations in python. *Geoscientific Model Development*, *15*(1), 15–43. https://doi.org/10.5194/gmd-15-15-2022

Hussain, Md., & Mahmud, I. (2019). pyMannKendall: A python package for non parametric mann kendall family of trend tests. *Journal of Open Source Software*, *4*(39), 1556. https://doi.org/10.21105/joss.01556

Ibáñez, C., Caiola, N., Barquín, J., Belmar, O., Benito, X., Casals, F., Fennessy, S., Hughes, J., Palmer, M., Peñuelas, J., Romero, E., Sardans, J., & Williams, M. (2022). Ecosystem-level effects of re-oligotrophication and N:P imbalances in rivers and estuaries on a global scale. *Global Change Biology*, *n/a*(n/a). https://doi.org/10.1111/gcb.16520

Janssen, P., Chevalier, R., Chantereau, M., Dupré, R., Evette, A., Hémeray, D., Mårell, A., Martin, H., Rodrigues, S., Villar, M., & Greulich, S. (2023). Can vegetation clearing operations and reprofiling of bars be considered as an ecological restoration measure? Lessons from a 10-year vegetation monitoring program (loire river, france). *Restoration Ecology, 31*(3), e13704. https://doi.org/10.1111/rec.13704

Jones, A. S., Jones, T. L., & Horsburgh, J. S. (2022). Toward automating post processing of aquatic sensor data. *Environmental Modelling and Software, 151*, 105364. https://doi.org/10.1016/j.envsoft.2022.105364

Jones, J. B., Stanley, E. H., & Mulholland, P. J. (2003). Long-term decline in carbon dioxide supersaturation in rivers across the contiguous united states. *Geophysical Research Letters, 30*(10), 2003GL017056. https://doi.org/10.1029/2003GL017056

Kirk, L., & Cohen, M. J. (2023). River corridor sources dominate CO_2 emissions from a lowland river network. *Journal of Geophysical Research: Biogeosciences, 128*(1), e2022JG006954. https://doi.org/10.1029/2022JG006954

Koehler, B., Landelius, T., Weyhenmeyer, G. A., Machida, N., & Tranvik, L. J. (2014). Sunlight-induced carbon dioxide emissions from inland waters. *Global Biogeochemical Cycles, 28*(7), 696–711. https://doi.org/10.1002/2014GB004850

Lynch, J. K., Beatty, C. M., Seidel, M. P., Jungst, L. J., & DeGrandpre, M. D. (2010). Controls of riverine CO_2 over an annual cycle determined using direct, high temporal resolution pCO_2 measurements. *Journal of Geophysical Research: Biogeosciences, 115*(G3), 2009JG001132. https://doi.org/10.1029/2009JG001132

Millero, F. J. (1979). The thermodynamics of the carbonate system in seawater. *Geochimica et Cosmochimica Acta, 43*(10), 1651–1661. https://doi.org/10.1016/0016-7037(79)90184-4

Minaudo, C., Meybeck, M., Moatar, F., Gassama, N., & Curie, F. (2015). Eutrophication mitigation in rivers: 30 years of trends in spatial and seasonal patterns of biogeochemistry of the loire river (1980–2012). *Biogeosciences, 12*(8), 2549–2563. https://doi.org/10.5194/bg-12-2549-2015

Moatar, F., Descy, J. P., Rodrigues, S., Souchon, Y., Floury, M., Grosbois, C., Minaudo, C., Leitao, M., Wantzen, K. M., & Bertrand, F. (2022). Chapter 7 – The loire river basin. In K. Tockner, C.

Zarfl, & C. T. Robinson (Eds.), *Rivers of Europe (Second Edition)* (pp. 245–271). Elsevier. https://doi.org/10.1016/B978-0-08-102612-0.00007-9

Moatar, F., Fessant, F., & Poirel, A. (1999). pH modelling by neural networks. Application of control and validation data series in the middle loire river. *Ecological Modelling*, *120*(2–3), 141–156. https://doi.org/10.1016/S0304-3800(99)00098-8

Moatar, F., & Meybeck, M. (2005). Compared performances of different algorithms for estimating annual nutrient loads discharged by the eutrophic River Loire. *Hydrological Processes*, *19*(2), 429–444. https://doi.org/10.1002/hyp.5541

Moatar, F., Miquel, J., & Poirel, A. (2001). A quality-control method for physical and chemical monitoring data. Application to dissolved oxygen levels in the river loire (france). *Journal of Hydrology*, *252*(1–4), 25–36. https://doi.org/10.1016/S0022-1694(01)00439-5

NOAA. (n.d.). *Trends in atmospheric carbon dioxide*. Global Monitoring Laboratory - Carbon Cycle Greenhouse Gases. https://gml.noaa.gov/ccgg/trends/data.html

Odum, H. T. (1956). Primary Production in Flowing Waters. *Limnology and Oceanography*, *1*(2), 102–117. https://doi.org/10.4319/lo.1956.1.2.0102

Raymond, P. A., Caraco, N. F., & Cole, J. J. (1997). Carbon dioxide concentration and atmospheric flux in the hudson river. *Estuaries*, *20*(2), 381. https://doi.org/10.2307/1352351

Raymond, P. A., Hartmann, J., Lauerwald, R., Sobek, S., McDonald, C., Hoover, M., Butman, D., Striegl, R., Mayorga, E., Humborg, C., Kortelainen, P., Dürr, H., Meybeck, M., Ciais, P., & Guth, P. (2013). Global carbon dioxide emissions from inland waters. *Nature*, *503*(7476), 355–359. https://doi.org/10.1038/nature12760

Raymond, P. A., Zappa, C. J., Butman, D., Bott, T. L., Potter, J., Mulholland, P., Laursen, A. E., McDowell, W. H., & Newbold, D. (2012a). Scaling the gas transfer velocity and hydraulic geometry in streams and small rivers. *Limnology and Oceanography: Fluids and Environments*, *2*(1), 41–53. https://doi.org/10.1215/21573689-1597669

Raymond, P. A., Zappa, C. J., Butman, D., Bott, T. L., Potter, J., Mulholland, P., Laursen, A. E., McDowell, W. H., & Newbold, D. (2012b). Scaling the gas transfer velocity and hydraulic

geometry in streams and small rivers. *Limnology and Oceanography: Fluids and Environments*, *2*(1), 41–53. https://doi.org/10.1215/21573689-1597669

Reed, A. P., Stets, E. G., Murphy, S. F., & Mullins, E. A. (2021). Aquatic-terrestrial linkages control metabolism and carbon dynamics in a mid-sized, urban stream influenced by snowmelt. *Journal of Geophysical Research: Biogeosciences*, *126*(9), e2021JG006296. https://doi.org/10.1029/2021JG006296

Rocher-Ros, G., Harms, T. K., Sponseller, R. A., Väisänen, M., Mörth, C. M., & Giesler, R. (2021). Metabolism overrides photo-oxidation in CO2 dynamics of Arctic permafrost streams. *Limnology and Oceanography*, *66*(S1), S169–S181. https://doi.org/10.1002/lno.11564

Rocher-Ros, G., Sponseller, R. A., Bergström, A., Myrstener, M., & Giesler, R. (2020). Stream metabolism controls diel patterns and evasion of CO_2 in arctic streams. *Global Change Biology*, *26*(3), 1400–1413. https://doi.org/10.1111/gcb.14895

Seabold, S., & Perktold, J. (2010). *Statsmodels: Econometric and statistical modeling with python*. 92–96. https://doi.org/10.25080/Majora-92bf1922-011

Thiéry, D. (2018). *ÉROS: A semi-global hydrological modelling application for a catchment area divided into sub-basins | BRGM*. https://www.brgm.fr/en/software/eros-semi-global-hydrological-modelling-application-catchment-area-divided-sub-basins

Trentman, M. T., Hall, R. O., & Valett, H. M. (2023). Exploring the mismatch between the theory and application of photosynthetic quotients in aquatic ecosystems. *Limnology and Oceanography Letters*. https://doi.org/10.1002/lol2.10326

Truong, C., Oudre, L., & Vayatis, N. (2020). Selective review of offline change point detection methods. *Signal Processing*, *167*, 107299. https://doi.org/10.1016/j.sigpro.2019.107299

Tsypin, M., & Macpherson, G. L. (2012). The effect of precipitation events on inorganic carbon in soil and shallow groundwater, konza prairie LTER site, NE kansas, USA. *Applied Geochemistry*, *27*(12), 2356–2369. https://doi.org/10.1016/j.apgeochem.2012.07.008

Van Vliet, M. T. H., Franssen, W. H. P., Yearsley, J. R., Ludwig, F., Haddeland, I., Lettenmaier, D. P., & Kabat, P. (2013). Global river discharge and water temperature under climate change. *Global Environmental Change*, *23*(2), 450–464. https://doi.org/10.1016/j.gloenvcha.2012.11.002

Vihermaa, L. E., Waldron, S., Garnett, M. H., & Newton, J. (2014). Old carbon contributes to aquatic emissions of carbon dioxide in the Amazon. *Biogeosciences*, *11*(13), 3635–3645. https://doi.org/10.5194/bg-11-3635-2014

Wallin, M. B., Audet, J., Peacock, M., Sahlée, E., & Winterdahl, M. (2020). Carbon dioxide dynamics in an agricultural headwater stream driven by hydrology and primary production. *Biogeosciences*, *17*(9), 2487–2498. https://doi.org/10.5194/bg-17-2487-2020

Young, F. L., Colman, B. P., Carter, A. M., Fiejó De Lima, R., Shangguan, Q., Payn, R. A., & DeGrandpre, M. D. (2025). Variability and Controls of p CO_2 and Air-Water CO_2 Fluxes in a Temperate River. *Journal of Geophysical Research: Biogeosciences*, *130*(2), e2024JG008434. https://doi.org/10.1029/2024JG008434

Zhang, T., Li, J., Pu, J., Martin, J. B., Khadka, M. B., Wu, F., Li, L., Jiang, F., Huang, S., & Yuan, D. (2017). River sequesters atmospheric carbon and limits the CO2 degassing in karst area, southwest China. *Science of the Total Environment*, *609*, 92–101. https://doi.org/10.1016/j.scitotenv.2017.07.143

Abril, G., & Borges, A. V. (2019). Ideas and perspectives: Carbon leaks from flooded land: Do we need to replumb the inland water active pipe? Biogeosciences, 16(3), 769–784. https://doi.org/10.5194/bg-16-769-2019

Abril, G., Bouillon, S., Darchambeau, F., Teodoru, C. R., Marwick, T. R., Tamooh, F., Ochieng Omengo, F., Geeraert, N., Deirmendjian, L., Polsenaere, P., & Borges, A. V. (2015). Technical note: Large overestimation of pCO2 calculated from pH and alkalinity in acidic, organic-rich freshwaters. Biogeosciences, 12(1), 67–78. https://doi.org/10.5194/bg-12-67-2015

Aho, K. S., Hosen, J. D., Logozzo, L. A., McGillis, W. R., & Raymond, P. A. (2021). Highest rates of gross primary productivity maintained despite CO 2 depletion in a temperate river network. Limnology and Oceanography Letters, 6(4), 200–206. https://doi.org/10.1002/lol2.10195

Amaral, J., Suhett, A., Melo, S., & Farjalla, V. (2013). Seasonal variation and interaction of photodegradation and microbial metabolism of DOC in black water Amazonian ecosystems. Aquatic Microbial Ecology, 70(2), 157–168. https://doi.org/10.3354/ame01651

Appling, A. P., Hall, R. O., Yackulic, C. B., & Arroita, M. (2018). Overcoming Equifinality: Leveraging Long Time Series for Stream Metabolism Estimation. Journal of Geophysical Research: Biogeosciences, 123(2), 624–645. https://doi.org/10.1002/2017JG004140

Battin, T. J., Lauerwald, R., Bernhardt, E. S., Bertuzzo, E., Gener, L. G., Hall, R. O., Hotchkiss, E. R., Maavara, T., Pavelsky, T. M., Ran, L., Raymond, P., Rosentreter, J. A., & Regnier, P. (2023). River ecosystem metabolism and carbon biogeochemistry in a changing world. Nature, 613(7944), 449–459. https://doi.org/10.1038/s41586-022-05500-8

Baulon, L., Allier, D., Massei, N., Bessiere, H., Fournier, M., & Bault, V. (2022). Influence of low-frequency variability on groundwater level trends. Journal of Hydrology, 606, 127436. https://doi.org/10.1016/j.jhydrol.2022.127436

Bernal, S., Cohen, M. J., Ledesma, J. L. J., Kirk, L., Martí, E., & Lupon, A. (2022). Stream metabolism sources a large fraction of carbon dioxide to the atmosphere in two hydrologically contrasting headwater streams. Limnology and Oceanography, 67(12), 2621–2634. https://doi.org/10.1002/lno.12226

Binet, S., Charlier, J.-B., Jozja, N., Défarge, C., & Moquet, J.-S. (2022). Evidence of long-term biogeochemical interactions in carbonate weathering: The role of planktonic microorganisms and riverine bivalves in a large fluviokarst system. Science of the Total Environment, 842, 156823. https://doi.org/10.1016/j.scitotenv.2022.156823

Bogard, M. J., & Del Giorgio, P. A. (2016). The role of metabolism in modulating CO_2 fluxes in boreal lakes. Global Biogeochemical Cycles, 30(10), 1509–1525. https://doi.org/10.1002/2016GB005463

Butman, D., & Raymond, P. A. (2011). Significant efflux of carbon dioxide from streams and rivers in the united states. Nature Geoscience, 4(12), Article 12. https://doi.org/10.1038/ngeo1294

Cole, J. J., Cole, J. J., Caraco, N. F., & Caraco, N. F. (2001). Carbon in catchments: Connecting terrestrial carbon losses with aquatic metabolism. Marine and Freshwater Research, 52(1), 101. https://doi.org/10.1071/MF00084

Cole, J. J., Prairie, Y. T., Caraco, N. F., McDowell, W. H., Tranvik, L. J., Striegl, R. G., Duarte, C. M., Kortelainen, P., Downing, J. A., Middelburg, J. J., & Melack, J. (2007). Plumbing the global

carbon cycle: Integrating inland waters into the terrestrial carbon budget. Ecosystems, 10(1), 171–184. https://doi.org/10.1007/s10021-006-9013-8

Coynel, A., Etcheber, H., Abril, G., Maneux, E., Dumas, J., & Hurtrez, J.-E. (2005). Contribution of small mountainous rivers to particulate organic carbon input in the bay of biscay. Biogeochemistry, 74(2), 151–171.

Deirmendjian, L., & Abril, G. (2018). Carbon dioxide degassing at the groundwater-stream-atmosphere interface: Isotopic equilibration and hydrological mass balance in a sandy watershed. Journal of Hydrology, 558, 129–143. https://doi.org/10.1016/j.jhydrol.2018.01.003

Diamond, J. S., Bernal, S., Boukra, A., Cohen, M. J., Lewis, D., Masson, M., Moatar, F., & Pinay, G. (2021). Stream network variation in dissolved oxygen: Metabolism proxies and biogeochemical controls. Ecological Indicators, 131(September), 108233. https://doi.org/10.1016/j.ecolind.2021.108233

Diamond, J. S., Moatar, F., Cohen, M. J., Poirel, A., Martinet, C., Maire, A., & Pinay, G. (2022). Metabolic regime shifts and ecosystem state changes are decoupled in a large river. Limnology and Oceanography, 67(S1). https://doi.org/10.1002/lno.11789

Dodds, W. K., & Smith, V. H. (2016). Nitrogen, phosphorus, and eutrophication in streams. Inland Waters, 6(2), 155–164. https://doi.org/10.5268/IW-6.2.909

Duvert, C., Butman, D. E., Marx, A., Ribolzi, O., & Hutley, L. B. (2018). CO2 evasion along streams driven by groundwater inputs and geomorphic controls. Nature Geoscience, 11(11), Article 11. https://doi.org/10.1038/s41561-018-0245-y

Etcheber, H., Taillez, A., Abril, G., Garnier, J., Servais, P., Moatar, F., & Commarieu, M. V. (2007). Particulate organic carbon in the estuarine turbidity maxima of the gironde, loire and seine estuaries: Origin and lability. Hydrobiologia, 588(1), 245–259. https://doi.org/10.1007/s10750-007-0667-9

Floury, M., Delattre, C., Ormerod, S. J., & Souchon, Y. (2012). Global versus local change effects on a large european river. Science of the Total Environment, 441, 220–229. https://doi.org/10.1016/j.scitotenv.2012.09.051

He, H., Wang, Y., Liu, Z., Bao, Q., Wei, Y., Chen, C., & Sun, H. (2022). Lake metabolic processes and their effects on the carbonate weathering CO2 sink: Insights from diel variations in the hydrochemistry of a typical karst lake in SW china. Water Research, 222, 118907. https://doi.org/10.1016/j.watres.2022.118907

Hotchkiss, E. R., Hall Jr, R. O., Sponseller, R. A., Butman, D., Klaminder, J., Laudon, H., Rosvall, M., & Karlsson, J. (2015). Sources of and processes controlling CO2 emissions change with the size of streams and rivers. Nature Geoscience, 8(9), 696–699. https://doi.org/10.1038/ngeo2507

Humphreys, M. P., Lewis, E. R., Sharp, J. D., & Pierrot, D. (2022). PyCO2SYS v1.8: Marine carbonate system calculations in python. Geoscientific Model Development, 15(1), 15–43. https://doi.org/10.5194/gmd-15-15-2022

Hussain, Md., & Mahmud, I. (2019). pyMannKendall: A python package for non parametric mann kendall family of trend tests. Journal of Open Source Software, 4(39), 1556. https://doi.org/10.21105/joss.01556

Ibáñez, C., Caiola, N., Barquín, J., Belmar, O., Benito, X., Casals, F., Fennessy, S., Hughes, J., Palmer, M., Peñuelas, J., Romero, E., Sardans, J., & Williams, M. (2022). Ecosystem-level effects of re-oligotrophication and N:P imbalances in rivers and estuaries on a global scale. Global Change Biology, n/a(n/a). https://doi.org/10.1111/gcb.16520

Janssen, P., Chevalier, R., Chantereau, M., Dupré, R., Evette, A., Hémeray, D., Mårell, A., Martin, H., Rodrigues, S., Villar, M., & Greulich, S. (2023). Can vegetation clearing operations and reprofiling of bars be considered as an ecological restoration measure? Lessons from a 10-year vegetation monitoring program (loire river, france). Restoration Ecology, 31(3), e13704. https://doi.org/10.1111/rec.13704

Jones, J. B., Stanley, E. H., & Mulholland, P. J. (2003). Long-term decline in carbon dioxide supersaturation in rivers across the contiguous united states. Geophysical Research Letters, 30(10), 2003GL017056. https://doi.org/10.1029/2003GL017056

Kirk, L., & Cohen, M. J. (2023). River corridor sources dominate CO2 emissions from a lowland river network. Journal of Geophysical Research: Biogeosciences, 128(1), e2022JG006954. https://doi.org/10.1029/2022JG006954

Koehler, B., Landelius, T., Weyhenmeyer, G. A., Machida, N., & Tranvik, L. J. (2014). Sunlight-induced carbon dioxide emissions from inland waters. Global Biogeochemical Cycles, 28(7), 696–711. https://doi.org/10.1002/2014GB004850

Lynch, J. K., Beatty, C. M., Seidel, M. P., Jungst, L. J., & DeGrandpre, M. D. (2010). Controls of riverine CO_2 over an annual cycle determined using direct, high temporal resolution pCO_2 measurements. Journal of Geophysical Research: Biogeosciences, 115(G3), 2009JG001132. https://doi.org/10.1029/2009JG001132

Millero, F. J. (1979). The thermodynamics of the carbonate system in seawater. Geochimica et Cosmochimica Acta, 43(10), 1651–1661. https://doi.org/10.1016/0016-7037(79)90184-4

Minaudo, C., Meybeck, M., Moatar, F., Gassama, N., & Curie, F. (2015). Eutrophication mitigation in rivers: 30 years of trends in spatial and seasonal patterns of biogeochemistry of the loire river (1980–2012). Biogeosciences, 12(8), 2549–2563. https://doi.org/10.5194/bg-12-2549-2015

Moatar, F., Descy, J. P., Rodrigues, S., Souchon, Y., Floury, M., Grosbois, C., Minaudo, C., Leitao, M., Wantzen, K. M., & Bertrand, F. (2022). Chapter 7 — The loire river basin. In K. Tockner, C. Zarfl, & C. T. Robinson (Eds.), Rivers of Europe (Second Edition) (pp. 245–271). Elsevier. https://doi.org/10.1016/B978-0-08-102612-0.00007-9

Moatar, F., Fessant, F., & Poirel, A. (1999). pH modelling by neural networks. Application of control and validation data series in the middle loire river. Ecological Modelling, 120(2–3), 141–156. https://doi.org/10.1016/S0304-3800(99)00098-8

Moatar, F., & Meybeck, M. (2005). Compared performances of different algorithms for estimating annual nutrient loads discharged by the eutrophic River Loire. Hydrological Processes, 19(2), 429–444. https://doi.org/10.1002/hyp.5541

Moatar, F., Miquel, J., & Poirel, A. (2001). A quality-control method for physical and chemical monitoring data. Application to dissolved oxygen levels in the river loire (france). Journal of Hydrology, 252(1–4), 25–36. https://doi.org/10.1016/S0022-1694(01)00439-5

NOAA. (n.d.). Trends in atmospheric carbon dioxide. Global Monitoring Laboratory - Carbon Cycle Greenhouse Gases. https://gml.noaa.gov/ccgg/trends/data.html

Raymond, P. A., Caraco, N. F., & Cole, J. J. (1997). Carbon dioxide concentration and atmospheric flux in the hudson river. Estuaries, 20(2), 381. https://doi.org/10.2307/1352351

Raymond, P. A., Hartmann, J., Lauerwald, R., Sobek, S., McDonald, C., Hoover, M., Butman, D., Striegl, R., Mayorga, E., Humborg, C., Kortelainen, P., Dürr, H., Meybeck, M., Ciais, P., & Guth, P. (2013). Global carbon dioxide emissions from inland waters. Nature, 503(7476), 355–359. https://doi.org/10.1038/nature12760

Raymond, P. A., Zappa, C. J., Butman, D., Bott, T. L., Potter, J., Mulholland, P., Laursen, A. E., McDowell, W. H., & Newbold, D. (2012). Scaling the gas transfer velocity and hydraulic geometry in streams and small rivers. Limnology and Oceanography: Fluids and Environments, 2(1), 41–53. https://doi.org/10.1215/21573689-1597669

Reed, A. P., Stets, E. G., Murphy, S. F., & Mullins, E. A. (2021). Aquatic-terrestrial linkages control metabolism and carbon dynamics in a mid-sized, urban stream influenced by snowmelt. Journal of Geophysical Research: Biogeosciences, 126(9), e2021JG006296. https://doi.org/10.1029/2021JG006296

Rocher-Ros, G., Harms, T. K., Sponseller, R. A., Väisänen, M., Mörth, C.-M., & Giesler, R. (2021). Metabolism overrides photo-oxidation in CO2 dynamics of Arctic permafrost streams. Limnology and Oceanography, 66(S1), S169–S181. https://doi.org/10.1002/lno.11564

Rocher-Ros, G., Sponseller, R. A., Bergström, A., Myrstener, M., & Giesler, R. (2020). Stream metabolism controls diel patterns and evasion of CO2 in arctic streams. Global Change Biology, 26(3), 1400–1413. https://doi.org/10.1111/gcb.14895

Seabold, S., & Perktold, J. (2010). Statsmodels: Econometric and statistical modeling with python. 92–96. https://doi.org/10.25080/Majora-92bf1922-011

Truong, C., Oudre, L., & Vayatis, N. (2020). Selective review of offline change point detection methods. Signal Processing, 167, 107299. https://doi.org/10.1016/j.sigpro.2019.107299

Tsypin, M., & Macpherson, G. L. (2012). The effect of precipitation events on inorganic carbon in soil and shallow groundwater, konza prairie LTER site, NE kansas, USA. Applied Geochemistry, 27(12), 2356–2369. https://doi.org/10.1016/j.apgeochem.2012.07.008

Van Vliet, M. T. H., Franssen, W. H. P., Yearsley, J. R., Ludwig, F., Haddeland, I., Lettenmaier, D. P., & Kabat, P. (2013). Global river discharge and water temperature under climate change. Global Environmental Change, 23(2), 450–464. https://doi.org/10.1016/j.gloenvcha.2012.11.002

Vihermaa, L. E., Waldron, S., Garnett, M. H., & Newton, J. (2014). Old carbon contributes to aquatic emissions of carbon dioxide in the Amazon. Biogeosciences, 11(13), 3635–3645. https://doi.org/10.5194/bg-11-3635-2014

Wallin, M. B., Audet, J., Peacock, M., Sahlée, E., & Winterdahl, M. (2020). Carbon dioxide dynamics in an agricultural headwater stream driven by hydrology and primary production. Biogeosciences, 17(9), 2487–2498. https://doi.org/10.5194/bg-17-2487-2020

Young, F. L., Colman, B. P., Carter, A. M., Fiejó De Lima, R., Shangguan, Q., Payn, R. A., & DeGrandpre, M. D. (2025). Variability and Controls of pCO_2 and Air-Water CO_2 Fluxes in a Temperate River. Journal of Geophysical Research: Biogeosciences, 130(2), e2024JG008434. https://doi.org/10.1029/2024JG008434

Zhang, T., Li, J., Pu, J., Martin, J. B., Khadka, M. B., Wu, F., Li, L., Jiang, F., Huang, S., & Yuan, D. (2017). River sequesters atmospheric carbon and limits the CO_2 degassing in karst area, southwest China. Science of the Total Environment, 609, 92–101. https://doi.org/10.1016/j.scitotenv.2017.07.143